A Diagnostic Tool for Neuropathy Assessment on the Plantar Surface of the Foot

by

Vitale Kyle Castellano

A thesis submitted to the Graduate Faculty of
Auburn University
in partial fulfillment of the
requirements for the Degree of
Master of Science

Auburn, Alabama
August 8, 2020

Neuropathy, Threshold Sensitivity, Machine Design, Computer Numerical Control, Finite Element Analysis, Semmes-Weinstein Monofilament Assessment

Approved by

Michael Zabala, Chair, Assistant Professor of Mechanical Engineering
Robert L. Jackson, Professor of Mechanical Engineering
Chad Rose, Assistant Professor of Mechanical Engineering

Abstract

Neuropathy is categorized as a loss of sensation in the extremities, particularly in the hands and feet. It is often found in people with diabetes and is present in 40-60 million people. Symptoms include burning, numbness, shooting pain, and an electrical sensation. Those who have neuropathy are at an increased risk of puncturing their feet as they may step on a sharp object and not even feel it. This can result in infection, amputation, ulceration, and even death. There are a variety of tests used for neuropathy diagnosis, which includes vibration analysis via tuning forks, electrical stimulation, and monofilament assessment. The Semmes-Weinstein monofilament assessment is the most popular tool used to diagnose neuropathy. It utilizes a nylon monofilament which is applied normal to the surface of the foot, noninvasively, until it buckles. At the instant that the monofilament buckles it is assumed to apply a constant force to the skin. The most popular monofilament is the 5.07 gauge monofilament, which is advertised to produce 10 grams of equivalent force at buckling. However, there is a lack of consistent testing methodology when using the monofilament technique and other factors likely also affect the accuracy of the assessment. For example, the monofilaments are influenced by temperature, humidity, fatigue, insertion speed, and angle of insertion. Although the monofilaments produce a specific force at the instant they buckle, they are capable of being over-inserted, resulting in greater amounts of contact force. In this thesis a study involving theoretical contact mechanics and finite element analysis was conducted showing that the amount of insertion depth and the monofilament diameter both affect the amount of force produced as the monofilament is applied to human skin. The results of this study showed that the more the monofilament evaluator is inserted into the human skin the greater the contact force and normal stress produced. Likewise, if the diameter increases then the contact force will increase, but conversely the normal stress will decrease. Surface plots visually depicted

the contact force and normal stress as functions of insertion depth and monofilament diameter. These factors are likely to make it challenging to apply the correct amount of force with the monofilament. Although some clinicians are skilled enough to use the monofilaments repeatably and accurately, others may struggle to do this. This compromises the ability of a clinician to monitor a person's degree of neuropathy and to study the effects of treatments. A new standardized method and corresponding tool was developed which can objectively measure an individual's sensation lost caused by neuropathy. This new method involves a computer numerical control machine which can apply the monofilament to many locations on the plantar surface of the foot at a variety of forces using only a single monofilament. The machine was developed over the course of two years, with three distinct prototypes. These included an initial prototype, followed by Mk1 and Mk2 prototypes. Mk1 was built within the first year and is fully operational. The most important feature of the machine is that it applies the monofilament by using a feedback loop between a load cell and a stepper motor. This is ultimately what makes the device more accurate than the hand applied monofilament assessment when used in preliminary pilot testing. This diagnostic tool is fully capable of mapping out an individual's threshold sensitivity and is designed to be used on 95% of the world's population. The results of the assessment are documented using a picture of the patient's foot for both the patient and clinician to observe. Moreover, a new testing methodology was developed specifically for this device, which uses randomization and false-positive assessments in its protocol. The randomization feature is specifically for the location testing order and consequently removes both the clinical and patient bias during the test. Additionally, a false-positive check is given a 10% chance of occurring per testing location. This new methodology also systematically homes in on the patient's threshold sensitivity. All of these features help standardize the testing procedure and are currently absent in the manual

monofilament evaluation. A provisional patent application was filed on the design and functionality of the diagnostic tool and it is anticipated that it could become a more accurate screening tool for neuropathy assessment.

Acknowledgments

I would like to thank Dr. Zabala for all of his mentorship, advisement, and support throughout my time at Auburn University. It has been a pleasure to have worked in the Auburn University Biomechanical Engineering Lab for the last two years where I have been able to be apparent of many enjoyable projects and ground break research. I have learned a lot from him and feel that I have become a better engineer through his mentorship. I look forward to continuing to work with him in the future, especially in my PhD research.

I would also like to thank my committee members Dr. Jackson and Dr. Rose for their support in my research and for serving on my defense. Their feedback has been invaluable and ultimately has made my thesis better. I am very grateful that they were able to serve on my defense and am glad I was given the opportunity to take my research in different areas than I originally anticipated.

I also would like to thank Dr. Burch and Dr. Commander for all of their support and insight throughout the development of this device. Dr. Burch has provided much of his engineering knowledge towards the device, while Dr. Commander has provided medical insight vital for the success of this project. I learned a lot from both of them and am grateful for the opportunity to have worked beside them. I am also grateful for Dr. Brock for being a good liaison between the Edward via College of Osteopathic Medicine (VCOM) and Auburn University throughout this design project. I am appreciative to VCOM for funding my research for the past few years and look forward to continuing to work with them in the future of my research project.

I am also grateful for all of my lab mates in the Auburn University Biomechanical Engineering Lab for their support and friendship over the last two years. Jordan Coker, Jake Larson, Austin Harris, Taylor Wright Oldfather, Amelia Falcon, Scott Kennedy, Raju Gupta, Reed Rodich,

Chase Mathews, Scot Carpenter, Grace Gray, and Anthony Marino have all been great to work alongside with and I happy to call them all friends.

I also would like to thank Hayden Burch for his time and commitment in this research project. He developed a good concept which was a great starting point for me when I started my graduate studies. We then came together and over the course of a summer we improved the machine dramatically by developing a new method of applying the monofilament using a feedback loop between a stepper motor and a load cell. This device allowed the machine to be far more accurate and repeatable. I learned a lot from him and implemented a lot of things he taught me about coding in other scripts and functions I wrote. I couldn't have done it without him and am grateful he worked so hard with me on this project. met

Additionally, I would like to acknowledge Dr. Tippur for taking the time to meet with me and my dad when I was looking at graduate schools. Before I came to Auburn he would always answer my questions regarding undergraduate courses I should take to better prepare myself for graduate school at Auburn. I also took many courses with Dr. Tippur and valued his availability for help outside of class and for challenging me to think critically about the course material.

I also appreciate the help I received from Michael Knotts in manufacturing some of the components of my device, as well as Howard Chen for his advice in using GRBL software in my machine. I also need to acknowledge the help from Professor Arnold and Chad Bailey from the Auburn University College of Architecture, Design, and Construction, School of Industrial and Graphic Design for their assistance in manufacturing the acrylic foot plate and front panel of my device with their laser cutters. The foot plate was a vital component and could only be made using a laser cutter. I need to also acknowledge Dr. Brady and the Auburn University Office of

Innovation Advancement & Commercialization for their guidance and assistance in filling the provisional patent application on the device.

I am grateful to Auburn University and the Samuel Ginn College of Engineering for allowing me to attend and for giving me the privilege to attend my dream school. I had always wanted to attend Auburn University and am glad that I was able to do so.

I would also like to take the time to thank professors from my undergraduate education at Kennesaw State University (Southern Polytechnic State University), where I earned my Bachelor of Science in Mechanical Engineering Technology. I would like to thank Dr. Nasseri for taking me under her wing and teaching me what engineering research is all about. Together we conducted research in biomedical engineering and manufacturing engineering, working with her motivated me that I needed to pursue graduate education and I am glad I did. I became a better engineer because of her and will always be grateful to her. I also would like to acknowledge Professor Conrey for being a good mentor for me during my undergraduate studies and for all his advice and guidance he gave me. We had many good conversations and I always felt welcomed in the MET program because of him.

I also would like to thank Professor Turner for her support and always answering my questions. Professor Turner was my statics professor and to this day I believe that statics it the foundation for engineering education and I am grateful to have learned from her. I also need to acknowledge Professor Sweigart for being my professor is so many engineering courses at SPSU. I spent a lot of time in his courses, but I feel that I became a better engineer from learning from him. Professor Winsor is also a professor I would like to thank, he is a fellow Auburn Alumni and because of him I was able to hone my SolidWorks skills which allowed me to become a professional at SolidWorks by obtaining the CSWP. He was also a fantastic professor and I

always looked forward to his lectures. Other SPSU professors I would like to thank are Professor Emert, Dr. Russell, Dr. Stollberg, Dr. Ritter, Dr. Thackston, Professor Ilksoy, Professor Duff, Professor Jenkins, Dr. Trebits, and Dr. Pascu.

There are also a number of teachers from high school, middle school, and elementary school that I would like to acknowledge for working with me and instilling in me a passion for learning. They include Mrs. Stiers, Mrs. Stuler, Mr. Turner, Mr. Englebert, Mr. Tozier, Mrs. Whittaker, Mrs. Waddell, Mrs. Williams, Mr. Hamm, Mrs. Wilson, Mrs. Godby, Mr. Gathing, Mr. Miller, Mrs. Winkler, Mrs. Pickens, Mrs. Artzer, Mrs. Harrison, Mrs. Ingram, Mrs. Foster, Mr. Newton, Mrs. Waters, Mrs. McEntyre, Mrs. Reese, Mrs. Bialek, Mr. Cotton, Mrs. McGlumphy, Mrs. Hunt, Mrs. Woodring, Mrs. Stils, Mrs. Gravitt, Ms. Reis, and Mrs. Mallanace. I also would like to acknowledge my 6th grade technology teacher, Mr. Taylor, who first introduced me to the area of STEM and for recognizing my hard work ethic. Since then I always knew I would end up in a STEM field.

I also need to sincerely thank Mr. Johnson, my high school engineering teacher and fellow Auburn Alumni. I learned so much from him both in the classroom and at Robotics Club. To this day I still use things he taught me and in fact when building my machine I used 80/20 Aluminum profiles, which we used in Robotics Club. I also got the idea of using a laser cutter to manufacture my acrylic plates from him, as we had one in high school and used it for various projects. I could never thank him enough for introducing me to the world of engineering, it is hard for me to believe that I would have pursued engineering in college and as a career path without him. Sometimes there is that one person in your life that makes a big difference and to me Mr. Johnson is that person. I will always remember him and continue to take the things he taught me throughout my life.

I would also like to thank some close friends, starting with Elliot Boerman, my best friend from West Forsyth High School. Elliot is one of the hardest working people I know and has been a true friend since I have known him. I would also like to thank both Ben Semmens and Cory Culberson for all of their support and camaraderie. I meet them the first week I was in Auburn and we all became good friends. We would often work together in class projects and they are by far the best group I have worked with. I also would like to thank Kurt Jacobson, Thomas Kosko, Tim Slaughter, Dan Homisak, Mushfequr Kotwal, Thomas Smith, Nathan Buck, Paul Schwan, Sams Khan, Daniel Bain, Taylor Bounds, and Herve Sobtaguim for their friendship.

Some other people I would like to thank are Dr. Jenkins, Dr. Beach, Dr. Sessions, Dr. Cofrancesco, and Dr. Cleaver for all of their support and help throughout my life.

Lastly, I would like to thank my family for all of their love and support, especially during my time during my graduate studies. To my mother I would like to thank her for all of her support, for working with me when I was younger, and for being the best teacher I have ever had. Without her I would never had overcome my reading and learning disability, as well as my speech impediment when I was in elementary school. She helped me learn good study habits and better writing techniques that I still use to this day. To my father I would like to thank him for always supporting me and for always having fun with me. We bonded over fast cars, speakers, and fishing. We have always had an enjoyable time together as father and son fixing and building things. Both of my loving parents have always supported my academic aspirations and without them I would have never developed my work ethic which has taken me far. I would also like to thank my brother Kevin, my best friend, for always being there for me. We have always brought out the best in each other and I am glad he is my brother. I also would like to thank my little buddy Rudy for always making me laugh and smile, even to this day. I would also like to

thank my grandfather and grandmother, Mario and Concetta Marino, for their love and support. Although I only got to spend a couple of years getting to know my grandfather, I would like to think he would have liked to see me become an engineer, as he worked with many. I never met my grandmother, she came to America from Italy as a little girl to escape fascism, and she is the bravest person I have ever heard of by doing so. I would also like to thank my grandparents, Vic and Val Castellano, for all of their love and support. They have always given kind words of encouragement and I am very grateful for them for always thinking of me. I would also like to thank my Zsi Zsi, Uncle Dan, and Zsi Zsi Fred for always thinking of me and for their love and support throughout my life. In addition, I would like to thank my Aunt Connie, Aunt Katie, Uncle John, Uncle Frank, and Aunt Pam for their love and support.

I think that in most people's lives there is often one person that without you would have turned out different, however I am fortunate and grateful to have many. From my family, to my friends, and to my teachers I have been bettered as a person and will always remember them all for the kindness they have given me.

War Eagle!

Table of Contents

List of Tables

Table of Figures

Chapter 1: Introduction and Background

1.1 Neuropathy Disease Background

Neuropathy is a disease that causes a loss of sensation in a person's extremities. The most common type is peripheral neuropathy, which results in nerve damage of the hands and feet of individuals who have type 2 diabetes [1, 2, 3, 4]. "Peripheral" is defined as beyond (the brain), while "neuro" is attributed to nerves, and "pathy" is disease [5]. In other words, peripheral neuropathy is the disease of nerves away from the brain. In 2019, 463 million adults have been reported to have diabetes and it is estimated that by 2045 this number will reach 700 million [4]. Sometimes referred to as "diabetic foot", complications associated with neuropathy affect 40 to 60 million people [4]. Burning feet is one of the most common symptoms related to neuropathy [6]. People also experience shooting pain, an electrical sensation, and numbness [7, 8, 9]. Additionally, individuals with neuropathy often cannot sense pressure or pain as a result of their sensation loss [10]. This often results in patients stepping on an object and puncturing their foot. This puts this cohort at an increased risk of developing ulcers [11, 12]. In fact, individuals with diabetic neuropathy are at greater risk of developing infections, which can lead to amputations and even death [12]. Individuals who have diabetes are 10 to 20 times more likely to have a lower limb amputation, which occurs on average every 30 seconds worldwide as a result of neuropathy complications [4].

1.2 Current Neuropathy Assessment Tools

There are a number of different methods employed to measure a person's degree of neuropathy. Application of warm and cold temperatures, vibratory analysis, nerve conduction, and electrodiagnostic studies have all been used [11]. A device called a Neurometer®, which employs a rapid current threshold detection method, uses electrodes to deliver current stimulations

corresponding to certain frequencies and has been used for neuropathy diagnosis [12]. Vibration perception threshold testing has also been conducted with the use of a biothesiometer [7]. Tuning forks applied to the patient have also been used as a method to measuring an individual's sensation loss, specifically the 128 Hz tuning fork [3, 7, 9]. It has also been proposed that using the reflectance spectra for human skin can be used to study ulceration and neuropathy by monitoring an individual's oxygen level [13]. However, the most common method for quantifying an individual's neuropathy is with a Semmes-Weinstein monofilament. In the 1800s horsehair filaments were used to assess for neuropathy, but in the 1960s Semmes and Weinstein developed nylon monofilaments to evaluate an individual's sensory perception [14, 15]. These first monofilaments were developed to be used on the hands of those affected with brain injuries [16]. These monofilaments, made of a single fiber of nylon, and are calibrated to reproduce a consistent buckling stress [11]. They were developed to control the force applied to the skin and to minimize the vibration as a result of the clinician's hand [17]. They are a popular choice for neuropathy assessment because they are noninvasive, easy to use, quick, and are relatively cheap when compared to other testing methods [11, 16]. The monofilament is applied perpendicular to the skin until it bends [16, 18]. As the monofilament is inserted the amount of force it produces increases until it buckles, which in theory makes this a reproducible test [14]. There are different monofilaments to choose from which correlate to different amounts of applied buckling forces. They can range from 0.008 to 300 grams of force, however they are typically expressed using an evaluator size [9]. The evaluator size, or monofilament gauge, is related to the logarithm of the force applied in grams of force, which is an application of "Weber's Law" relating perceived sensation ratio to the stimulus intensity [9, 15, 16, 18]. There are 5 classifications of plantar threshold sensitivity: normal (0.008-0.4 grams-force), diminished light touch (0.6-2.0 grams-

force), diminished protective sensation (4.0-8.0 grams-force), loss of protective sensation (10-180 grams-force), and deep pressure sensation only (300 grams-force) [9]. It is the 10-gram monofilament, or 5.07 evaluator, that is used most extensively to measure an individual's threshold of sensation [8, 9, 16]. It has been reported that the monofilament test is fully capable of controlling the applied force and has great sensitivities and repeatability requirements when the monofilament has been properly calibrated [17]. Wang et al. found that the monofilament assessment has good accuracy when compared to nerve conduction studies for diabetic peripheral neuropathy [19].

1.3 Semmes-Weinstein Monofilament Accuracy Factors

The Semmes-Weinstein monofilament assessment is not foolproof, as the actual force produced is dependent on many factors. The impact speed and the angle of insertion can affect the force produced [18]. The monofilament evaluators can also be affected by the temperature and humidity [14]. Fatigue is also a factor; Chikai and Ino found that after the monofilament was used 10 times it no longer produced its rated force and was 10% off this value [18]. There are also quality differences between monofilaments of the same evaluator size [17]. Inconsistencies in the diameter and the length of the monofilaments are potential sources of error against the rated supplied force [17]. McGill, Molyneaux, and Yue found in their study that as the monofilament length was reduced it caused an increase in the buckling force applied [20]. There are also inconsistencies in the literature of how to conduct an assessment using Semmes-Weinstein monofilaments, which makes it difficult to characterize this method's real world accuracy [11]. This makes it challenging to monitor potential treatments for neuropathy. It is because of the lack of a standardized testing methodology and the clinician bias associated with applying the monofilament by hand that has inspired a new device to be created.

Chapter 2: Modeling the Effects of Monofilament Insertion Depth and Diameter for Neuropathy Assessment on Human Skin

2.1 Abstract

Background: Neuropathy is a disease which results in the loss of sensation in the extremities. A method for assessing the degree of neuropathy is with a monofilament evaluator which buckles at a prescribed force depending on the filament diameter. However, as this assessment is conducted by the clinician's hand, the true force delivered is unknown. Therefore, the purpose of this study was to model the effects of both insertion depth and monofilament diameter on the contact force and normal stress produced on human skin.

Methods: Theoretical contact mechanics equations were used to understand the relationship between insertion depth, monofilament diameter, and applied force. SolidWorks© FEA was used to evaluate a 0.5 mm diameter monofilament, which is reported to provide a contact force of 10 grams of force, at 14 different insertion depths. The theoretical equations produced surface plots detailing how the monofilament insertion depth and diameter affected the force and stress produced. The FEA contact forces and normal stresses were validated against the results of the theoretical calculations.

Findings: The theoretical contact mechanics showed that higher levels of insertion and larger diameter monofilaments produced greater amounts of contact force. The normal stress increased with insertion depth but decreased with monofilament diameter. The FEA contact force consistently had an 8.9% difference from the theoretical result. To produce exactly 10 grams of force the monofilament must be inserted 0.604 millimeters.

Interpretation: The results showed that small differences in insertion depth and monofilament diameters had a large effect on the force delivered.

Keywords: *Neuropathy, Semmes-Weinstein Monofilament, Contact Mechanics, FEA, Boussinesq Half-Space, Modeling*

2.2 Introduction

Neuropathy is a disease, commonly associated with diabetes, which results in a loss of sensation on the plantar surfaces of the hands and feet. Symptoms often include tingling, burning, numbness, and false sensations akin to having something in contact with the skin. In a research survey conducted by Brouwer et al. they found that the most frequent symptom of neuropathy was burning feet [6]. Severe cases of neuropathy can result in an individual stepping on an object and unknowingly puncturing their foot. Peripheral neuropathy puts individuals at an increased risk of ulceration [11, 12]. Nather et al. reported that neuropathy can result in infection, amputation, and even death [12].

The gold standard for assessing the degree of neuropathy is with a Semmes-Weinstein monofilament test. This method involves inserting a monofilament, similar to that of fishing line, noninvasively into human skin. There are many different gauges of these monofilament evaluators which produce different amounts of force when they buckle. However, the actual force produced by these monofilaments are highly sensitive to many different parameters. For example, Chikai and Ino compared a manual monofilament assessment with an automated process looking at how insertion speed and angle affected measurements [18]. They found that after 10 applications of the monofilament the buckling force decayed by 10% of its initial value, which validated much of their background research [18]. They also found that the velocity and the insertion angle also affected the value of the buckling force in both automated and manual applications of the monofilament [18]. Haloua, Sierevelt, and Theuvenet found that these monofilaments are

dependent on the temperature and the humidity in which they are stored, resulting in different buckling forces than advertised [14]. Furthermore, an extensive literature review by Dros et al. found that there is a lack of standard testing methodology [11]. This, with the lack of accuracy of this test, raises questions about its justification [11].

This modeling study examined how changes in the depth of insertion and the diameter of the monofilament affects the amount of force and stress produced on the skin. Accordingly, this study was designed to ensure that the monofilament was inserted normal to the skin, i.e. normal to the plantar surface of the foot. This orientation of insertion is easily achieved with both theoretical equations and finite element analysis (FEA).

One of the most common monofilaments used produces an equivalent force of 10 grams when used on the plantar surface of the foot to the point of buckling. The monofilament is advertised to produce this force at the instant that it buckles but can actually exceed its rated value if it is continued to be inserted. The subsequent inability of the clinician to apply a consistent normal force presents challenges for assessment of future treatments to combat this disease. Therefore, it is important to develop an understanding of how insertion depth affects the evaluation process and why special consideration needs to be taken when performing this test on patients.

In order to demonstrate the influence that the insertion depth had on the contact force and normal stress, theoretical contact mechanics were used to show the dependence on the insertion depth for monofilaments of various diameters. Furthermore, FEA was conducted via SolidWorks© Simulation for the 10-gram rated monofilament, which is one of the most common used for neuropathy assessment. The FEA simulations were used to calculate the contact force and to measure the normal stress. FEA simulations are a powerful tool that lets users model the effects of bodies under load, or in this experiment bodies in contact with one another. It can also be used as

an iterative process in order to test different combinations of fixtures, loads, and settings to compare results between simulations. However, caution should be taken when utilizing the FEA process to ensure results are validated and accurate. For this reason, the FEA results of this study were verified against theoretical results and were also subjected to a sensitivity analysis [21].

It was hypothesized that the depth of insertion and the diameter of the monofilament both affect the amount of force and stress produced on the skin as a result of contact. Moreover, it was hypothesized that as the insertion depth increases the contact force and normal stress increases. Furthermore, it is hypothesized that as the diameter of the monofilament becomes larger the contact force will proportionally increase, but the normal stress will decrease.

2.3 Methods

2.3.1 Theoretical Equations

In this study theoretical contact mechanics equations were chosen that would best demonstrate the effect of insertion depth on the force and stress produced on the skin for monofilaments of different diameters. This problem was modeled as a Boussinesq problem, where there is a rigid indenter being inserted into an elastic half space. In this study, the nylon was considered rigid when compared to human skin. Sneddon took Boussinesq equations and applied Hankel transforms to derive relevant equations for a cylindrical indenter applied normal to the surface [22]. Sneddon looked at the relationships between depth of penetration and force, in addition to stress profiles as a result of the contact. The first equation derived by Sneddon (Eq. 1) shows the relationship between load (P) and the depth of penetration (D). Here a is the radius of the circular face and η is the Poisson's ratio of the half space. The other variable, μ, is the modulus of rigidity, also known as the shear modulus, and is defined in Eq. 2. Additionally, E is the modulus of elasticity.

Combining Eq. 1 and 2 leads to a complete expression, Eq. 3, for the load (P) in terms of E, a, D, and η. This theoretical equation was used to compare to the FEA results when the monofilament is inserted normal to the skin. The FEA experiments were validated with theoretical results to ensure that the simulation performed as expected [21].

$$P = \frac{4\mu a D}{1-\eta} \quad \text{Eq. 1}$$

$$\mu = \frac{E}{2(1+\eta)} \quad \text{Eq. 2}$$

$$P = \frac{2EaD}{(1+\eta)(1-\eta)} \quad \text{Eq. 3}$$

Sneddon also derived an expression for the normal stress profile caused by the indenter, where ρ is the incremental radial distance from the center of the indenter up to the edge of the indenter (Eq. 4). However, in this study it was necessary to set ρ equal to zero to calculate the normal stress at the center of contact, because at the edge of the indenter the stress becomes theoretically infinite [23]. This produces a singularity and, theoretically, it cannot be measured. However, in reality infinite stress will not occur due to the rounded edges of the indenter and non-linear properties, such as plasticity. This equation was rewritten to a more readily applied form in Eq. 5. This equation was used to compare the normal stress found at the center of the indenter when in contact with the human skin sample.

$$\sigma_{zz} = \frac{2\mu D}{\pi(1-\eta)\sqrt{a^2-\rho^2}} \quad \text{Eq. 4}$$

$$\sigma_{zz} = \frac{ED}{\pi(1+\eta)(1-\eta)a} \quad \text{Eq. 5}$$

2.3.2 Finite Element Analysis Setup

SolidWorks© Simulation was utilized for this modeling experiment between the monofilament evaluator and a human skin sample. The monofilament was modeled as a thin cylinder with an overall length of 40.0 mm and a diameter of 0.500 mm, equivalent to a standard 10-gram evaluator. The actual monofilament is made of nylon, so in the simulation nylon 6/10 was used. The chosen nylon has a Young's Modulus of 8.30 GPa, a Poisson's ratio of 0.28, a density of 1400 kg-m^3, and a yield strength of 139 MPa, as reported in the SolidWorks material database. The impacted specimen was a rectangular block with human skin material properties as follows: Young's Modulus of 250 kPa [24], Poisson's ratio of 0.48 [24], and density of 1116 kg-m^3 [24]. The overall dimensions of the specimen were 2.00 mm width, 2.00 mm height, and 1.50 mm depth. This size was chosen in order to reduce the complexity and computation time of the simulation. Both components were inserted into a SolidWorks© assembly in which the end of the monofilament was in immediate contact with the sample. Fig. 1 shows the monofilament in contact with a human skin specimen. A static analysis was employed for all trials assuming linear elastic material properties. The simulation was set up with a fixture on the back face of the sample, shown in green arrows, opposite that of the contact with the monofilament. All of the other faces of the specimen where unconstrained and free.

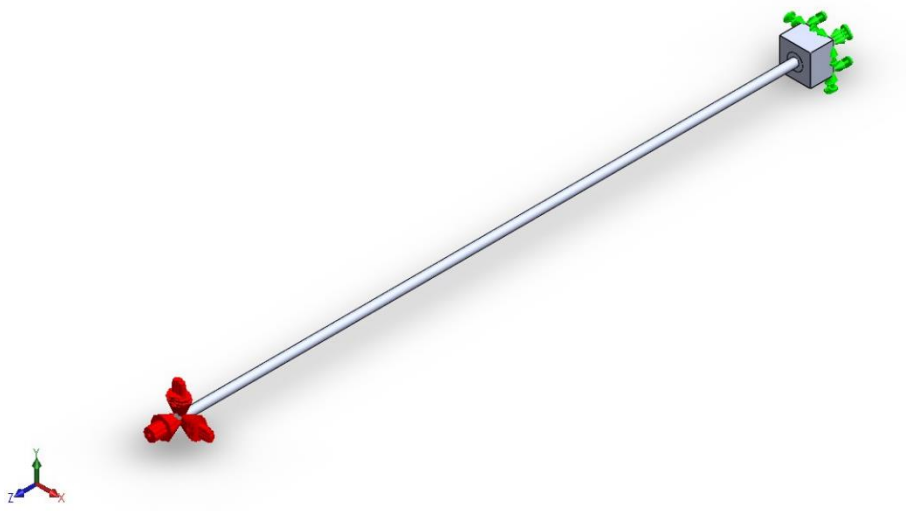

Figure 2-1: Contact Assembly-Nylon Monofilament in Initial Contact with Human Skin Specimen

The monofilament was given a prescribed displacement at the opposite end of the surface-to-surface contact, shown in red arrows. The displacements considered for this study were 0.025, 0.050, 0.075, 0.100, 0.200, 0.300, 0.400, 0.500, 0.600, 0.700, 0.800, 0.900, 1.000, and 1.250 mm. These displacements were defined in the z direction, whereas the x and y directions where set to 0 mm. It was necessary to set the x and y directions to zero in this simulation to properly define how the monofilament is supposed to interact with the specimen. The contacting surfaces between the specimen and the monofilament were given a no penetration condition and a friction coefficient of 0.37 [25]. The no penetration condition allows for the monofilament to deform the specimen and to create an impact crater representative of the insertion. Mesh parameters included a curvature-based mesh with a maximum element size of 0.250 mm and a minimum of 12 elements in a circle. However, mesh control settings were utilized at the end of the monofilament and a circular region, with a 1.00 mm diameter, on the face of the specimen to further refine the mesh. This parameter was set to have an element size of 0.050 mm. Dong et al. used a similar process of having an extremely fine mesh at the area of contact and a coarse mesh farther away [26]. When considering

contact mechanics it is important to have a fine mesh, which does increase the computational time. Nonetheless, mesh controls allow for areas of interest to have a much finer mesh than the surrounding areas, which are not as important. This provided a good balance between a good quality mesh and run time. It should also be noted that an H-adaptive study was employed which served as a way to further refine the mesh at areas of interest, such as the contacting surfaces. The mesh was refined as a result of the stresses that occurred in the model in order to reach the target accuracy threshold [27]. This level of mesh refinement is similar to surface roughness, at a large scale a surface may have very little roughness, but at a smaller scale it may appear to be extremely rough. The associated H-adaptive parameters included setting the target accuracy to 98%, or 2% error, and setting the accuracy bias to global. The target accuracy is a parameter for the strain energy norm [27] and was used as a criteria to justify that the simulation completed. The accuracy bias was set to global to prevent the presence of singularities, which meant that the FEA simulation focused on getting accurate results on a global scale [27]. Additional study parameters included selecting the options for improving the accuracy for no penetration contacting surfaces, setting the incompatible bonding options to more accurate and using the FEEPlus iterative solver, which works well with the H-adaptive solving method.

After simulation, numerous results were reviewed including the contact force, normal stress, and the accuracy achieved in the simulation. Sensors were placed at the center of the human skin specimen, where the monofilament made initial contact. Sensors were configured to measure the values of forces and stresses, which are automatically updated for each simulation. The contact force was calculated by the software and is shown as a set of vectors, whereas the stress is depicted with contour plots. Once a simulation has been setup it was duplicated and modified to reflect different parameters such as the insertion depth. This ensured that all settings remained the same

from one simulation to another. All 14 simulations took a total runtime of 3 hours and 20 minutes. All simulations where performed on a Dell Inspiron 7559 with an upgraded Samsung 860 EVO m.2 solid state drive and 16 gigabytes of RAM. It also utilizes a 2.6 GHz Intel Quad Core i7-6700HQ.

2.4 Results

The first set of results are based off of the theoretical Eq. 3 and 5, where the amount of force and stress are both functions of depth of insertion and the diameter of the monofilament. Furthermore, when using Eq. 3 the units are in Newtons, however, to be consistent with neuropathy studies, which use Semmes-Weinstein monofilaments, the force is expressed in grams-force (gF). This was achieved by dividing Newtons by gravity, 9.81 $m\text{-}s^{-2}$, and then multiplying by one-thousand. The values for normal stress are all expressed in kilopascals (kPa). When using Young's modulus and Poisson's ratio for human skin [24] the following surface plot, Fig. 2, was produced. It shows that as the depth of insertion increased, so did the contact force. The same was seen as the diameter of the monofilament increased. Another surface plot was created to show the normal stress as a function of insertion depth and diameter, Fig. 3. Here, the greatest amount of stress occurred when the amount of insertion increased, but the diameter decreased.

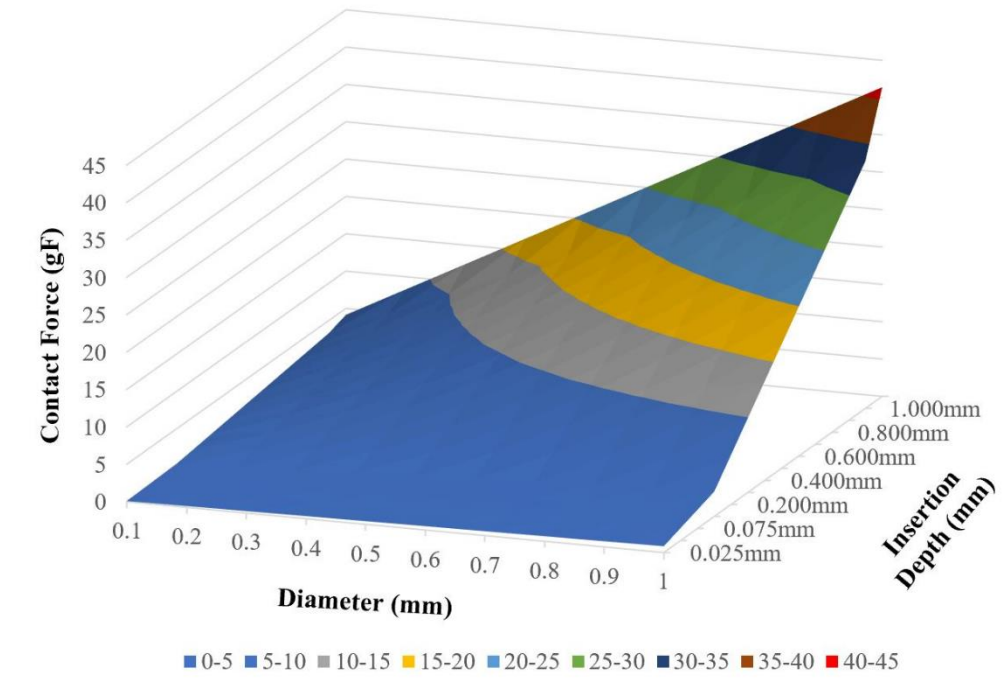

Figure 2-2: Contact Force Surface Plot- Contact Force as a Function of Insertion Depth and Diameter for Human Skin

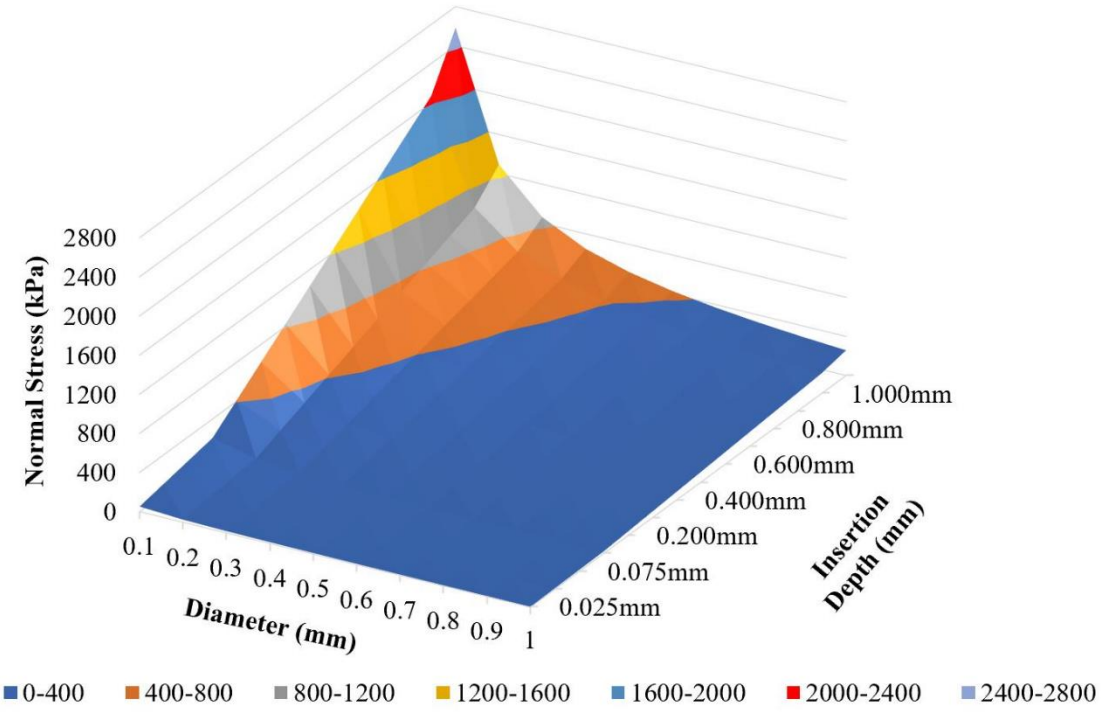

Figure 2-3: Normal Stress Surface Plot- Normal Stress as a Function of Insertion Depth and Diameter for Human Skin

Direct relationships are extrapolated from the surface plots for specific monofilaments. Since the 10-gram monofilament is one of the most popularly used, which has a diameter of 0.5 mm, the following plot was produced to show the relationship between the contact force and normal stress against the depth of insertion. Fig. 4 shows a clear linear relationship for both the contact force and normal stress These theoretical solutions were used to validate the FEA results.

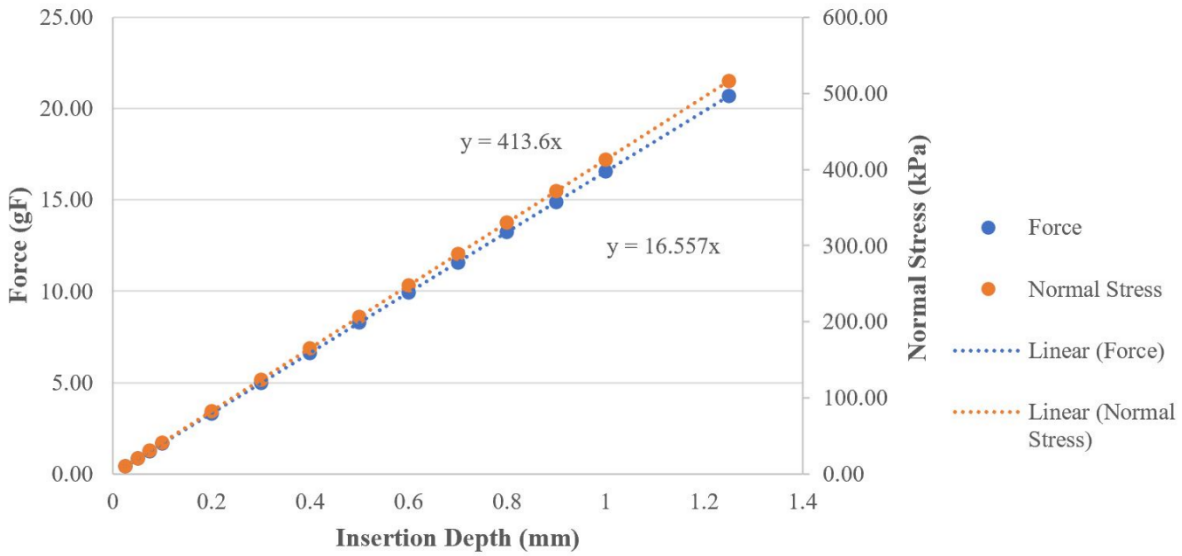

Figure 2-4: 10-gram Monofilament Contact Theoretical Relationships-Theoretical Contact Force and Normal Stress versus Depth of Insertion for a 10-gram Monofilament with a 0.5 mm Diameter

The first FEA results depicted in Table 1, show the contact force and normal stress for a 10-gram monofilament inserted normal to the surface of the sample. Both the theoretical contact force and normal stress are also provided and are used to calculate a percent error against the FEA results. The FEA contact force had an average percent error of 8.9% compared to the theoretical. The normal stress average percent error was 2.4%, but most of the individual percent errors were less than 1% when compared to the theoretical. Only five insertion depths yielded a normal stress

percent error greater than 1%. Also, all simulations in this study achieved the 2% error criteria in five iterations. Each simulation completed at a value of 1.5%.

Table 2-1: FEA Contact Force and Normal Stress for 10-gram Monofilament Applied Normal to the Surface

Depth (mm)	FEA Force (gF)	Theoretical Force (gF)	Error		FEA Normal Stress (kPa)	Theoretical Normal Stress (kPa)	Error		Total Relative Strain Energy Norm Error
0.025	0.45	0.41	8.90%		10.26	10.34	0.78%		1.52%
0.050	0.90	0.83	8.90%		20.52	20.68	0.78%		1.52%
0.075	1.35	1.24	8.91%		30.76	31.02	0.83%		1.52%
0.100	1.80	1.66	8.89%		41.06	41.36	0.72%		1.52%
0.200	3.61	3.31	8.90%		82.08	82.72	0.78%		1.52%
0.300	5.41	4.97	8.89%		118.96	124.08	4.13%		1.52%
0.400	7.21	6.62	8.90%		164.31	165.44	0.69%		1.52%
0.500	9.02	8.28	8.91%		205.28	206.80	0.73%		1.52%
0.600	10.82	9.93	8.91%		246.11	248.16	0.83%		1.52%
0.700	12.62	11.59	8.90%		287.41	289.52	0.73%		1.52%
0.800	14.43	13.25	8.93%		348.36	330.88	5.28%		1.52%
0.900	16.23	14.90	8.92%		366.85	372.24	1.45%		1.52%
1.000	18.03	16.56	8.89%		386.90	413.60	6.46%		1.50%
1.250	22.54	20.70	8.90%		566.56	517.01	9.58%		1.52%

These results are made possible because of the H-adaptive mesh used in the simulations. Fig. 5 highlights the detail of the mesh when the monofilament is applied to the specimen. The H-adaptive mesh refined itself at the areas of contact in order to gain an understanding of how the monofilament affected the specimen. Zooming in reveals smaller mesh elements, which appear unclear in the overall image. Fig. 5 also shows how the contact between the two components and the resulting stress required a finer mesh for analysis. Futhermore each of the 14 simulation studies had its own unique mesh to reflect the different displacments used.

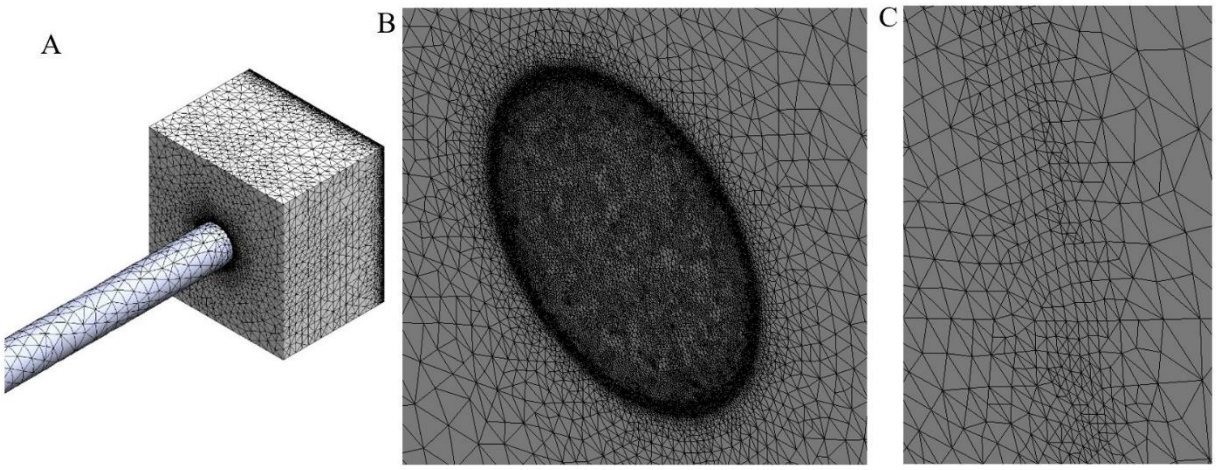

Figure 2-5: FEA H-Adaptive Contact Mesh- Mesh Utilized for 10-gram Monofilament for 0.600 mm Insertion Depth

A) Large Scale View

B) Medium Scale View

C) Small Scale View

SolidWorks© FEA also produced detailed displacement and stress plots of the results for a 10-gram rated monofilament. Fig. 6a and 6b shows the displacement plot created as a result of the contact between the monofilament and specimen when the insertion depth was 0.600 mm. An impact crater formed at the center of contact and extends into the specimen. Likewise, Fig. 6c and 6d depicts the normal stress plot. Fig. 6a and 6c are displayed in an undeformed state, whereas 6b and 6d are in a one-to-one deformed state. The monofilament was hidden for these plots in order to see the crater formed. Examples of these plots were generated for all 14 insertion depths and all showed similar contour plots.

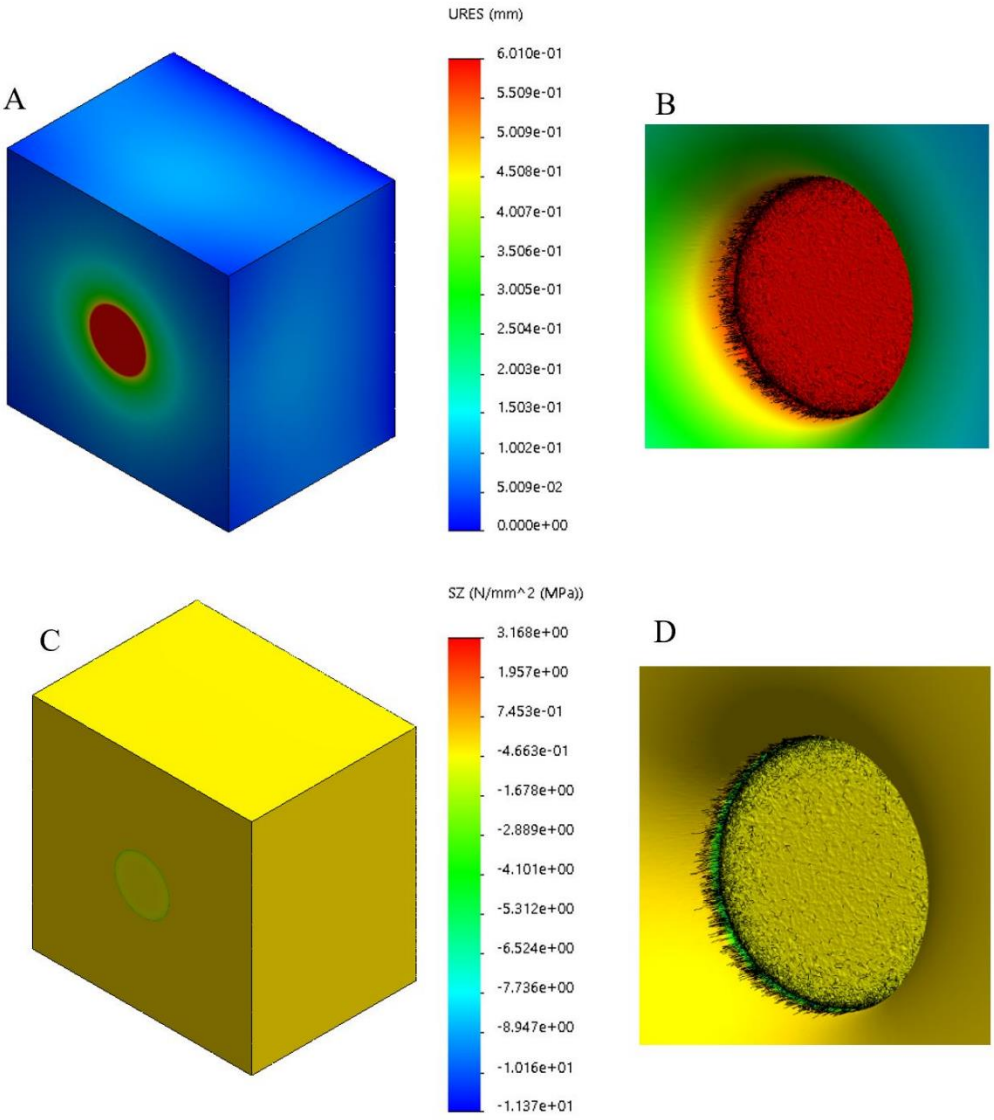

Figure 2-6: FEA Displacement and Stress Plots- Human Skin Specimen Displacement and Normal Stress Plots for 0.600 mm Insertion Depth

A) Displacement Plot

B) Displacement Plot Close-Up

C) Normal Stress Plot

D) Normal Stress Close-Up

2.5 Discussion

The results verified that the initial hypothesis was correct, in which an increase in insertion depth yielded greater amounts of contact force and normal stress. Furthermore, as the diameter became larger the contact force increased, but the normal stress decreased. If the diameter decreased, the area also decreased, which allowed higher stresses to be induced. When using the theoretical equations for the 10-gram monofilament a linear relationship existed between the contact force and normal stress when evaluated against insertion depth. The more an indenter is inserted into a material the greater the force produced. Likewise, if the force increased, the corresponding normal stress increased, since the contact area did not change its physical shape. However, what is most insightful is that in order for the 10-gram monofilament to produce its rated contact force it must be inserted approximately 0.604 mm. If the monofilament is inserted 0.700 mm than the contact force will become 12.00 gF. Increasing the penetration depth only by 0.100 mm will cause this standard monofilament to exceed its rated force. Also, since these monofilaments are supposed to be applied by hand it would be exceedingly difficult to precisely stop applying the monofilament at exactly 0.604 mm. It is also worth noting that the material properties of human skin differ from one person to another, which could influence the insertion depth required to obtain a certain amount of contact force. This would also make it challenging to get the monofilament to achieve the desired force output.

The FEA model performed very well when compared to three different validation checks. It is noteworthy that the contact force had a percent error of 8.9% for all insertion depths. The results showed that the contact force percent error was independent of the insertion depth. All of the normal stresses were typically within 1.0% of the theoretical. The total relative strain energy norm error was 1.52%, which was within the 2.0% allowed for this study. The parameters used for this

simulation study proved to be very effective and correlated well to the results obtained through the theoretical contact mechanics equations. The displacement and stress plots also proved to be insightful since the crater formed as a result of the contact was studied. Some of this error could be improved by setting the accuracy parameter to 99%, however this would require more than five iterations to solve per configuration. Both the contact force and normal stress FEA results were sensitive to the insertion depth. This was verified by the theoretical results and by the percent errors for the contact force and normal stress. Lastly, the root mean squared error was 0.92 and 15.91 for the contact force and normal stress data, respectfully.

The theoretical and experimental FEA results indicate that small differences in insertion depth have large effects on the force delivered via the monofilament. Although some clinicians may be able to accurately and repeatedly use a Semmes-Weinstein monofilament, caution must be used when attempting to recreate the correct force delivered over multiple applications of the monofilament.

Although this study assumed that the nylon monofilament and human skin were linear elastic, further studies should consider using nonlinear or hyperelatstic variants of the material properties. This would require a nonlinear FEA which could take a long time to set up and find adequate settings. Another area of future work could involve nonlinear dynamic buckling analysis using the work of Russell and White in order to model the buckling behavior of the monofilament when it comes in contact with the skin [28]. The research of Szalai may also be useful for nonlinear simulations [29]. Nonlinear mechanical properties of human skin should be considered for future FEA [30].

2.6 Conclusion

This study sought out to understand how insertion depth and the diameter of the monofilament affected neuropathy assessment on human skin. The contact force and normal stress were examined using FEA and validated using theoretical equations. All FEA simulations performed well compared to theoretical contact mechanics, but there is some room for improvement. One such area of improvement would be considering nonlinear material properties of both monofilament and skin to gain better insight into the details of contact. Overall, using SolidWorks© Simulation was an effective way of running all 14 simulations and had many useful features that helped model the studies close to real life conditions.

Finally, the results indicate that it would be extremely difficult to accurately apply a consistent contact force by hand for assessing neuropathy. As such, caution must be taken when using hand applied monofilaments for neuropathy assessment.

Chapter 3: The Neuropathy Device

3.1 Introduction

Results gained from Chapter 2 have indicated that a better method of quantifying an individual's loss of sensation is needed. The current manual method is subjectively based on the clinician. Although some clinicians may be able to accurately apply the monofilament for multiple locations, inter- and intra-clinician variations are always a factor. This makes it challenging to not only determine an individual's threshold sensitivity, but also to monitor the efficacy of potential treatments. A new methodology is required which makes the assessment more accurate and repeatable. The resulting solution to this problem is a machine which automates the hand applied assessment method. This machine standardizes the testing procedure and has the ability to map out the patent's threshold sensitivity.

3.2 Design Objectives

There were many objectives considered when designing the initial neuropathy device prototype. The first criteria were that it had to be easy to assemble and to manufacture. This needed to be a device that with a set of instructions anyone could assembly within a few hours. Additionally, only a few tools should have to be used to put it together, such as a set of hex key allen wrenches, a crescent wrench, screw driver, a level, and a pair of pliers. The device had to be built by no more than two individuals, but preferably one individual. The prototype needed to be modular and adaptable, meaning that's its components should be able to be adjusted and repositioned to various individuals to be assessed using it. This flexibility also allowed the machine to be changed based on future requirements during the design process. This saved money during the development phase since the initial prototype can be altered to reflect new design requirements. The machine had to

be compact and relatively lightweight. This meant that the machine had to weigh less than 75 pounds and was capable of being transported from one exam room to another. Although the device needed to utilize the current nylon monofilament, improvements to the testing methodology would also be valuable. The most important criteria were that the machine must be noninvasive and safe. It is paramount that the device did not cause harm to human subjects and should have adequate safety features to prevent harm. These included not having sharp edges and appropriate electrical safety measures to prevent electrical shock. Using quality stepper motors and power supplies with built in safety precautions was mandatory. The design had to be comfortable for the patient to place their foot on. Human subjects are flat on their back during the test, to replicate the current testing methodology, and the machine had to be adjustable to accommodate this pose and an individual's comfort level. The person's foot needed to be held in place during the test to prevent excessive motion during the test, but the subject must still remain comfortable. The machine had to be easy to disinfect between patients as to not transfer bacteria to the patients. In addition, the device had to accommodate at least 95% of the world's population. There also needed to be a way to reevaluate the same locations on the subject's foot for future clinical assessments. Other criteria that had to be met was that the prototype had to be capable of providing a range of force stimuli to the plantar surface of the foot. At the least it needed to produce three different levels of force, however a range of forces would be preferred. Ideally the machine would be capable of applying forces between 0.2 and 10.0 grams of force (gF) to any location on the foot, preferably using a single monofilament. The targeted accuracy needed to be within ±0.5 gF, while the targeted resolution was desired to be in increments of 0.1 gF. The assessment cannot take a long time to complete in order to prevent the patients from becoming fatigued. This meant that the assessment

time should take roughly 10 to 15 minutes per foot, however the quicker the better. Lastly a future commercial version of the machine must be mass produced at around $1,000.00 at volume.

3.3 Electronics Background

3.3.1 Stepper Motor Background

Various electronic components were sourced to design and build the neuropathy prototypes. Stepper motors and their associated components were some of the most important elements used in this research project. A stepper motor is a motor that rotates in “steps”, rather than continuously [31]. It is built upon the fundamentals of a servo motor, but unlike a servo the stepper motor does not require an error amplifier or a position sensor [31]. Without speed and positioning verification stepper motors are classed as an open loop drive, where servo motors are defined as a closed loop drive [32]. They run off of direct current and are comprised of multiple coils of wire grouped into phases around a rotor [33, 34]. The motor rotates one step at a time when the phases are turned on in a sequential order [33]. Each motor has a built in step angle, which is based off of the position of the coil windings [32]. Stepper motors are ideal components for positioning applications because of their precise steps, especially in CNC machines and 3D printers [33]. Stepper motors also have maximum torque at low speeds, which is ideal for CNC systems [33]. One of the few downsides of stepper motors is that they are not efficient when it comes to energy consumption, which is because of how much electrical current they draw when not moving [33]. This can generate a lot of heat, but cooling fans can be used to keep stepper motors running cool [33]. Although there are methods to reduce the current when the motor is idle it can reduce the holding torque needed to hold the motor in place [31]. If the holding torque is too low or is completely off the load could cause the motor to slip, especially in vertical applications. The faster a stepper motor

rotates the less available torque there is for the motor to use [31]. There are three types of stepper motors which include permanent magnet stepper, variable reluctance stepper, and hybrid synchronous stepper motor [34]. A permanent magnet stepper motor has a magnetic rotor which rotates when the stator windings create an opposite magnetic polarity than the rotor [34]. The variable reluctant stepper motor uses a rotor with teeth which rotates when the stator coils are activated in a certain order [34]. The hybrid synchronous motor has a magnetic rotor with fine teeth, as well as a stator with its own set of teeth [34]. The rotor is also divided into two regions with opposite polarity, which like the other types of stepper motors is rotated when the windings are energized in a specific type of order [34]. There are a variety of ways these coils are energized to induce motion. In single-coil excitation the coils are energized one at a time [34]. In full step drive mode, two coils are always energized, which results in higher amounts of torque from the motor [34]. The half step drive mode operates with one coil activated at one instance, followed by two the next instance, which doubles the resolution of the stepper motor [34]. Nonetheless, the most popular control method is microstepping, where sine waves are used to control the amount of current to the coil windings [34]. Microstepping gives increased resolution to the system but does not necessarily make the device more accurate [35]. In fact, microstepping will reduce the available torque the stepper motor produces during operation [35, 36]. The stepper motor driver connects to the stepper motor and gives the commands necessary to turn the phases on and off [32]. Its primary functions are to control the phase current and energize the phases in a specific sequence to cause the desired motion [32]. The machine controller is used to issue the instructions to the stepper motor driver and is concerned with the position and distance needed to move to the correct location [32]. Typical machine controllers are Arduinos, Raspberry Pi controllers, and

custom controllers specifically used for CNC operation. Some popular CNC software used on machines include GRBL, Linux CNC, and Planet CNC.

3.3.2 Computer Numerical Control and Gcode Background

The computer numerical control (CNC) machine can trace its lineage back to before the 1800s. Early machine tools, like John Wilkinson's boring machine is considered one of the first inventions to automate manufacturing, which was created in 1775 [37]. In 1805, punch cards were used by Joseph Marie Jacquard in textile manufacturing looms, although the first punch cards were invented by Basile Bouchon in 1725 [37]. Later, punch cards were used in self-playing pianos and telegraphy [37]. Herman Hollerith would later invent the electromechanical punched card tabulator in 1889 which would eventually lead to the formation of IBM in 1924 [37]. These punch cards would be responsible for computer storage and numerical control machines [37]. Servomechanisms are also considered a predecessor to CNC and was invented by H. Calendar in 1896 [37]. Servomechanisms are automated devices that use error feedback to monitor performance and make adjustments, typically in position and speed applications involving hydraulic, pneumatics and electrical systems [37]. From servomechanisms came the automatically programmed tool (APT) programming language in 1956 which would eventually incorporate FORTRAN software [37]. APT was created by Douglas T. Ross and was used in some of the first numerical control machines up until the 1970s [37]. Numerical control (NC) machines were the direct predecessor to modern CNC machines and arose from the manufacturing needs of the military [37]. John T. Parsons, considered the father of NC, created and patented the first NC machine with the help of Frank L. Stulen out of a need to improve the manufacturing process of helicopter rotor blades [37]. The U.S. Air Force would later fund Parsons to work on the NC

machine, but ultimately MIT would be awarded the project [37]. These first machines closely resembled current CNC machines used today but with very complex control systems, such as magnetic tapes [37]. In the 1950s G-code, a NC programming language, was created in the MIT Servomechanisms Lab which was used to tell computerized machines how to execute manufacturing instructions [38]. In fact, the first NC machines were all text based to express geometry and toolpaths [38]. Patrick J. Hanratty created Pronto in 1957, a NC programming language for commercial use, which would lead the creation of CAD programs [38]. G-code actually stands for "geometric code" and includes many instructions related to positions, speeds, and feeds [39]. G-code is modal, which means that once a parameter is activated it remains activated until a new instruction is executed [39]. Table 3-2 comprises a list of common G-code functions from Autodesk [39]. An example of a G-code instruction is "G01 X2.5 Y3.75 F15 T01 S2000", where G01indicates a linear motion to the position (2.5, 3.75), with a feed rate of 15 mm/rev and spindle speed of 2000 rpm using tool number one.

Table 3-1: Common G-code Instructions

N	Line Number
G	Motion
X	Horizontal Position
Y	Vertical Position
Z	Depth
F	Feed Rate
S	Spindle Speed
T	Tool Selection
M	Miscellaneous Functions
I and J	Incremental Center of an Arc
R	Radius of an Arc

It was then in the 1960s that minicomputers were developed which reduced the overall size of the computing unit needed to control the automated machine and would lead to the current use of CNC machines [38]. The 1980s made computers cheaper and more available to the public which made CNCs readily available to more people and industries [38]. LinuxCNC was eventually created in 1989 by the National Institute of Standards and Technology and was an open-source software system used to control CNC machines [38]. It is because of microcontrollers and personal computers that CNC machines became more compact, powerful, and cost efficient [40].

3.3.3 Load Cell Background

A load cell is a type of transducer that converts a force or pressure into an electrical signal [41, 42]. There are hydraulic, pneumatic and strain gauge load cells to choose from for different applications [41, 42]. The hydraulic load cell works by sensing a change in pressure via a piston and cylinder assembly, whereas a pneumatic load cell senses a change in air pressure [41]. The strain gauge load cell uses a combination of strain gauges placed on a physical element which can sense an applied load [41]. In a bending bar setup two of the strain gauges measure compression and the other two measure tension [41]. Often the strain gauges are connected in a Wheatstone bridge to measure the small resistance changes caused by the applied load [41]. The Wheatstone bridge was originally created in 1833 by Samuel Hunter Christie, but was made popular in 1843 by Sir Charles Wheatstone [43, 44]. In essence, this bridge circuit is four resistors connected in a series-parallel arrangement with a supply voltage, where an output voltage difference is measured between the two parallel branches [44]. It resembles a diamond and its governing equation for the voltage output, based off of Kirchhoff's laws, is as follows [43, 44]:

$$V_{out} = \left(\frac{R_x}{R_3 + R_x} - \frac{R_2}{R_1 + R_2}\right) * V_{supply}$$

A common Wheatstone bridge is an HX711 amplifier. Furthermore, each strain gauge has a corresponding gauge factor which is the ratio of the change in electrical resistance per the ratio of the strain [41]. When the voltage difference is zero it is said to be balanced and is unbalanced when the difference is nonzero [44]. Lastly the following governing equation shows the ratio between the 4 resistor elements [43]:

$$\frac{R_1}{R_2} = \frac{R_3}{R_x}$$

3.4 Design

The neuropathy device was split up into three iterations over the course of development. The initial prototype was developed within the first few months, whereas Mk1 was developed over the course of a year. Mk1 was assembled and showed promise as an effective tool for neuropathy diagnosis during preliminary pilot testing. Mk2 is considered the final iteration of the design and featured many improvements over Mk1, making it easier to assembly and to operate. All iterations of the neuropathy device were created using SolidWorks© and involved using assemblies and subassemblies.

3.4.1 Initial Prototype

After considering all of the design objectives a few initial ideas were brainstormed. The one selected for development was the use of a computer numerical control (CNC) machine to move a piece of monofilament to any location on an individual's foot. Two coordinate systems were considered: one was a polar coordinate system and the other was a Cartesian coordinate system. The polar coordinate system had the potential of requiring less components to operate but would have resulted in a more complex computer program to operate. A polar coordinate system would also have had difficulties achieving the machine's ability to be used on 95% of the world's population. Ultimately, a Cartesian coordinate system was selected since there are more existing systems which use this type of setup. The design was based off of 3D printers, which operate a gantry system with a combination of belts and pulleys to move the filament extruder head mechanism. Typical 3D printers use a belt and pulley system in two of the principal directions (x and y) and use a lead screw in the third principal direction (z). Figure 3-1 shows the initial prototype used to develop subsequent versions of the neuropathy device. The frame was designed with aluminum T-slot profiles; which provided stability and gave the device its overall shape. An

acrylic cover plate was attached to the front of the device and was where the patient's foot was designed to be placed during the assessment. There is also an area where the patent's ankle rests which included grooves for straps to be used to hold the ankle in place. There are also guides where straps can be used to go over the individual's toes. The cover plate featured a grid of 275 holes with 0.25 in diameter holes spaced 0.50 in apart (Figure 3-2). Each hole corresponded to a location where the machine can test. This resulted in a 5 inch by 12 inch rectangular region, which can accommodate 95% of the world's foot size [45]. The machine was capable of moving the monofilament to any of these holes and inserting the monofilament through the hole until it contacted the patient's foot with the prescribed amount of force. The initial prototype was 16 inches long, 7.25 inches deep, and was 24 inches tall, with a weight of 20.5 pounds without the electrical components. Additionally, the foot plate can be cleaned using disinfectant wipes and spray cleaning agents, such as Opti-Cide® Max disinfectant cleaner, to kill the accumulation of bacteria as a result of patient assessments. The monofilament can also be cleaned with a wipe.

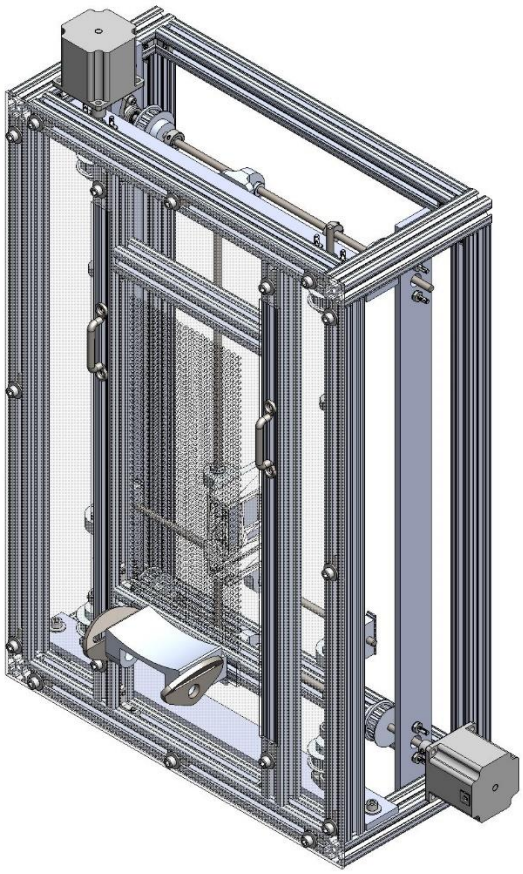

Figure 3-1: Intital Prototype

The gantry system is highlighted in Figure 3-3 and is used to move the monofilament to the corresponding test sites. This subassembly was responsible for the positioning of the monofilament to any location on the foot plate. Pulleys are used to convert the rotational motion of the stepper motors to linear motion of the monofilament. Belts interconnected the pulleys and the carriages, which attached to the monofilament holder device. Journal bearings are used to hold the rods in place during rotation. The gantry system directly connected to the monofilament holder device. The first iteration of the monofilament holder device (Figure 3-4) was designed by Hayden Burch, an Auburn University mechanical engineering undergraduate student. It utilized two stepper motors integrated with leadscrews, one translated the monofilament through the hole and the other

changed the effective length of monofilament, which affected the amount of force applied to the patient's skin. This method of changing the effective length to change the applied force is best understood using Euler's formula for column buckling [46]:

$$P_{cr} = \frac{\pi^2 EI}{{L_e}^2}$$

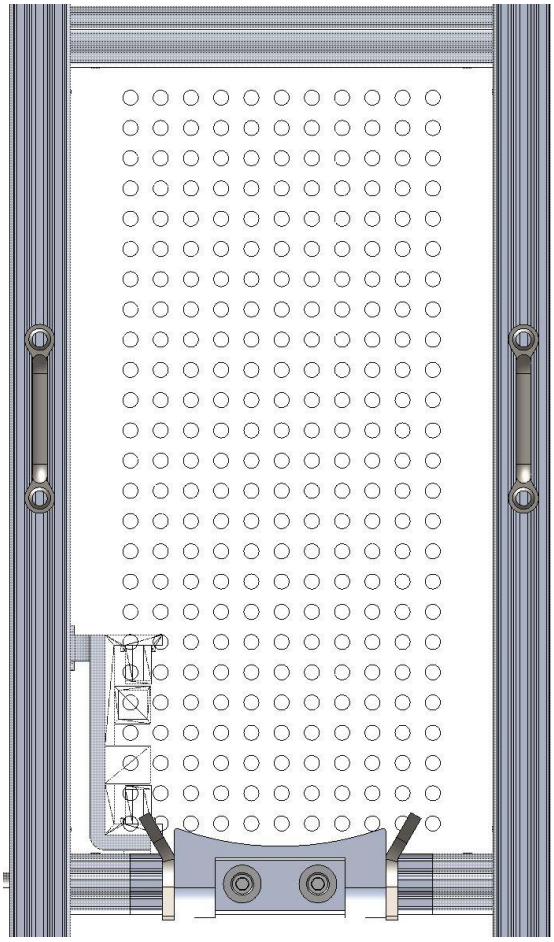

Figure 3-2: Initial Prototype Foot Plate Hole Grid

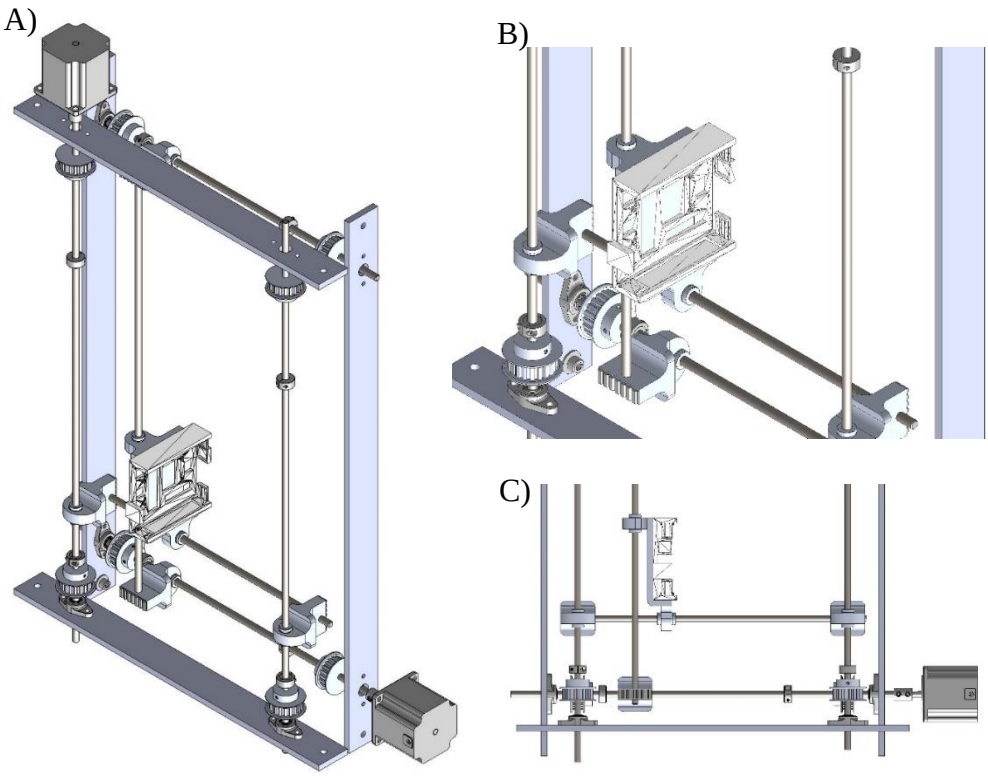

Figure 3-3: Initial Prototype Gantry System

A) Complete Gantry System
B) Gantry System Close-Up on Monofilament Holder
C) Gantry System Front View

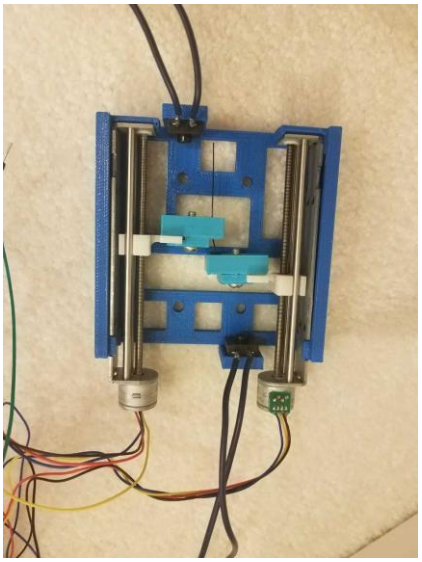

Figure 3-4: Initial Monofilament Holder Device

3.4.2 Mk1 Prototype

The initial prototype was used as the foundation for the Mk1 prototype (Figure 3-5) since it satisfied the majority of the design criteria. The initial prototype was compact, able to accommodate 95% of the world's population, was adaptable, and was modular enough to be upgraded with future improvements. Similar to the initial prototype, Mk1 used aluminum T-slot profiles to form its chassis. It also utilized GT2 timing belts and pulleys, which are very common in 3D printers and robots [47]. Belt tensioners were also installed on all four belts to ensure that the belts were in constant tension during operation. The gantry system used in Mk1 is very similar to the initial prototype but had been optimized to incorporate the entire monofilament holder, as shown in Figure 3-6. Self-locking external retaining rings were also installed in the gantry system to hold the rods securely in the journal bearing during operation. In this version of the gantry system the monofilament holder has been rotated 90 degrees and when not being used cannot be seen through the foot plate. Turn knobs were installed on the ends of the gantry system's rods, which can be used to manually move the monofilament holder when the machine is turned off. Mk1 used the same idea of a hole plate, but in this iteration it was recessed inward making it closer to the monofilament holder device (Figure 3-7). This allowed the monofilament to travel a smaller distance through the hole to make contact with the patient's foot, which saves time. The hole plate in this prototype had a higher resolution of holes than the initial prototype, with 1,029 holes, but still encompassed a 5 inch by 12 inch rectangular region. Each hole was 0.125 inches in diameter, spaced 0.250 inches center-to-center. Similar to the initial prototype, each hole corresponded to a testing location; however, in Mk1 a camera is used to take a picture of the patient's foot through the transparent foot plate. The camera is mounted behind the machine, as depicted in Figure 3-8, and was positioned so that it could capture the entire foot during machine operation. Typically this

camera would be mounted horizontally, but in the machine it is mounted vertically so that it maximizes the picture taken. The monofilament holder is out of view when the picture is taken. This picture can be used to select the testing locations on the foot. At the end of the assessment the results of the test are plotted on the same picture, serving as a threshold sensitivity map. This map can be used to document a person's degree of neuropathy and to monitor efficacy of potential treatments. An acrylic cover plate was also manufactured with engraved numbers used to document the placement of the clamping mechanism. This design's adjustable foot clamp mechanism, based on a Brannock device, provided light compression to the individual's foot. The clamping mechanism also featured a ball of the foot locator, which when combined with the engraved numbers on the cover plate, allows the patient's foot to be relocated to the same position from a previous assessment. The patient's toes are kept down during the assessment with a toe strap. Both the foot clamp and toe strap accommodated different foot sizes. The individual's ankle is to be placed in a curved holder which also featured a strap to prevent excessive motion during the assessment. The clamping mechanism (Figure 3-9) featured padded surfaces to make the patient comfortable during the assessment, which can all be cleaned with disinfectants. There are also stepper motor covers to prevent anyone from touching the stepper motors while the machine is on. Fans cool the stepper motors during operation to prevent excessive heat generation during operation. Mk1 was 18.5 inches wide, 24 inches tall, and 8 inches deep (19.75 inches deep with the inclusion of the camera mount and the clamping mechanism) and is roughly 45 pounds. The motor covers and manual knobs add another 5 inches to the height and width. The majority of components were 3D printed to reduce cost and can be subsequently injection molded for a future commercial version of the machine.

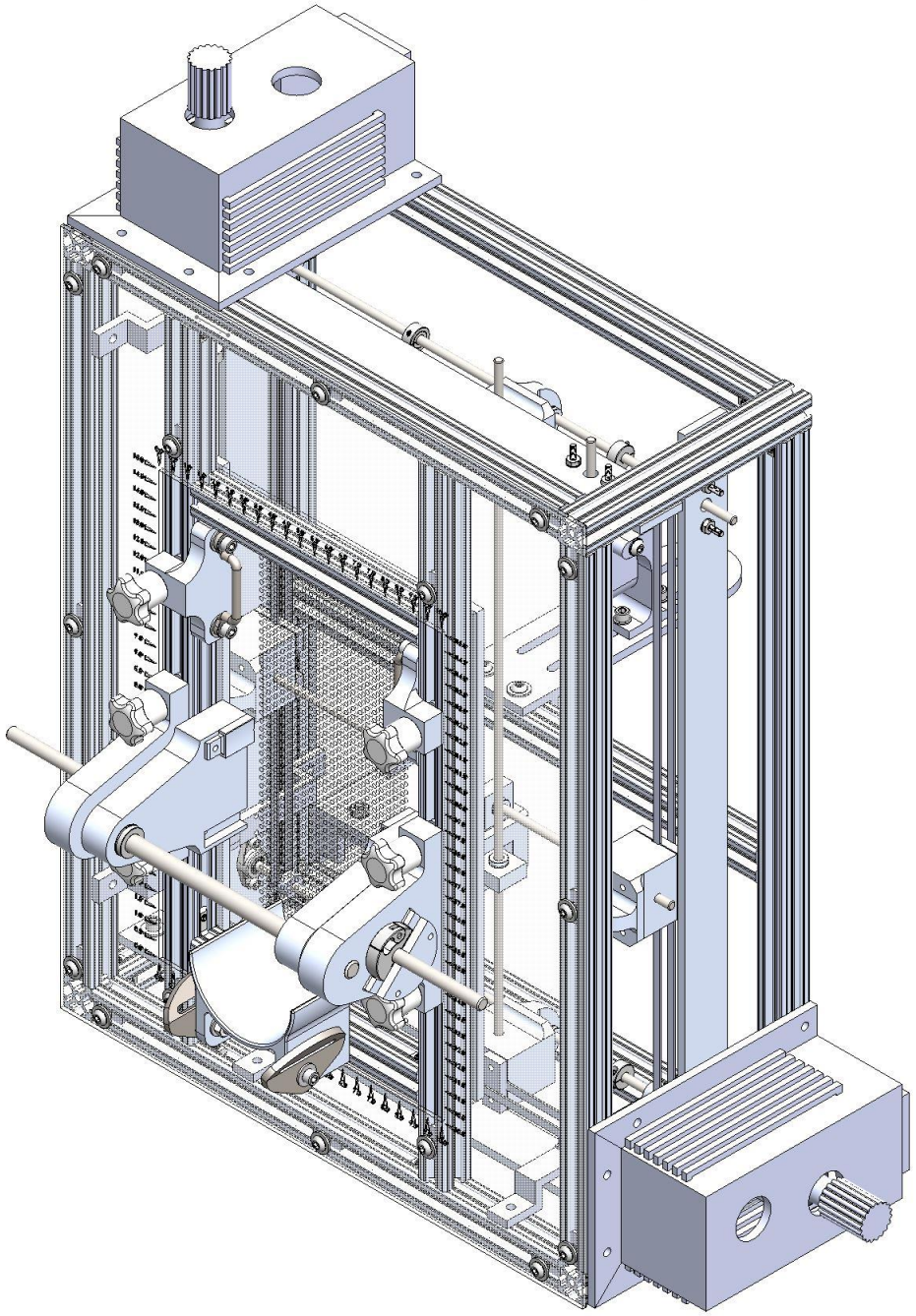

Figure 3-5: Mk1 Prototype

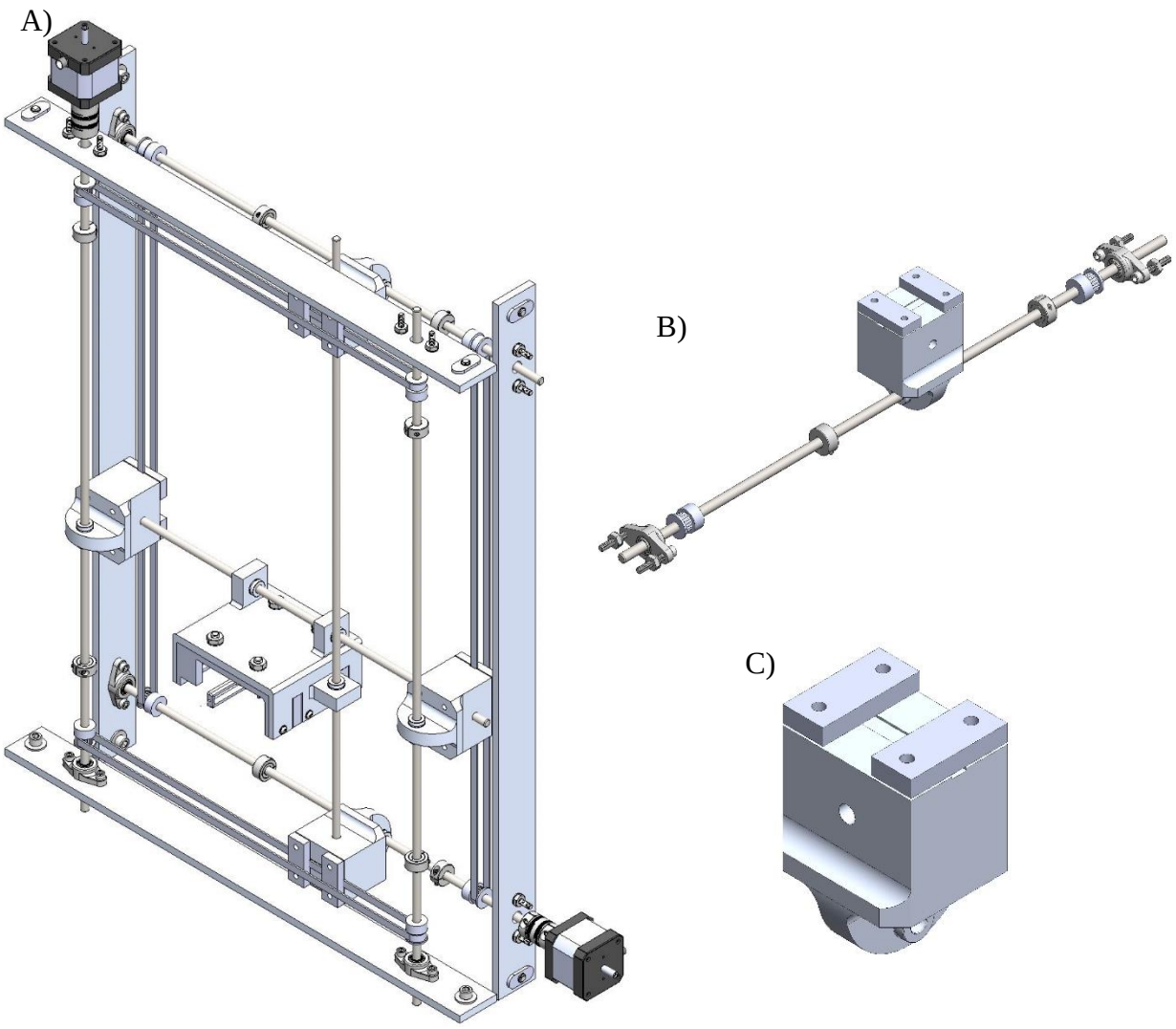

Figure 3-6: Mk1 Gantry System

A) Gantry Combined Assembly
B) Linear Motion Subassembly
C) Carriage

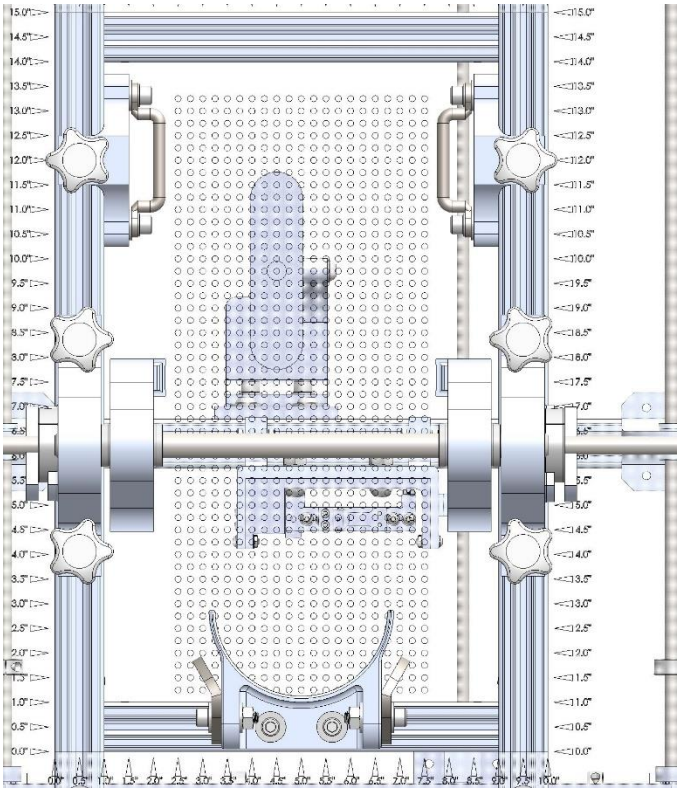

Figure 3-7: Mk1 Foot Plate

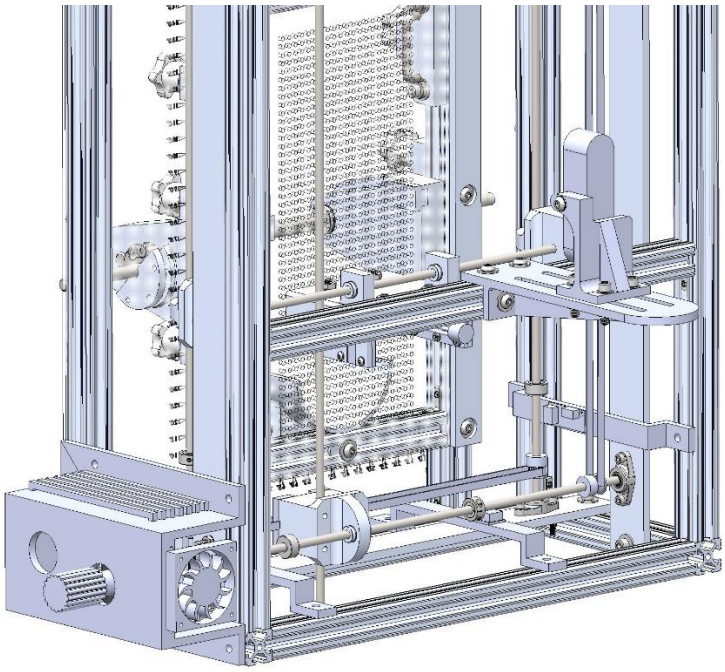

Figure 3-8: Camera Subassembly View

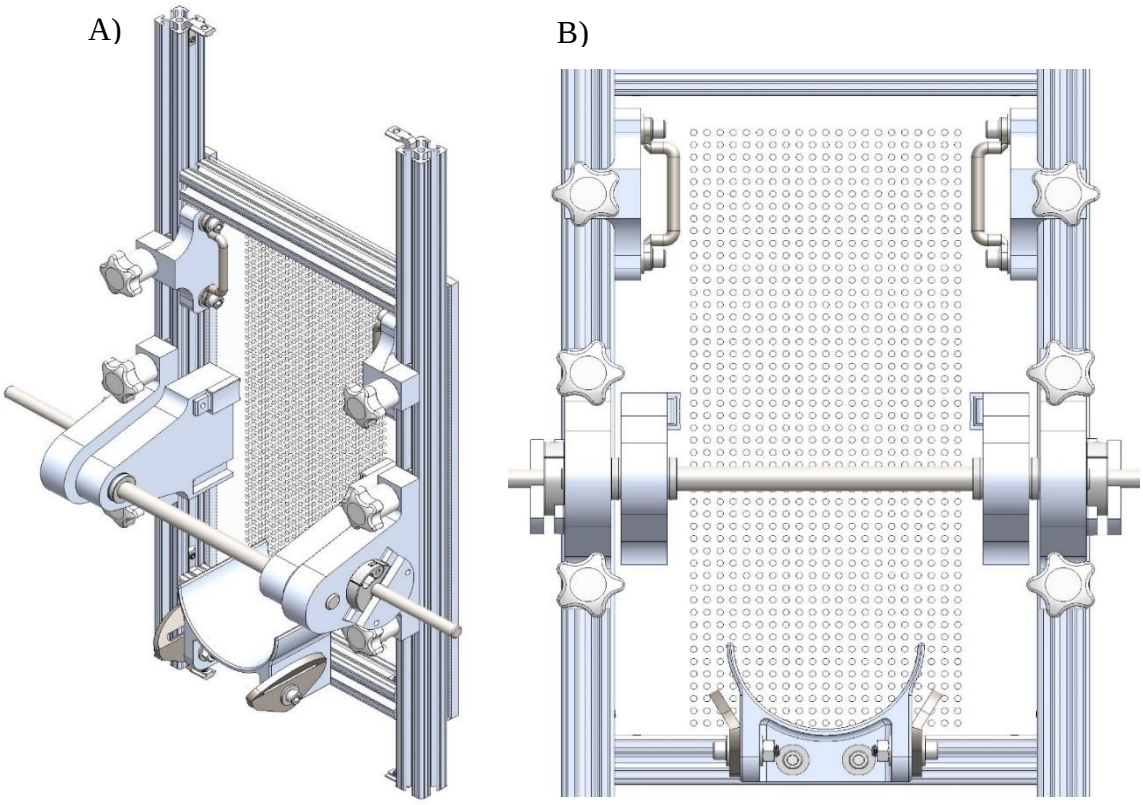

Figure 3-9: Foot Clamp Mechanism

A) Isometric View
B) Front View

Three monofilament holders were considered for the Mk1 prototype. Figure 3-10 showcases an iteration based on the one created by Hayden Burch, which operated on the principle of Euler's column buckling equation. Another version of this monofilament holder (Figure 3-11) was created, which included miniature ball bearing carriages and guide rails. The addition of these miniature components made the monofilament travel more smoothly and ensured the monofilament made it through the hole of the foot plate. Instead of having only one point of contact at the leadscrew, the use of the miniature components created a second contact point, which made a significant improvement.

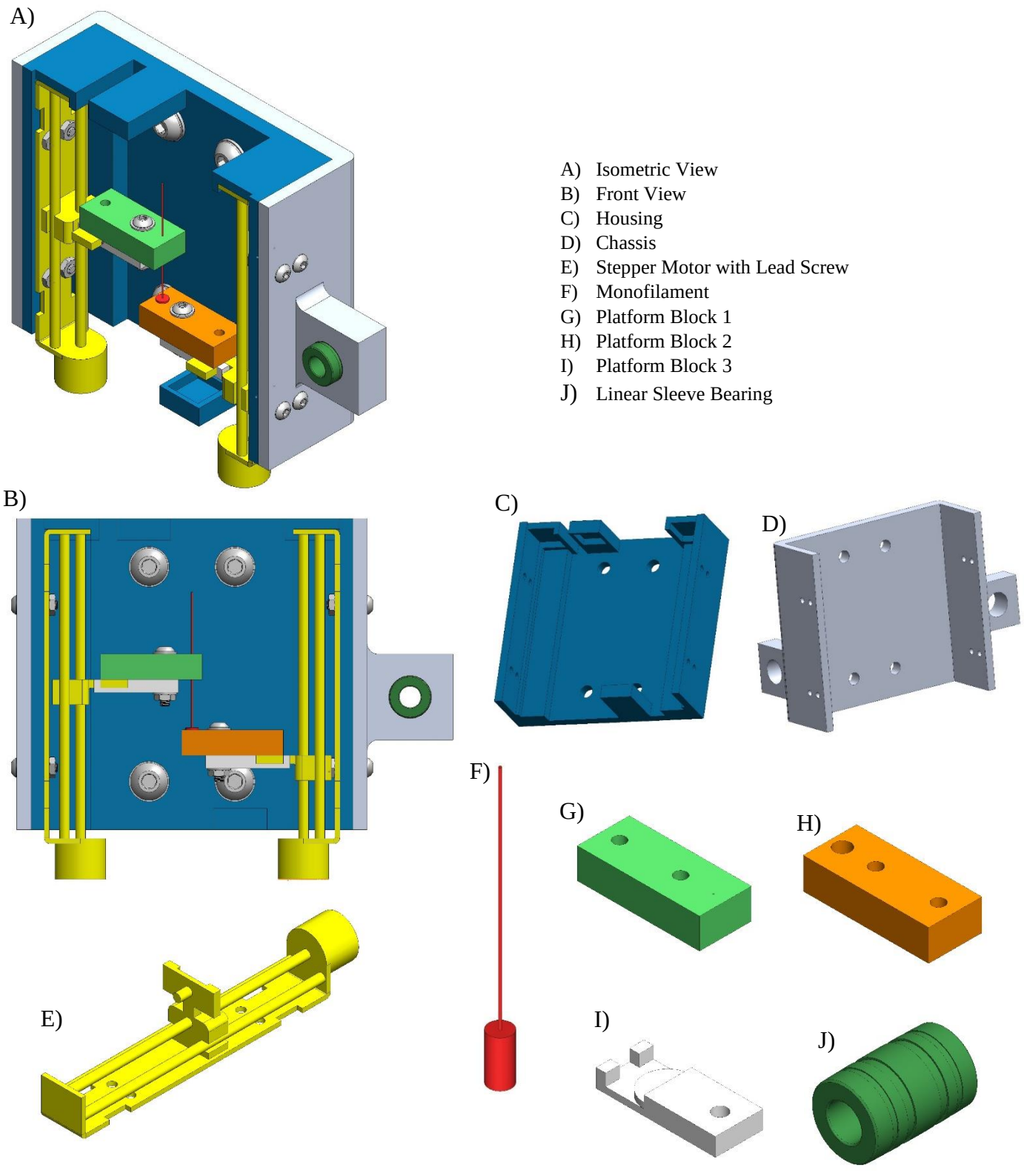

Figure 3-10: Mk1 Original Monofilament Holder

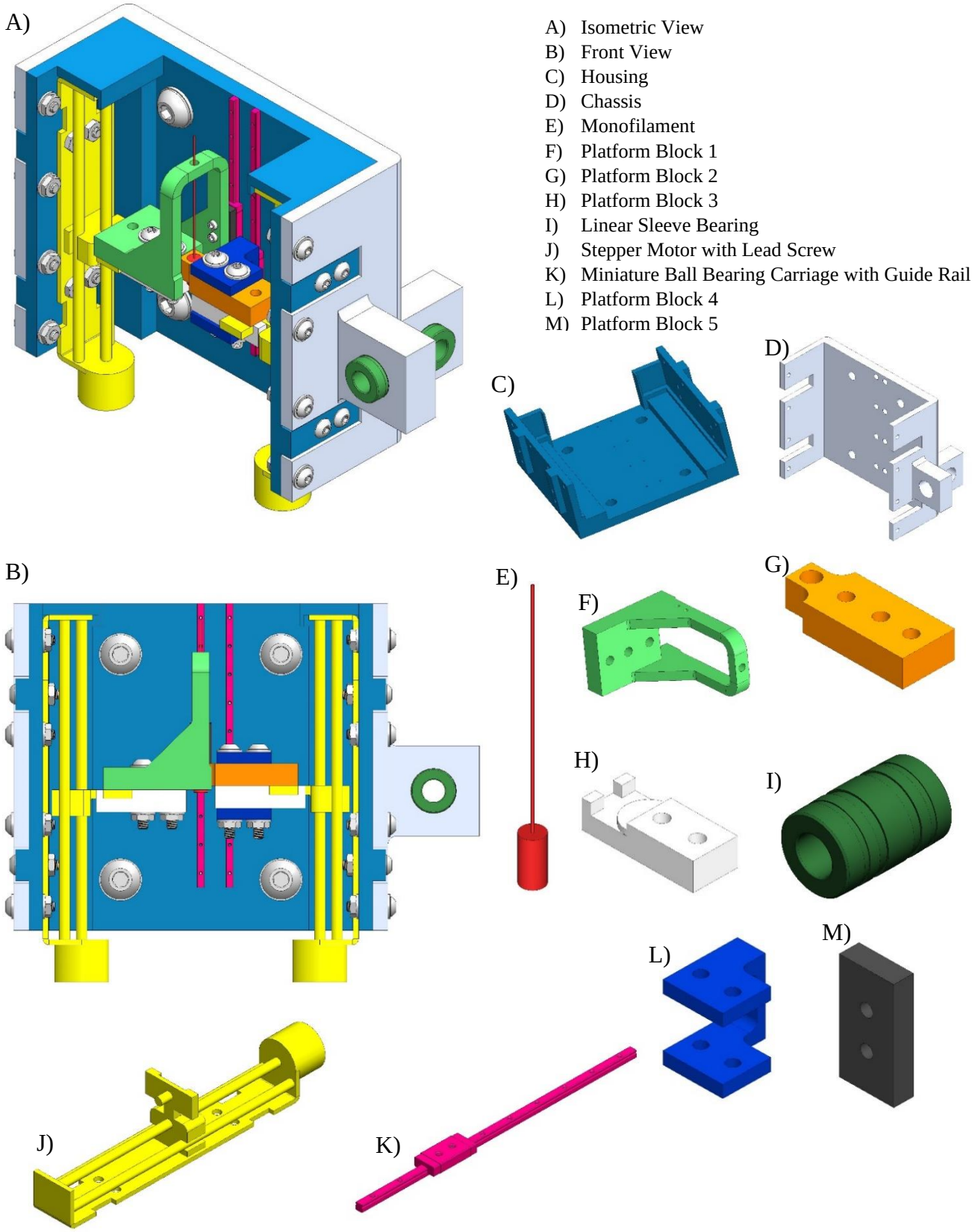

Figure 3-11: Mk1 Updated Monofilament Holder

Although controlling the effective length of the monofilament to alter the produced force was initially considered, a fundamentally new design was utilized because there are few commercially available monofilaments long enough to provide the range of pressures required for this machine. The most readily available monofilament for neuropathy assessment produces a contact force of 10 grams of force. Although it can produce forces larger than 10 grams by changing its effective length, in accordance to Euler's equation, it cannot theoretically produce forces less than 10 grams at buckling since it cannot increase its effective length. Alternatively, the machine could have been designed to use multiple monofilaments in order to apply a range of forces, but this was deemed ineffective. However, the underlying issue with using the method of changing the effective length is that it is still inaccurate and subjected to the current shortcomings associated with monofilament assessment. The monofilaments produce their rated force when they buckle, but if they are inserted too far they will exceed their rated capacity. There are other factors that affect the accuracy of these monofilaments, such as the angle of insertion, impact speed, humidity, temperature, and fatigue. Attaching the monofilament to a stepper motor and driving it forward an arbitrary amount to produce a force is very similar to the hand applied method, but both are displacement-based control methods. Also, this required a load cell to calibrate the effective length for each amount of force produced and would have to likely occur somewhere within the machine. Instead of this displacement-based method to control the monofilament a different approach was used to apply the monofilament. The monofilament is directly attached to a load cell which is connected to a platform driven by a stepper motor, as seen in Figure 3-12. In this design only one stepper motor is utilized. The monofilament is also inserted inside of a holder, which is used to keep the monofilament straight. This platform was also connected to a miniature ball bearing carriage and guide rail. The load cell is cantilevered off of this platform. Furthermore, the load cell and the

stepper motor are in linked together in a feedback loop, where the load cell constantly measures the amount of contact force the monofilament is applying to the person's foot. The stepper motor keeps moving the monofilament forward until it reaches the targeted contact force. As it gets closer to its targeted force it slows down the insertion speed until it reaches the prescribed force. The following lines of code from the Arduino Uno Function show the process of how the feedback loop samples the load cell and then reduces it speed until it reaches its target force.

```
if (scale.is_ready() && foo == 0){
  measuredload = scale.get_units_direct();
  if (measuredload < .25*inputload) {
    stop_motor = false;
    stepper.setSpeed(-20); }
  else if (measuredload < .5*inputload) {
    stop_motor = false;
    stepper.setSpeed(-15); }
  else if (measuredload < .75*inputload) {
    stop_motor = false;
    stepper.setSpeed(-10); }
  else if (measuredload < .9*inputload) {
    stop_motor = false;
    stepper.setSpeed(-7); }
  else if (measuredload < 1*inputload) {
    stop_motor = false;
    stepper.setSpeed(-5); }
  else {
    stop_motor = true;
    foo=1; }
}
```

This force based-control method is best used for loads above 2.0 grams of force, but can be used as low as 0.2 grams of force. This method's accuracy is more based on the skin surface, i.e. how thick and or coarse the skin is. This method proved to be very effective in pilot testing and will be utilized during future clinical trials. An added benefit is that the monofilament holder can be removed from the machine without having to disassemble it completely.

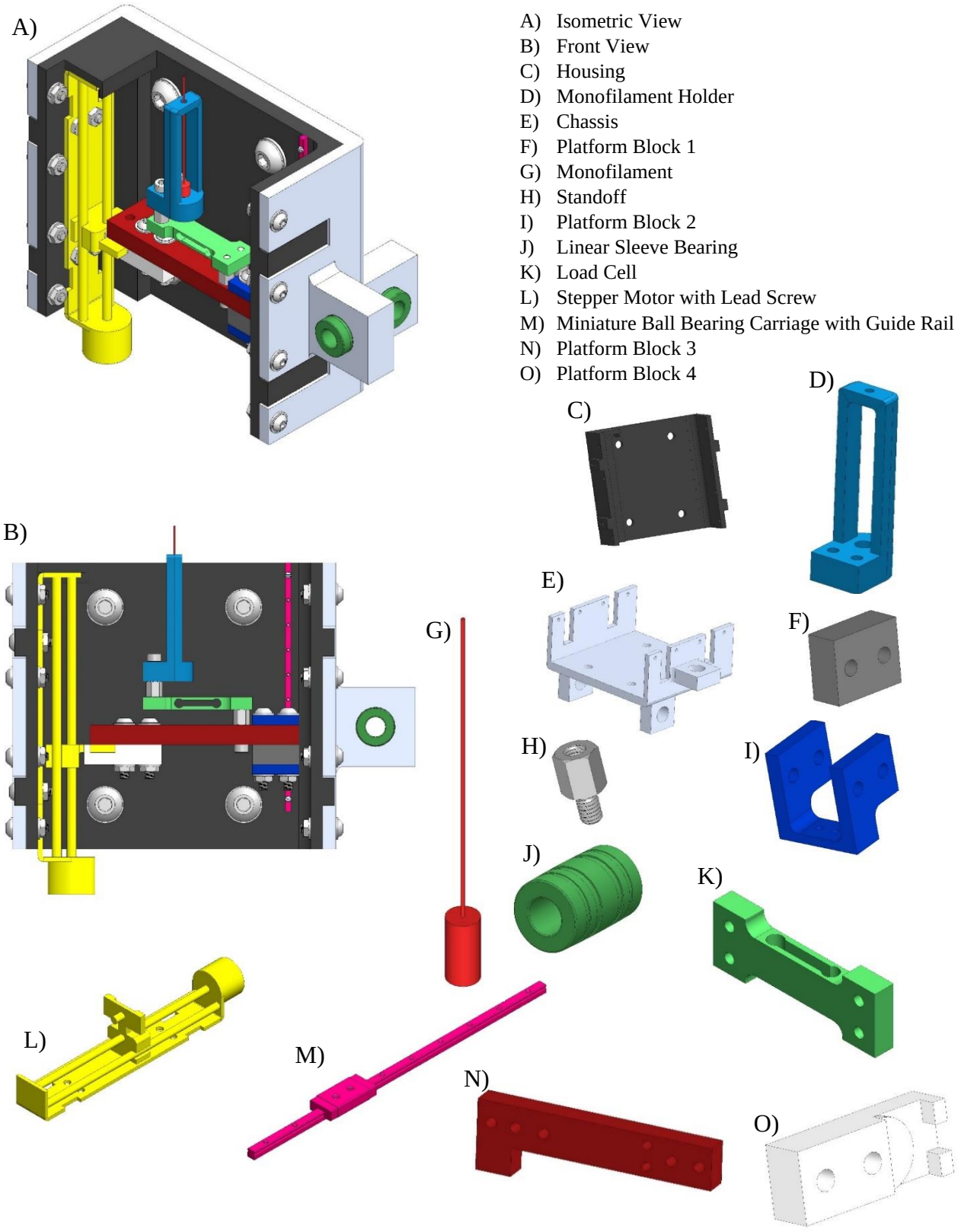

A) Isometric View
B) Front View
C) Housing
D) Monofilament Holder
E) Chassis
F) Platform Block 1
G) Monofilament
H) Standoff
I) Platform Block 2
J) Linear Sleeve Bearing
K) Load Cell
L) Stepper Motor with Lead Screw
M) Miniature Ball Bearing Carriage with Guide Rail
N) Platform Block 3
O) Platform Block 4

Figure 3-12: Mk1 Monofilament Holder with Load Cell

All electronics used to move the monofilament are on the other side of the foot plate, away from the patient. In the design, none of the electronics come in direct contact with the patient. The only components that touch the patient are the padded surfaces for the foot clamp mechanism, the foot plate, and the monofilament. The electronics include three stepper motors, three stepper motor drivers, limit switches, a load cell, a HX711 amplifier, an Arduino uno, an Arduino mega, a webcam, a power supply, and a buck converter. Figure 3-13 showcases the most prominent electrical components sourced for this device. A computer was also required to interface with the machine. Two of the stepper motors are SureStep STP-MTR-17040D. These stepper motors are bipolar NEMA 17, have a 3.81 lb-in of torque, are 1.7 amp per phase, and have 200 steps per revolution [48]. The STP-MTR-17040D were each connected to a STP-DRV-6575 stepper motor drivers, which are fully compatible with these motors and were microstepped between 200-20000 steps per revolution [48]. The stepper motor drivers were connected to a STP-PWR-4805 power supply, which outputs 48 volts DC to the stepper motor drivers [48]. The other stepper motor was a Walfront D8-MOTOR80, which featured a lead screw attached to the motor. It has 20 steps per revolution with a 0.800 amps per phase rating and was compatible with voltages between 9 to 12 volts [49]. The Walfront stepper motor was attached to a TB6600 stepper motor drive and was then connected to the buck converter. The buck converter was connected to the STP-PWR-4805 and converted the 48 volts DC down to 9 volts DV, to work with the Walfront stepper motor. Limit switches were installed inside of the machine and serve two purposes. The first is that they are used during the homing sequence, which calibrates the machine so that it can accurately move the monofilament from one location to another. The second purpose is for safety. If during operation of the device a limit switch is triggered it will stop the machine. This would occur if the stepper motors tried to move the monofilament outside of its defined range of motion. Physical hard stops

were also installed to act as a secondary means to stop the machine if it gets off track during use. Lastly the load cell used was an RB-Phi-203 100g Micro Load Cell. This load cell had a weight capacity of 100 grams, with a repeatability error of ±50 milligrams. It has a rated output of 600 μV/V and a 1 kΩ impedance [50]. Ultimately, Mk1 was built and a provisional patent application was filed showcasing its design and functionality. The machine was attached to a workbench (Figure 3-14), which had an adjustable height feature. This allowed the machine to accommodate a variety of examination tables and ensured that the subject's leg remains parallel to the exam table and is not elevated. Furthermore, the electronics are organized on a wooden board which was also attached to the workbench, as seen in Figure 3-15. The laptop used to interface with the machine was also placed on the workbench. This laptop runs through all of the relevant functions to control the machine and then interprets the results at the end of the assessment. The final cost to produce Mk1 was roughly $2,300.00 excluding the laptop.

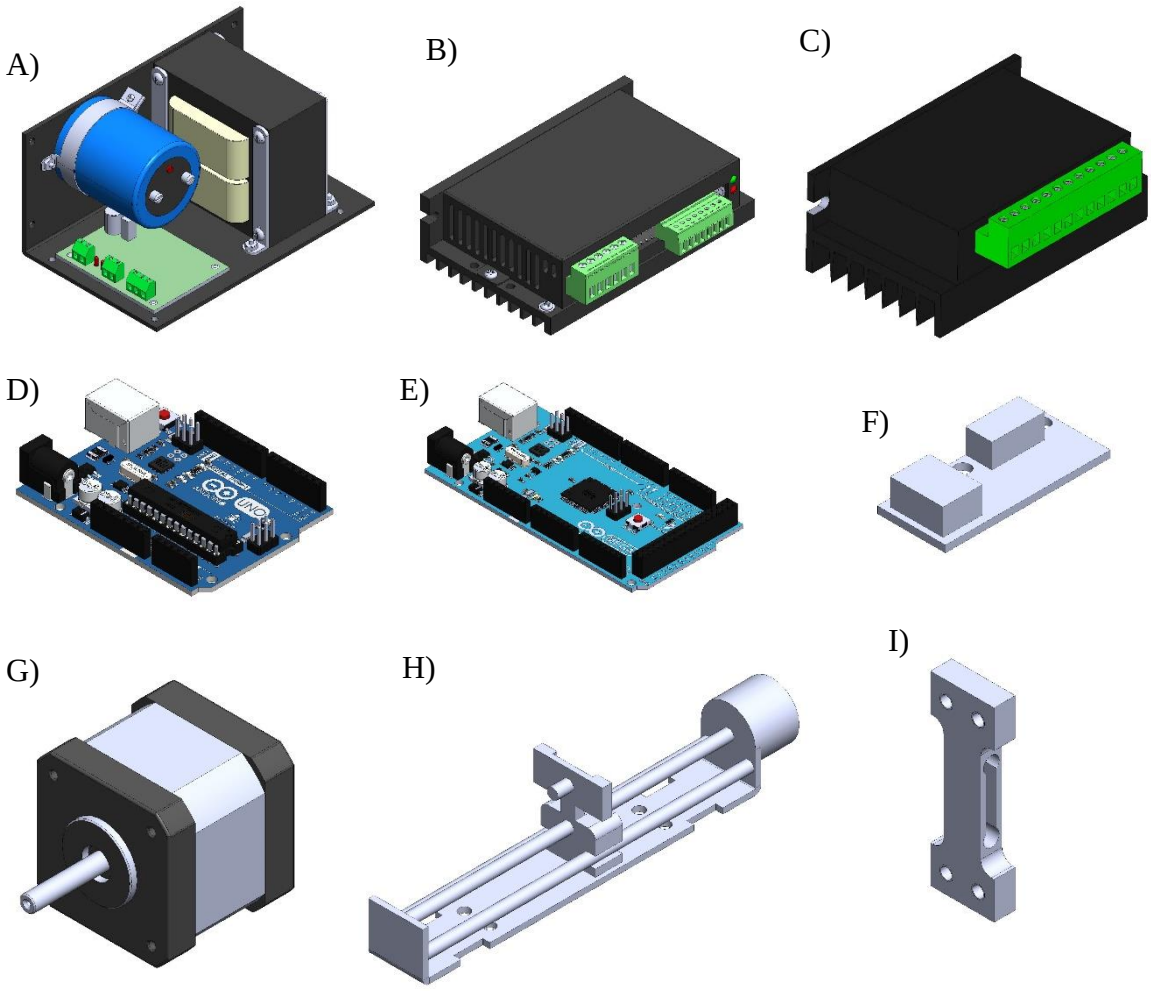

Figure 3-13: Mk1 Electronics

A) STP-PWR-4805 Power Supply
B) STP-DRV-6575 Stepper Motor Drive
C) TB6600 Stepper Motor Drive
D) Arduino Mega
E) Arduino Uno
F) Limit Switch
G) STP-MTR-17040D Stepper Motor
H) Walfront D8-MOTOR80 Stepper Motor
I) RB-Phi-203 100g Micro Load Cell

A) 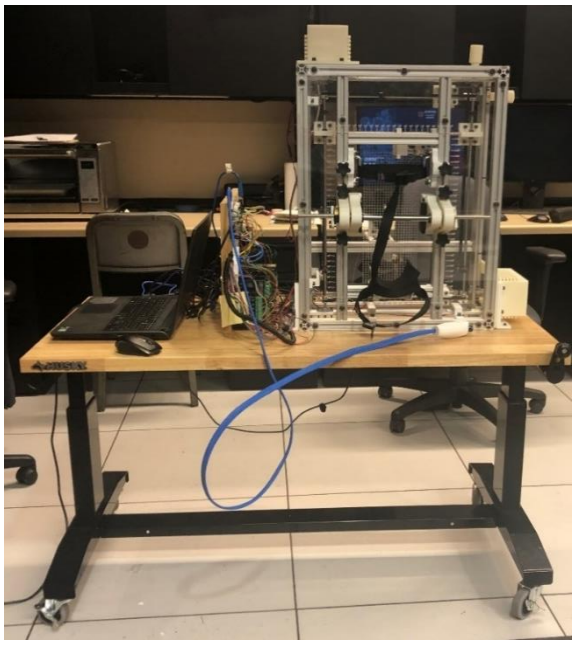 B) 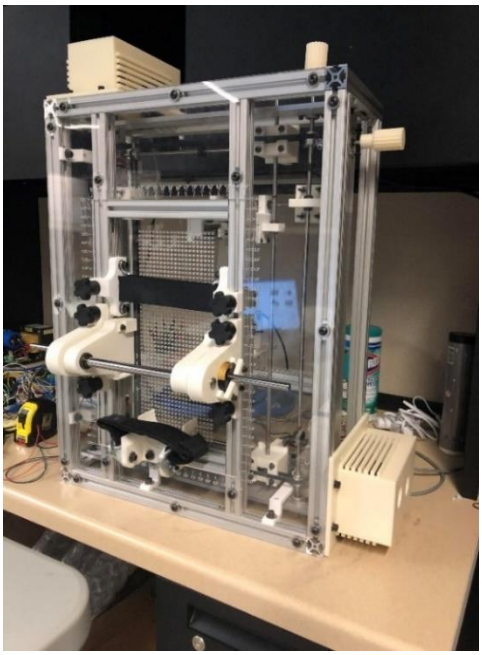

Figure 3-14: Assembled Mk1 Prototype

A) Mk1 Neuropathy Device on Adjustable Workbench
B) Mk1 Final Assembly

A) 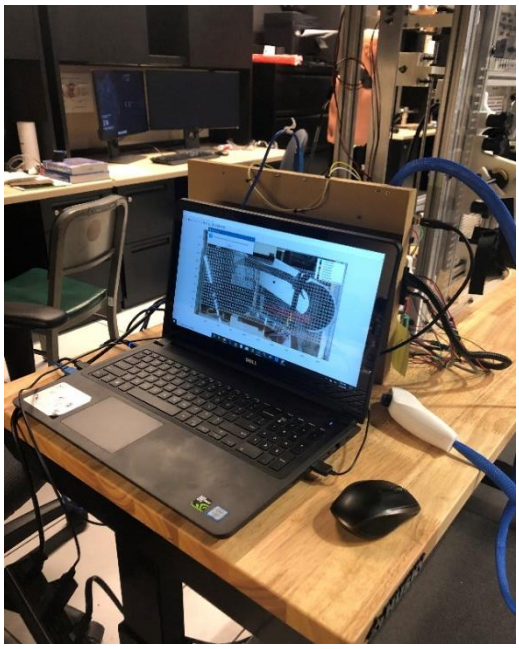 B) 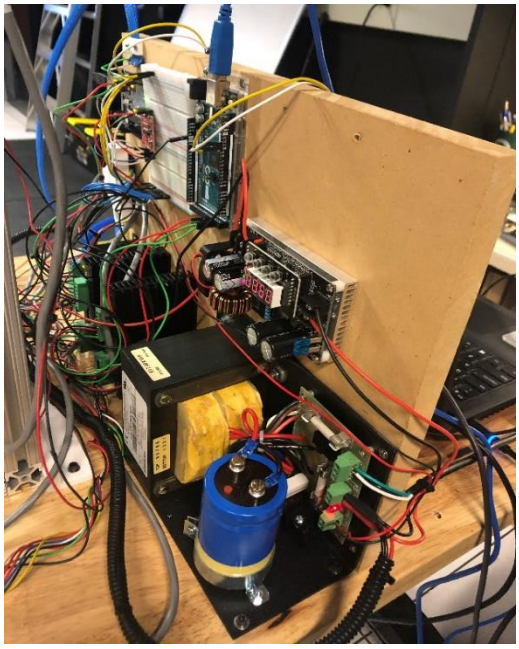

Figure 3-15: Electronics and Laptop

A) Laptop Interface with the Diagnostic Tool
B) Electronics Storage

3.4.3 Mk2 Prototype

Mk2 was the final iteration of the neuropathy device, depicted in Figure 3-16. It built upon the improvements of Mk1 but incorporated many usability enhancements. The first notable change were cover panels surrounding the entire machine, which keep anyone from reaching inside of the machine during use. These can be seen in Figure 3-17. The cover panels also served as an aesthetic feature. All panels are nontransparent, except for the foot plate with the grid array of holes. The foot plate maintained its 5 inch by 12 inch grid but each hole is now 0.1875 inches in diameter. The larger holes make it easier for the monofilament to go through the hole, since the monofilaments are seldom straight enough. The front cover plate still incorporated the engraved numbers used for positioning the clamping mechanism components. There is not a cover plate for the rear of the machine so that trained personnel can still easily change out the monofilament when needed. The foot plate had to remain transparent in order for the camera feature to still be utilized. Another improvement was that the clamping mechanism was connected to a pivot (Figure 3-18), which allows the patient to place their foot in the machine without the clamping structure getting in their way. The clamping structure can now be held up as the patient places their foot in the machine and is then locked in place. The clamping structure retained all functionality from Mk1 and is fully adjustable. This included the ability for the clamping mechanism to be used to relocate the subject's foot to the same position from a previous assessment. In the Mk2 prototype new stepper motors were selected to drive the x and y axis to accommodate for the increased weight of the gantry system. These stepper motors are the STP-MTR-17048D, which have 5.19 lb-in of torque and 2.0 amps per phase [48]. Also, two power supplies were selected to drive all three of the steppers, instead of using a buck converter to drive the Walfront D8-MOTOR80. These power supplies are the PSB48-240S and the PSB12-030-P, which output 48 volts DC and 12 volts DC,

respectively [48]. The rest of the electronics from Mk1 were also used in Mk2. The monofilament holder was also updated from Mk1. Unlike in the previous iteration, the monofilament holder in Mk2 was reoriented so that it can be accessed from above (Figure 3-19). This allows for the monofilament to be more easily changed out when needed. The gantry setup was also upgraded with larger rods and shaft holders that integrated into the carriages. The rods were increased from 6.35 mm (Mk1) to 8mm which resulted in a more rigid assembly and guaranteed that the rods did not bow and thus affect the accuracy of the system. The shaft holders were incorporated to improve the assembly process. Larger self-locking external retaining rings were also selected to be used to secure the rods of the gantry system to the journal bearings. In Mk2, a new setup was employed to connect the belts to the carriages. The belts are inserted around a curved profile and are then tied off. This assembly made it easier to create the necessary belt tension required, especially when paired with belt tensioners. The Mk1 monofilament holder, which implemented a load cell, was also refined to be smaller and more compact, seen in Figure 3-20. This updated monofilament holder featured limit switches which are used to ensure that the monofilament never over inserts into the patient's foot. The limit switches in the monofilament holder are also used to calibrate the device before each use. The size was similar to Mk1 with it measuring 18.5 inches wide by 24 inches tall by 10 inches deep (23 inches deep when considering the camera mount and the clamping mechanism). The motor covers and manual knobs add 5.25 inches to the width and height, respectfully.

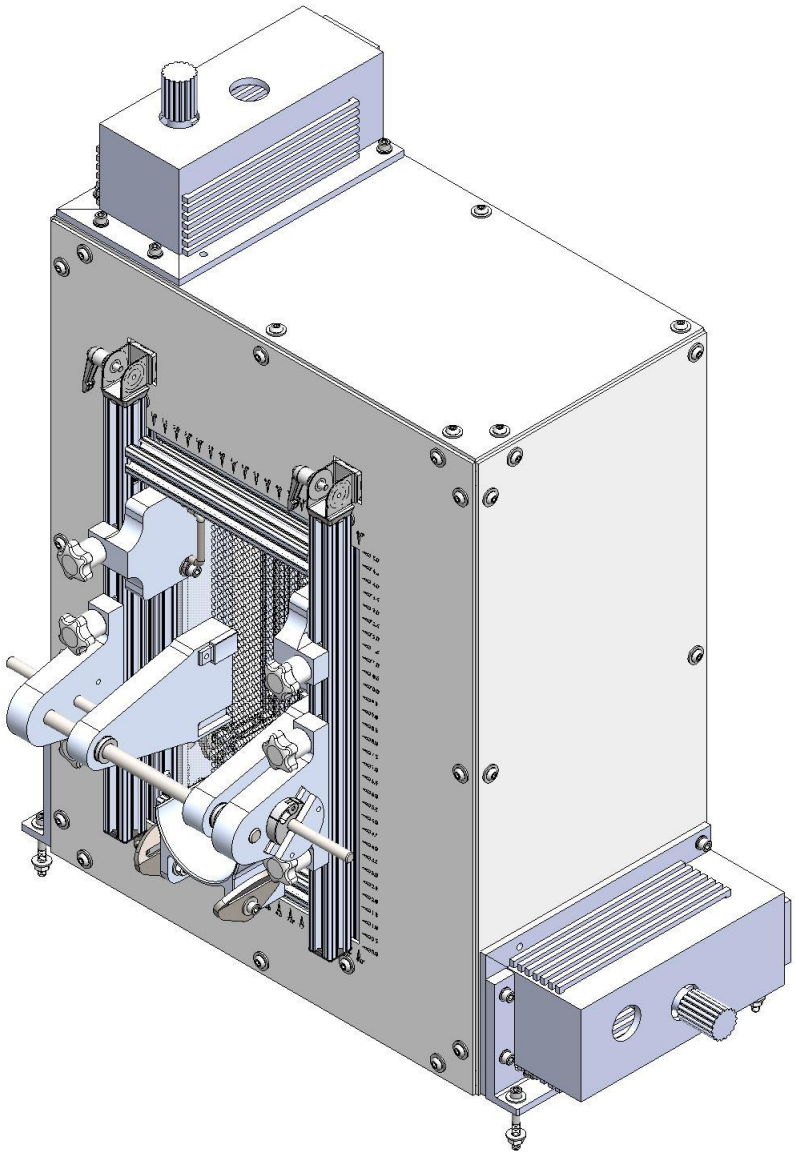

Figure 3-16: Mk2 Prototype

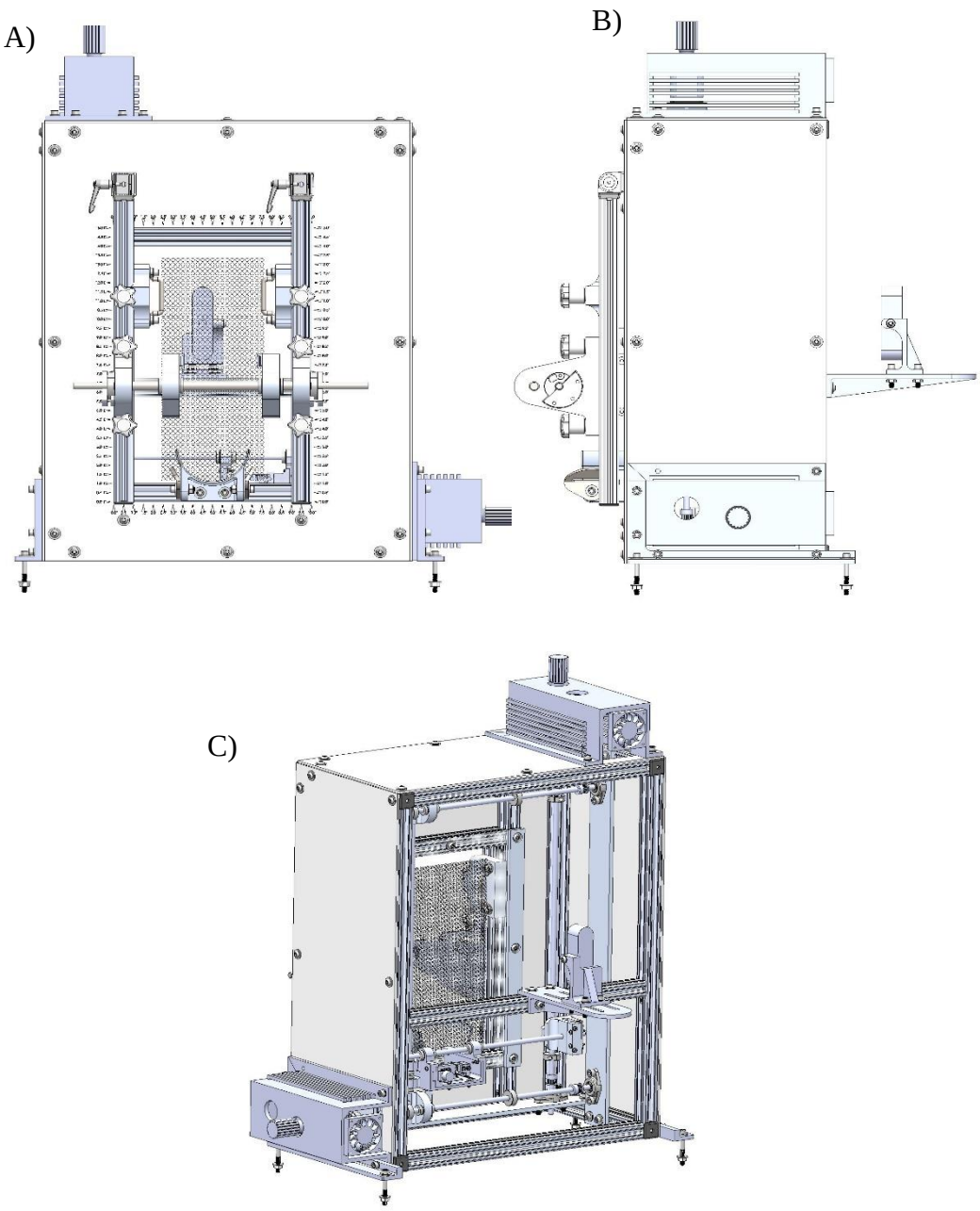

Figure 3-17: Mk2 Prototype with Cover Panels

A) Front View
B) Side View
C) Rear View

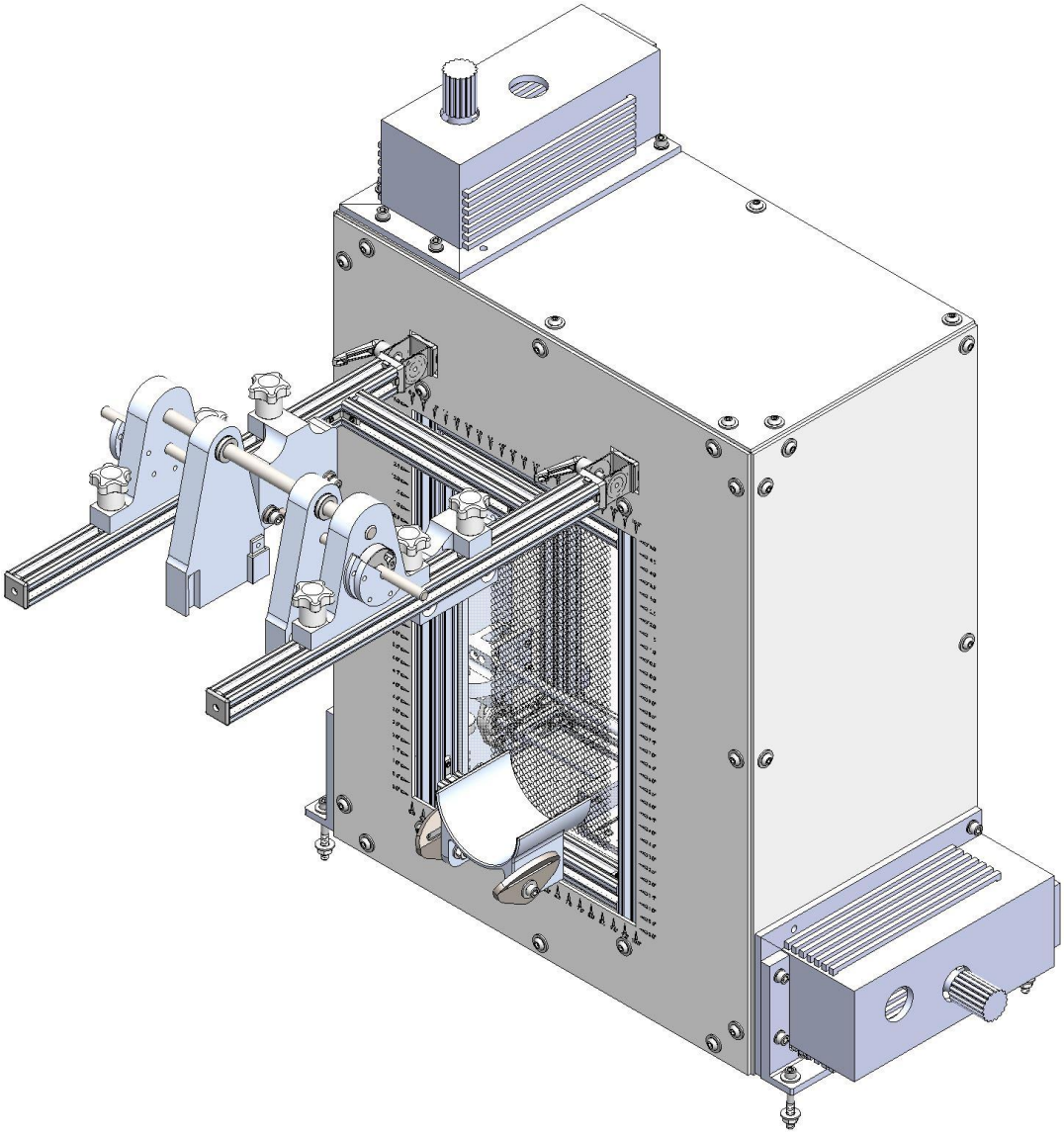

Figure 3-18: Foot Clamp Mechanism on Pivot

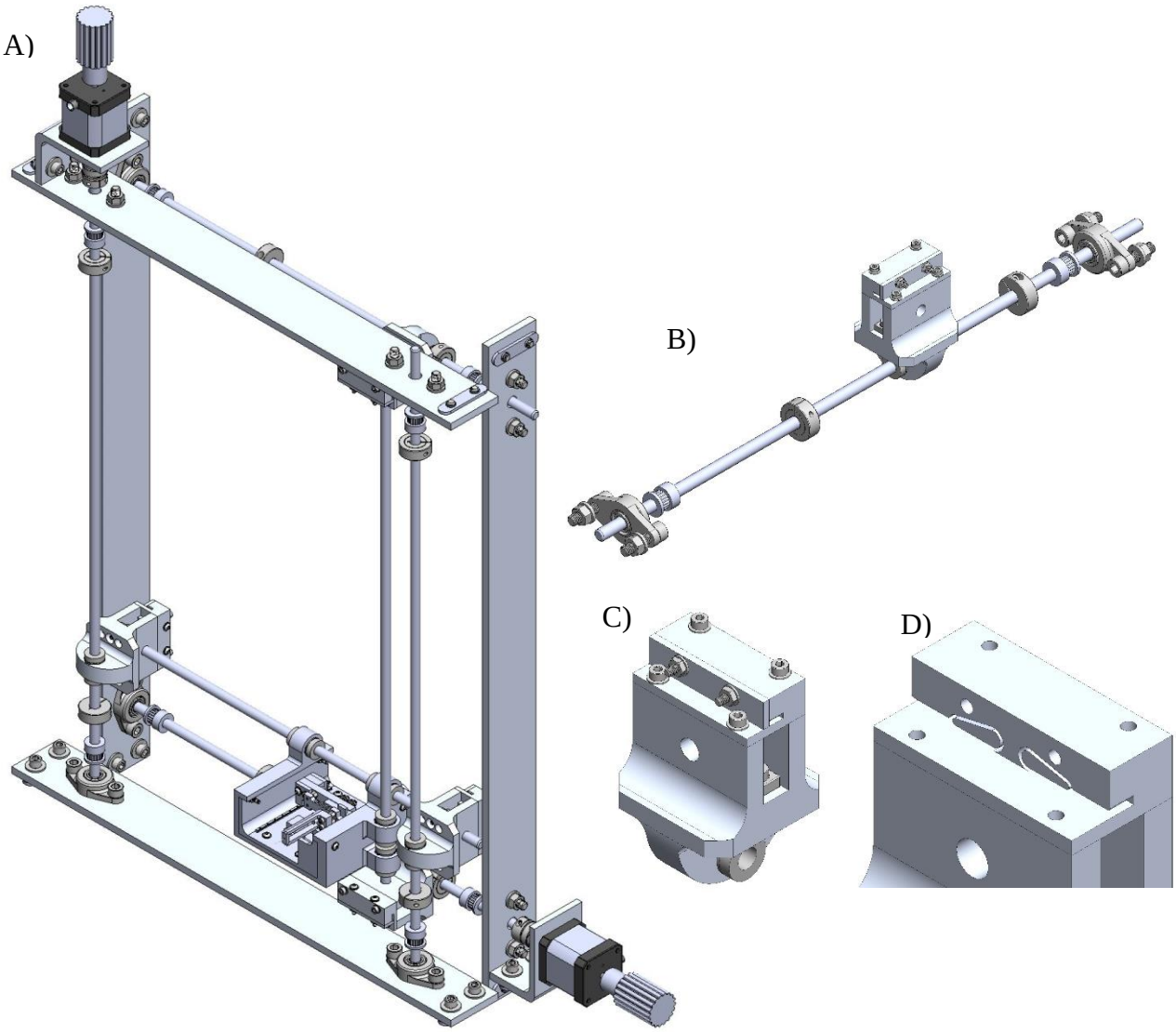

Figure 3-19: Mk2 Updated Gantry System

A) Gantry Combined Assembly
B) Linear Motion Subassembly
C) Updated Carriage
D) Updated Carriage without Belt Cover Plate

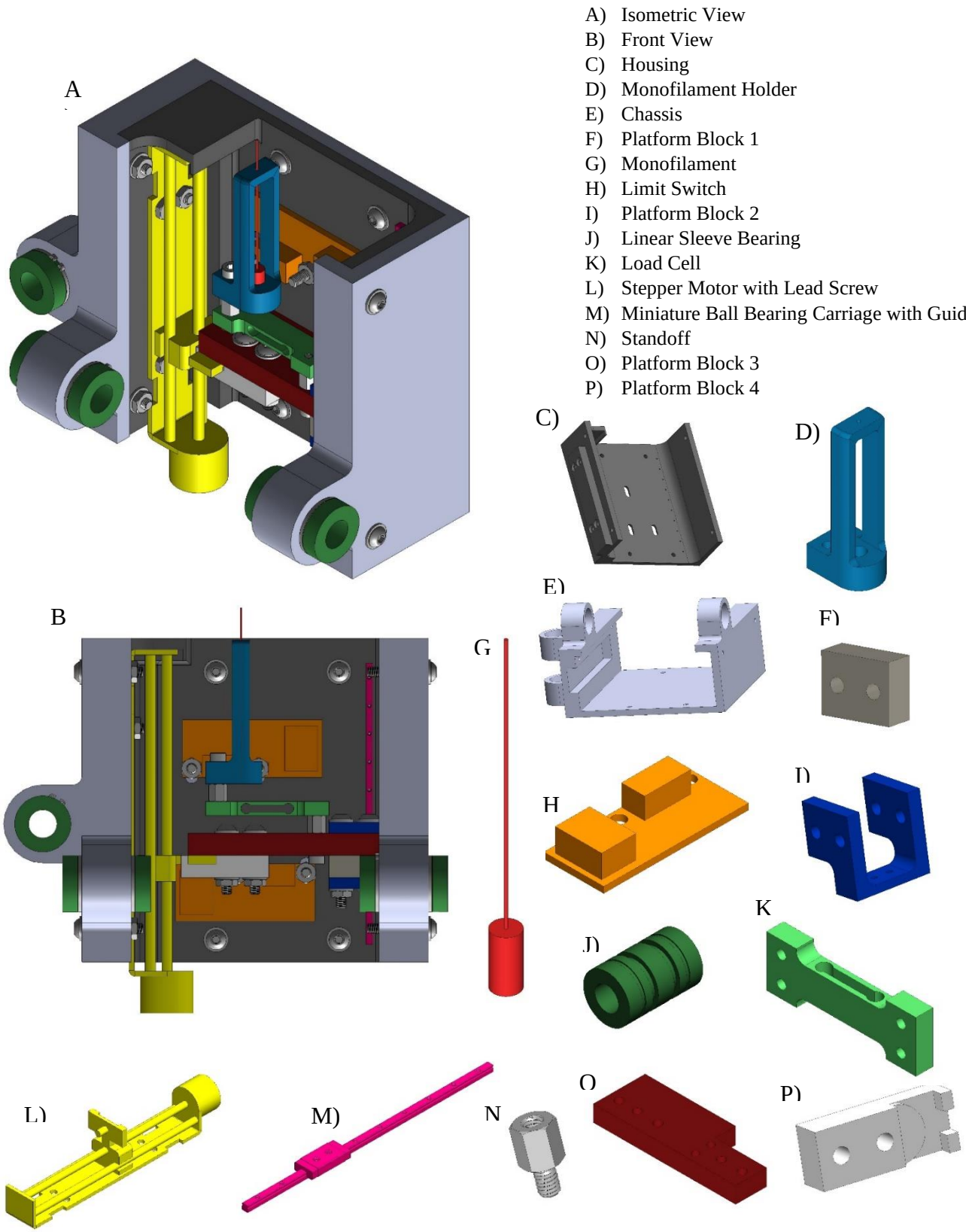

A) Isometric View
B) Front View
C) Housing
D) Monofilament Holder
E) Chassis
F) Platform Block 1
G) Monofilament
H) Limit Switch
I) Platform Block 2
J) Linear Sleeve Bearing
K) Load Cell
L) Stepper Motor with Lead Screw
M) Miniature Ball Bearing Carriage with Guide Rail
N) Standoff
O) Platform Block 3
P) Platform Block 4

Figure 3-20: Mk2 Monofilament Holder

Furthermore, a separate structure (Figure 3-21) was designed to hold all of the electrical components, such as the power supplies, stepper motor drivers, and Arduinos. This self-contained unit safely holds all of the electrical components and keeps them organized, shown in Figure 3-22. All components can be accessed for maintenance and troubleshooting by trained personnel. The size of this electrical storage cabinet is 8 inches by 10 inches by 24 inches. The total cost of all components is roughly $2,800.00, which includes all electrical components, with the exception of a computer.

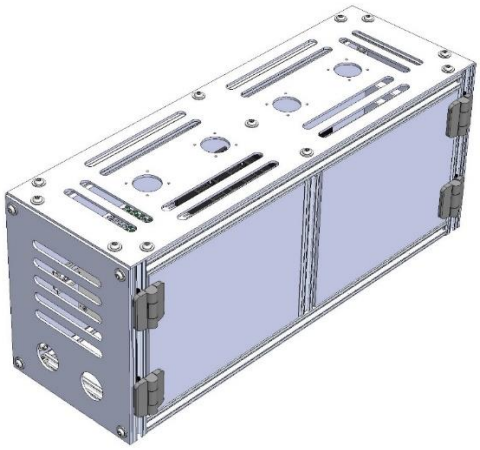

Figure 3-21: Electrical Storage Cabinet

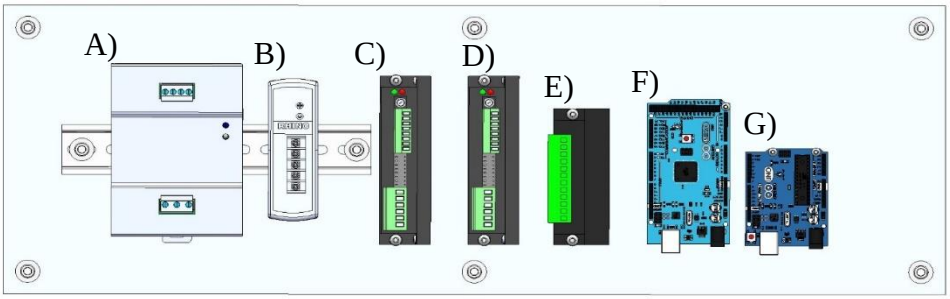

Figure 3-22: Mk2 Electrical Components

A) PSB48-240S Power Supply
B) PSB12-030-P Power Supply
C) STP-DRV-6575 Stepper Motor Drive for X Axis
D) STP-DRV-6575 Stepper Motor Drive for Y Axis
E) TB6600 Stepper Motor Drive for Z Axis
F) Arduino Mega
G) Arduino Uno

3.5 Positional and Force Accuracy of the Device

The gantry system produced in Mk1demonstrated a high degree of positional accuracy for both the x and y axis. Fifteen positional measurements were taken at a microtstepping factor of 20,000 steps/rev and a travel distance of 3.5 inches for each axis. Measurements were taken using a digital caliber between a fixed shaft collar and the linear sleeve bearing attached to the carriage. These components were initially contacting, and where instructed to move 3.5 inches, and then back to the zero position. The gantry was calibrated before each measurement and each axis were studied one at a time. Table 3-2 shows the measurement data, the averages, and percent error. Overall, for a 3.5-inch travel distance the positional accuracy demonstrated a percent error of less than 1.0% and overall consistency in the measured values for each axis. An interesting trend is that for the x axis the average distance was less than 3.5 inches, while the opposite held true for the y axis. The y axis in this gantry system is the vertical direction, which means there is a gravitational effect on the carriage. In this case gravity is moving the carriage marginally past the 3.5 inch mark.

Table 3-2: Positional Accuracy for X and Y Axis for a 3.5 inch Travel Distance

	Measurements	
Trial Number	Real Distance X (in)	Real Distance Y (in)
1	3.4825	3.502
2	3.477	3.502
3	3.478	3.5065
4	3.4815	3.504
5	3.4875	3.5
6	3.479	3.4985
7	3.4845	3.4995
8	3.4805	3.498
9	3.4795	3.5035
10	3.4795	3.5005
11	3.479	3.5015
12	3.484	3.502
13	3.4785	3.4995
14	3.481	3.5005
15	3.481	3.5005
Average	3.481	3.501
Average Percent Error	0.547	0.035

Another important positional accuracy study was also conducted, which examined the machine's ability to travel back to a previous destination over a smaller distance. Specifically, the machine was instructed to move 3.5 inches to 3.75 inches, then back to 3.5 inches, followed by 3.25 inches, and then finally back to 3.5 inches. This study was performed ten times per axis, independent of each other. Similarly, to the last study a microtstepping factor of 20,000 steps/rev was used and a digital caliber measured the relative distances. Table 3-3 and Table 3-4 showed that the percent error of the distance traveled was less than 1.0% for both the x and y axis. Furthermore, the data showed exceptional accuracy and repeatability when the gantry system returned to the 3.5-inch position for both the x and y axis.

Table 3-3: X Axis Repeatability Analysis

	X Axis				
	Distance 1 (in)	Distance 2 (in)	Distance 3 (in)	Distance 4 (in)	Distance 5 (in)
Real Distances	3.5	3.75	3.5	3.25	3.5
Trial Number					
1	3.4745	3.728	3.511	3.27	3.4795
2	3.4795	3.7215	3.5165	3.2665	3.474
3	3.478	3.729	3.512	3.267	3.479
4	3.4835	3.7235	3.512	3.2665	3.4705
5	3.482	3.724	3.5145	3.267	3.476
6	3.48	3.724	3.5135	3.2645	3.4745
7	3.481	3.7215	3.513	3.266	3.476
8	3.4765	3.7205	3.512	3.2645	3.473
9	3.4775	3.7245	3.512	3.2645	3.474
10	3.4765	3.723	3.5125	3.2645	3.47
Average	3.479	3.724	3.513	3.266	3.475
Percent Error	0.603	0.695	0.369	0.495	0.724
Percent Error Average D1 vs Average D3	0.977				
Percent Error Average D3 vs Average D5	1.089				
Percent Error Average D1 vs Average D5	0.122				

Table 3-4: Y Axis Repeatability Analysis

	Y Axis				
	Distance 1 (in)	Distance 2 (in)	Distance 3 (in)	Distance 4 (in)	Distance 5 (in)
Real Distances	3.5	3.75	3.5	3.25	3.5
Trial Number					
1	3.5005	3.7495	3.517	3.2665	3.501
2	3.5035	3.75	3.518	3.266	3.5015
3	3.5035	3.7505	3.516	3.268	3.502
4	3.502	3.749	3.5175	3.2655	3.5015
5	3.501	3.7515	3.517	3.2685	3.4985
6	3.4995	3.752	3.517	3.269	3.4995
7	3.4995	3.749	3.516	3.2695	3.501
8	3.5025	3.753	3.5175	3.2695	3.503
9	3.5035	3.752	3.519	3.273	3.5065
10	3.4995	3.751	3.5175	3.269	3.5045
Average	3.502	3.751	3.517	3.268	3.502
Percent Error	0.043	0.020	0.493	0.568	0.054
Percent Error Average D1 vs Average D3	0.450				
Percent Error Average D3 vs Average D5	0.436				
Percent Error Average D1 vs Average D5	0.011				

Meanwhile Table 3-5 highlights the gantry systems spacing accuracy when compared to the 0.25-inch distance it should have theoretically traveled from one location to another. The average positions were selected for this analysis. A noteworthy observation was that the percent error was better when the machine went from 3.5 to 3.75 inches and 3.5 to 3.25 inches, with the y axis performing better than the x axis. However, when going from 3.75 to 3.5 inches and 3.25 to 3.5 inches the percent errors were worse, roughly 16% error for the x axis and 6 percent error for the y axis. This implies that the machine had some difficulty going back to a previous position.

Table 3-5: Spacing Accuracy for X and Y Axis Between Average Positions

X-Axis				
Theoretical Difference	D2-D1	D2-D3	D3-D4	D5-D4
0.25	0.245	0.211	0.247	0.209
Percent Error	1.98	15.58	1.28	16.58
Y-Axis				
Theoretical Difference	D2-D1	D2-D3	D3-D4	D5-D4
0.25	0.249	0.234	0.249	0.233
Percent Error	0.3	6.6	0.48	6.62

The results extrapolated from Table 3-5 encouraged further analysis considering the physical hole that the monofilament must travel through. Each hole has a diameter of 0.125 inches, which means for a hole at 3.5 inches one edge would be at 3.4375 and the other edge would be 3.5625 inches. Likewise, the hole at 3.75 inches has an edge at 3.6875 and 3.8125 inches, while the hole at 3.25 inches has an edge at 3.1875 and another at 3.3125 inches. After aggregating the position data measured with digital calipers and comparing the values to the geometry of the holes, Table 3-6 showed that the percent error of the measured distance to the center of the hole was within 1.0% error for both the x and y axis, while to the percent error of the measured distance to the edges was typically greater. In essence this means that the gantry system was more accurate at positioning itself closer to the center of the hole than to the edges of the hole, regardless of the axis.

Table 3-6: Positional Accuracy Accounting for a 0.125 inch Hole

Hole at 3.5 inches		
Edge 1 (in)	Center (in)	Edge 2 (in)
3.4375	3.5	3.5625
	X Axis	Y Axis
D1	3.479	3.502
D2	3.513	3.517
D3	3.475	3.502
Average	3.489	3.507
Percent Error Edge 1 D1	1.204	1.862
Percent Error Edge 1 D2	2.193	2.320
Percent Error Edge 1 D3	1.081	1.873
Percent Error Edge 1 Average	1.493	2.018
Percent Error Center D1	0.603	0.043
Percent Error Center D2	0.369	0.493
Percent Error Center D3	0.724	0.054
Percent Error Center Average	0.320	0.197
Percent Error Edge 2 D1	2.347	1.712
Percent Error Edge 2 D2	1.392	1.270
Percent Error Edge 2 D3	2.466	1.701
Percent Error Edge 2 Average	2.068	1.561
Hole at 3.75 inches		
Left Edge (in)	Center (in)	Right Edge (in)
3.6875	3.75	3.8125
	X Axis	Y Axis
D2	3.724	3.751
Percent Error Edge 1 D2	0.988	1.715
Percent Error Center D2	0.695	0.020
Percent Error Edge 2 D2	2.323	1.620
Hole at 3.25 inches		
Left Edge (in)	Center (in)	Right Edge (in)
3.1875	3.25	3.3125
	X Axis	Y Axis
D4	3.266	3.268
Percent Error Edge 1 D2	2.466	2.540
Percent Error Center D2	0.495	0.568
Percent Error Edge 2 D2	1.401	1.330

Lastly the accuracy of the diagnostic tool in terms of its ability to apply a force was also examined. Although the device could not be used on human subjects for this thesis the accuracy was demonstrated on a soft microfiber towel. The towel was attached to the foot plate and the monofilament was applied to the surface. The machine was instructed to apply a 0.50 gF load to the towel, which was performed 15 times. Overall, the stepper motor load cell feedback loop showed promising accuracy, with a percent error of 14% for this surface. Although a microfiber towel is not an ideal substitute for human skin, it does showcase this methodology's repeatability, which is encouraging for a clinical study.

Table 3-7: Force Accuracy for 0.50 gF Applied on a Microfiber Towel

Trial Number	Force(gF)
1	0.54
2	0.58
3	0.59
4	0.56
5	0.57
6	0.54
7	0.57
8	0.63
9	0.59
10	0.59
11	0.56
12	0.54
13	0.57
14	0.56
15	0.56
Average	0.57
Percent Error	14.0

3.6 Device Operation Code

Once the patient places their foot in the machine the MATLAB script will then take a picture of the patient's foot though the transparent acrylic plate. From here the operator selects 13 locations to be assessed on the foot in order to determine the threshold sensitivity at each testing location. The MATLAB script then converts the locations selected from pixels to inches, rounding to the nearest quarter inch. The 13 locations are divided into 3 regions for evaluation: the 5 distal phalanges, the 5 metatarsal heads, and 3 locations on the heel. The 3 regions will be evaluated one at a time in a specific testing order. There are four unique testing order paths (Table 3-1) that can occur; the testing order path is randomly chosen by the machine. These testing order paths represent the most time efficient order in which the regions are evaluated, based on the relative distance between one another.

Table 3-8: Machine Testing Order Paths

	Testing Order Paths			
	1	2	3	4
1st	Heel	Distal Phalanges	Metatarsal Heads	Heel
2nd	Metatarsal Heads	Metatarsal Heads	Distal Phalanges	Distal Phalanges
3rd	Distal Phalanges	Heel	Heel	Metatarsal Heads

The computer program generates a random testing order for all of the locations within each of the 3 regions so as the patient will not able to predict the order in which locations are accessed. The operator selects the locations in each region but also does not know the order of occurrence because of this randomization. The randomization feature is executed by using the time-based randomization function (rng shuffle) in MATLAB. This results in neither the patient nor the operator knowing the testing order, removing any bias from assessment. The monofilament is then moved into location by the machine and the computer program begins the process of applying the

monofilament at specific loads. Once the monofilament has been applied to the patient's foot, a pushbutton with an LED light will start to blink. This pushbutton is housed in a 3D printed ergonomic handle, depicted in Figure 3-23. The patient will be instructed to press the button if they felt the monofilament and to not push the button if they did not feel it. The subject is given five seconds to press the blinking push button. This process is repeated for multiple pressures until the minimum threshold value is determined at the specific location. Originally the protocol applied the monofilament at increasing magnitude of force (0.2, 0.7, 2.0, 4.0, 6.0, 8.0, and 10.0 gF) until the patient could sense the monofilament. Although this was a straightforward approach it benefited patients with better sensation perception and hurt those who had greater degrees of sensation loss. This would have ultimately meant that healthier patients could complete the assessment quicker than unhealthy individuals. Instead the process outlined in Figure 3-24 works by homing in on the individual's threshold sensitivity by using the least amount of total applications of the monofilament as possible. The individual is first accessed with a 0.2 gF load applied, if they can feel it then the monofilament is moved to the next location. If the individual cannot feel the 0.2 gF then a 10.0 gF is applied. Furthermore, if the patient cannot feel the 10.0 gF then the assessment at this location ends, since they are incapable of sensing the greatest amount of force. If they can feel 10.0 gF then this will start a process to find what value of force between 0.2 gF and 10.0 gF they can sense. False positives are included in the computer program to detect patients giving inaccurate answers. In the code there is a 10% chance of a false positive occurring per testing location. A false positive will either occur before or after the threshold sensitivity is determined per location. A false positive will prompt the monofilament to move forward, but will not contact the individual's skin, this mimics the sound of an actual application of the monofilament. At the conclusion of a false positive test the LED pushbutton will light up and blink

to query the individual if they felt a force, despite one not being applied. Likewise, patients in the manual assessment verbally indicate when they have felt a positive force stimulus. The current manual monofilament test does not include false positive checks, randomization, and a homing sequence in the testing procedure. In this methodology a patient with a high degree of sensation loss should complete the assessment in the same amount of time it would take a healthy individual. A patient in the middle between these two spectrums will take more time to complete the assessment, but their time will still be improved by limiting the amount of times the monofilament is applied. Preliminary pilot testing showed that it takes between 7-12 minutes per foot with the above parameters.

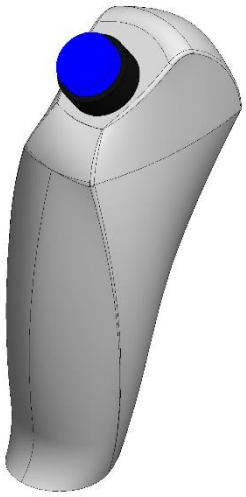

Figure 3-23: Pushbutton Response Handle

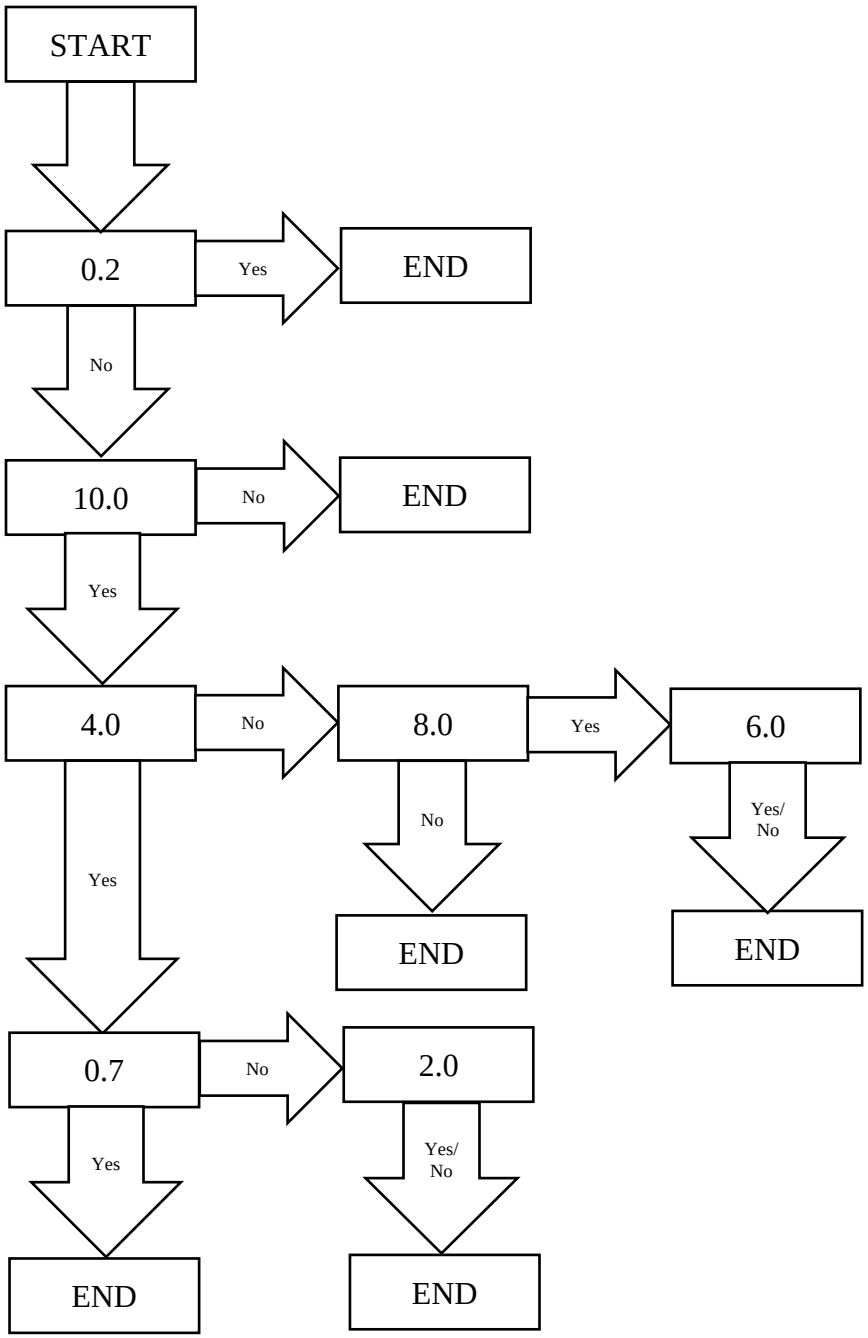

Figure 3-24: Monofilament Assessment Flowchart

The MATLAB script works in tandem with GRBL, an open source CNC operation software. GRBL is installed on the Arduino mega and is configured to be used with 2 stepper motors, and all of the necessary feeds and speeds. The MATLAB script sends g-code instructions through serial communication (usb ports) to GRBL, which is then interpreted to move the monofilament to the proper location. The g-code is generated in the MATLAB script based on the testing locations selected by the operator. This not only includes positional instructions but also to initiate a homing sequence before each use of the device. GRBL also sends MATLAB its current status when it is moving from one location to another, which is then used to know when the machine can begin to apply the monofilament. Another noteworthy feature is that the Arduino code developed to apply the monofilament is completely custom. This code is stored on the Arduino uno and also communicates with the MATLAB script, where MATLAB sends it the value at which to apply the monofilament. In return this code gives MATLAB the actual value applied and the patient's response to the monofilament applied (feel and no-feel). The code on the Arduino uno uses a nonblocking stepper motor library and a nonblocking HX711 amplifier library. These nonblocking libraries allow the load cell and stepper motor to read and write at the same time, allowing for seamless application of the monofilament. If nonblocking libraries were not used than the stepper motor and the load cell would have to take turns operating, which corresponds to less contact force measurements. The more often the load cell samples the amount of the force being applied to the patient's skin the more likely it will hit its targeted force. All of this code works together to make the neuropathy device be able to accurately apply a monofilament to a specific amount of force.

The threshold sensitivity maps produced are the most important results that the machine generates at the end of the assessment. They visually show the patient and the clinician at what point the subject is able to sense the load applied by the monofilament. The software generates a plot of each foot and also stores the data in an excel datasheet and a MATLAB workspace for future analysis. Although the machine has not been used in a clinical setting to date example figures of these threshold maps are provided to highlight this documenting feature, which is not used in the manual assessment. An example of a healthy foot can be seen in Figure 3-25, where the map shows the individual was able to sense very low amounts of force (0.2 and 0.7 grams of force). Whereas Figure 3-26 shows an individual starting to lose their diminished light touch sensitivity and are unable to sense forces less than 2.0 grams of force. Lastly, Figure 3-27 represents an unhealthy foot which includes locations where the individual could not sense the critical threshold sensitivity of 10.0 grams of force, which corresponds to a loss of protective sensation. This degree of neuropathy puts individuals at an increased risk of sustaining a puncture injury. This figure shows that the toes and metatarsal heads are the areas at the highest risk, while the heel has not reached this state yet. Although these threshold sensitivity maps are not based on actual results, these figures show what the diagnostic tool is capable of and how the results can be documented.

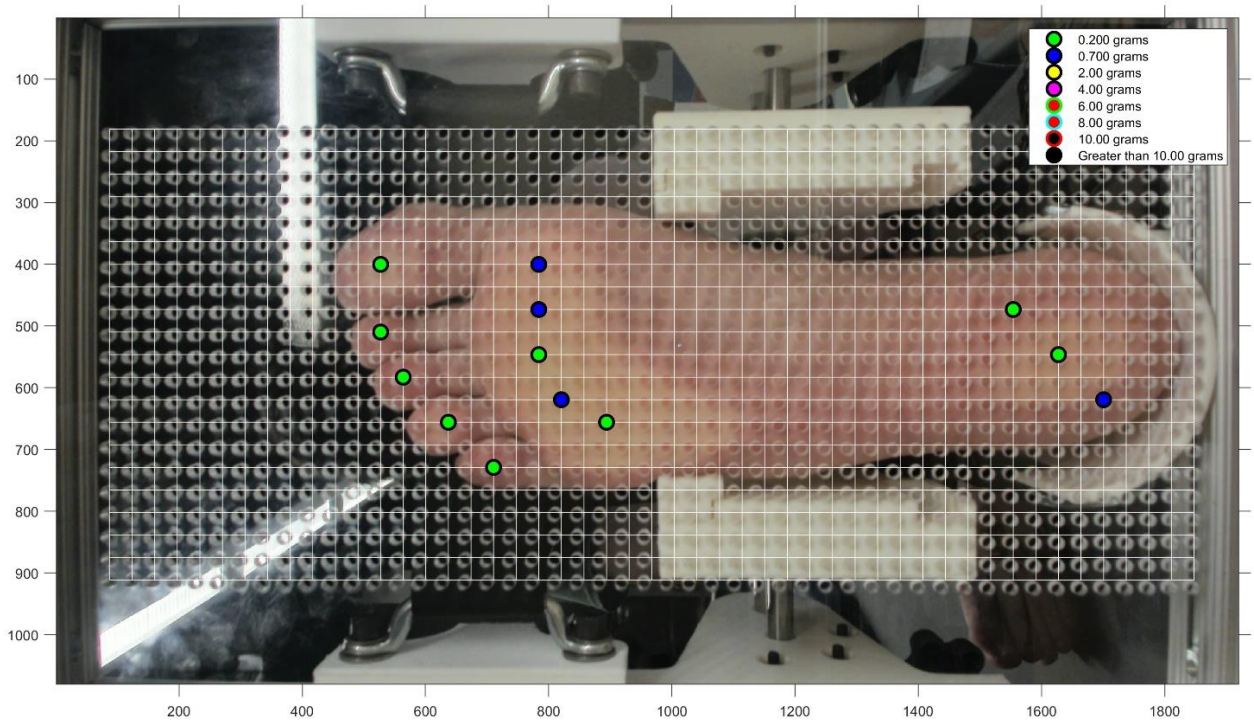

Figure 3-25: Representation of a healthy foot threshold sensitivity map

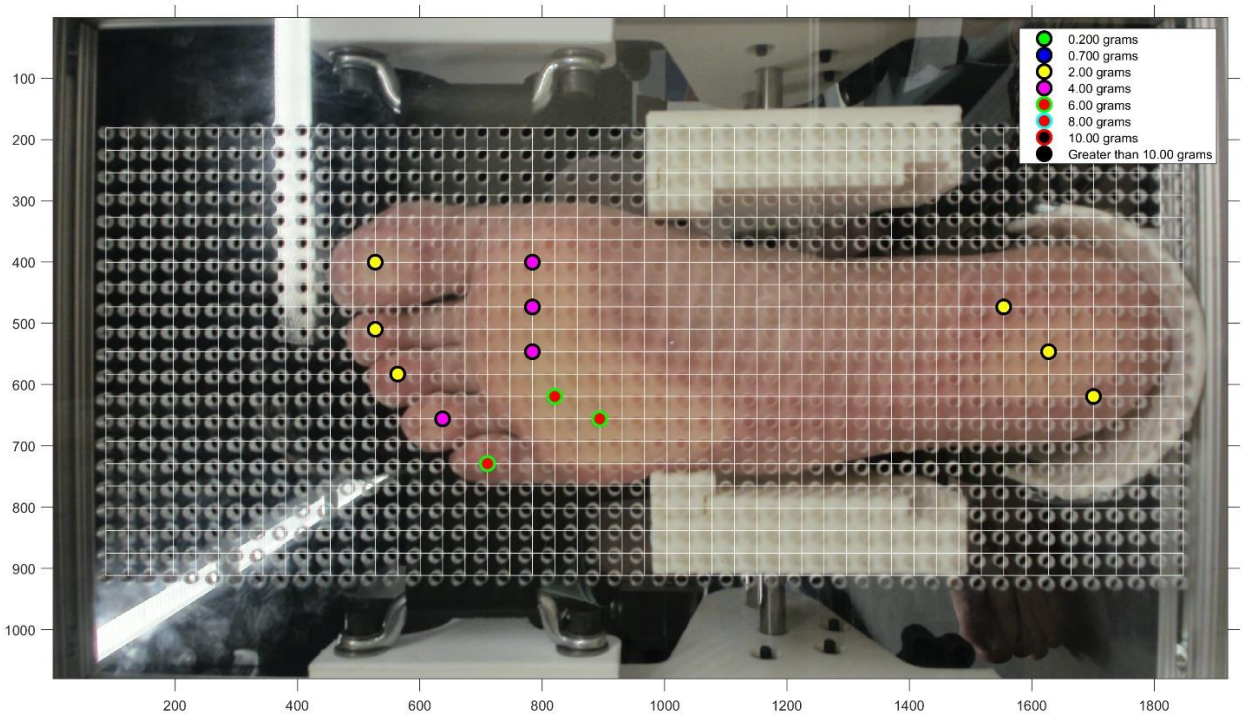

Figure 3-26: Representation of a moderately healthy foot threshold sensitivity map

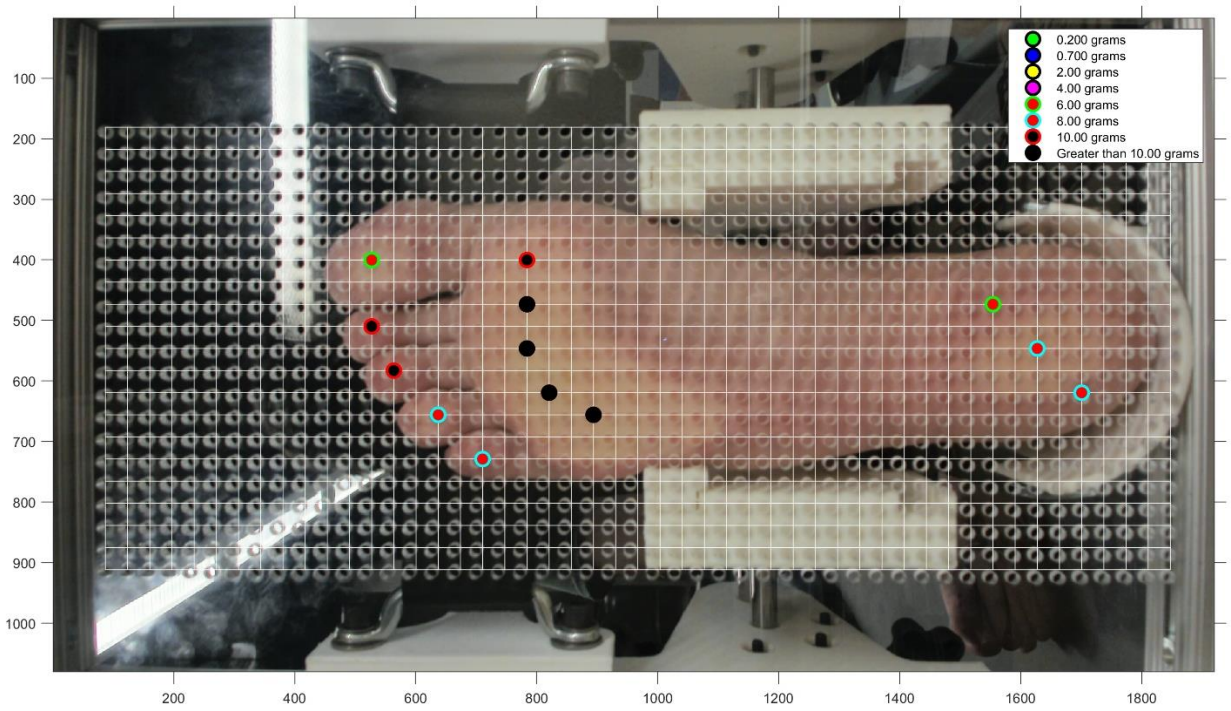

Figure 3-27: Representation of an unhealthy foot threshold sensitivity map

3.7 Foot Plate Finite Element Analysis

The acrylic foot plate was analyzed using SolidWorks© finite element analysis, since it is one of the most likely components of the machine to be subjected to fatigue. Although patients will be instructed to lightly press their foot against the foot plate, it is still a component that will see multiple loads. Also, the foot plate was manufactured using a laser cutter, which does generate a lot of heat in the acrylic causing thermal stresses. As such it was mandatory to understand the effects of load on the foot plate during the foot assessment. The Mk1 acyclic foot plate was used for the finite element analysis with an Elastic Modulus of 3.0 GPa, Poisson's Ratio of 0.35, and yield strength of 45 MPa, which were the material properties in the SolidWorks© material database. A linear elastic static study was employed, where a load was applied to an area representative of the plantar surface of the foot. The foot region, Figure 3-28, was based on anthropometric data for a foot representative of 5% of the USA population, which turned out to be a female foot. The

smallest foot was considered since it would yield the greatest amount of stress when loaded versus a larger foot. The foot region had a length from the heel to the ball of the foot of 159.7 mm [45], a heel width of 52.9 mm [45], and a breadth of 85.0 mm [45]. These dimensions were used as the basis for defining the foot region with arcs and parabolas helping to refine the shape. A normal compressive load was applied to this foot region with values of 10 lbs., 20 lbs., 30 lbs., 40 lbs., and 50 lbs. Furthermore, the foot plate was reduced in size by an inch along its border and was fixed along the outer faces. The front and back faces of the foot plate were not fixed and were free to be deformed by the applied load. Figure 3-29 highlights the boundary conditions of this model; the purple arrow are the force and the green arrows are the fixtures. Similar to the finite element analysis methodology of Chapter 2, an H-Adaptive study was used to simulate the effects of the load on the foot plate. The targeted accuracy was set to 98%, with a global accuracy bias, and utilized the iterative FEEPlus solver. A curvature-based mesh was employed for this study, with a maximum element size of 0.364 inches, a minimum element size of 0.073 inches, and a minimum of 12 elements in a circle. However, the H-Adaptive mesh will refine itself and will reduce the element size in areas of high stress for each iteration performed until it runs five times or achieves the 98% criteria. Figure 3-30 shows the final mesh produced when a 50 lb. load was applied to the foot plate.

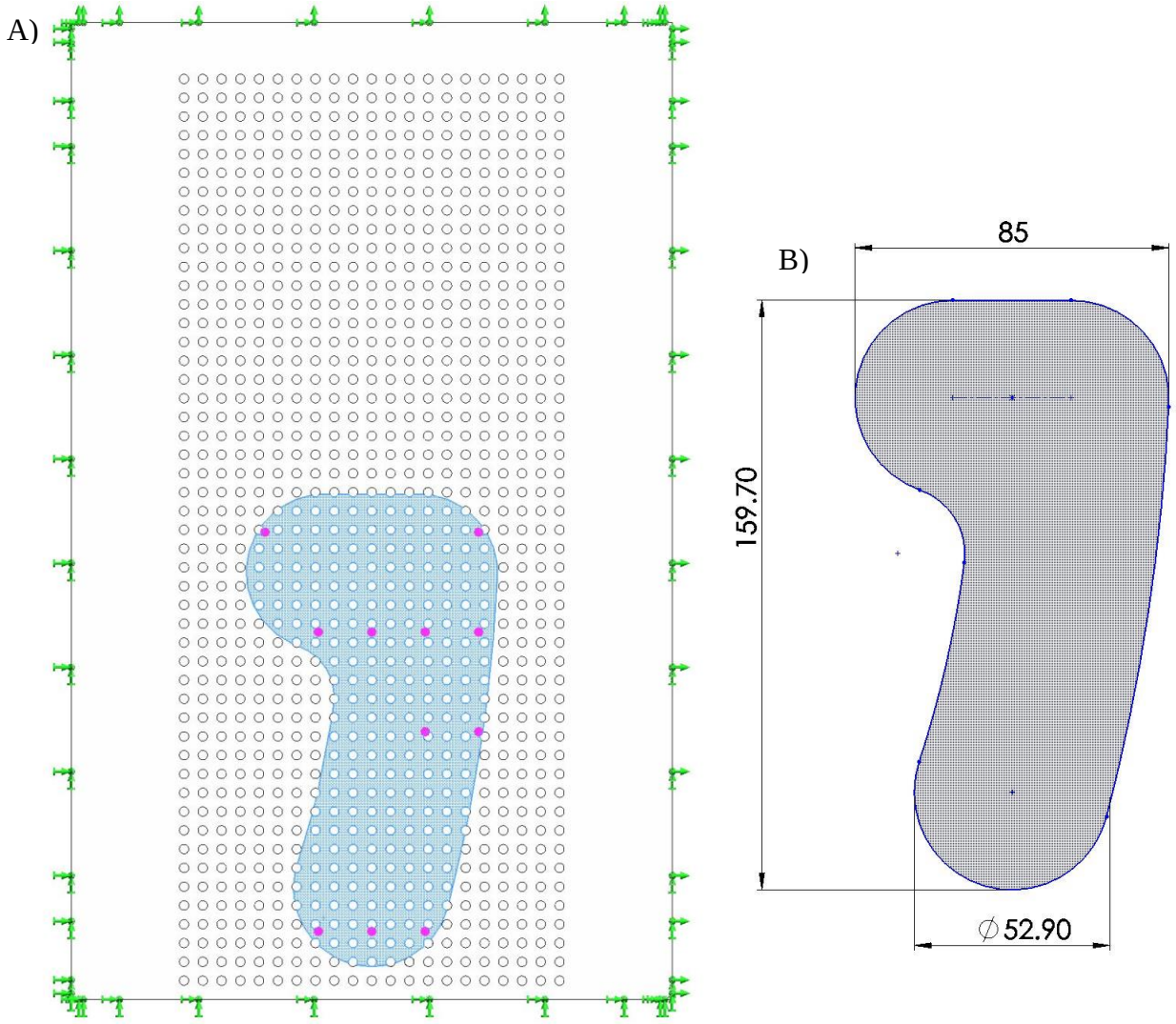

Figure 3-28: Foot Plate Load Region

A) Foot Region
B) Foot Sketch

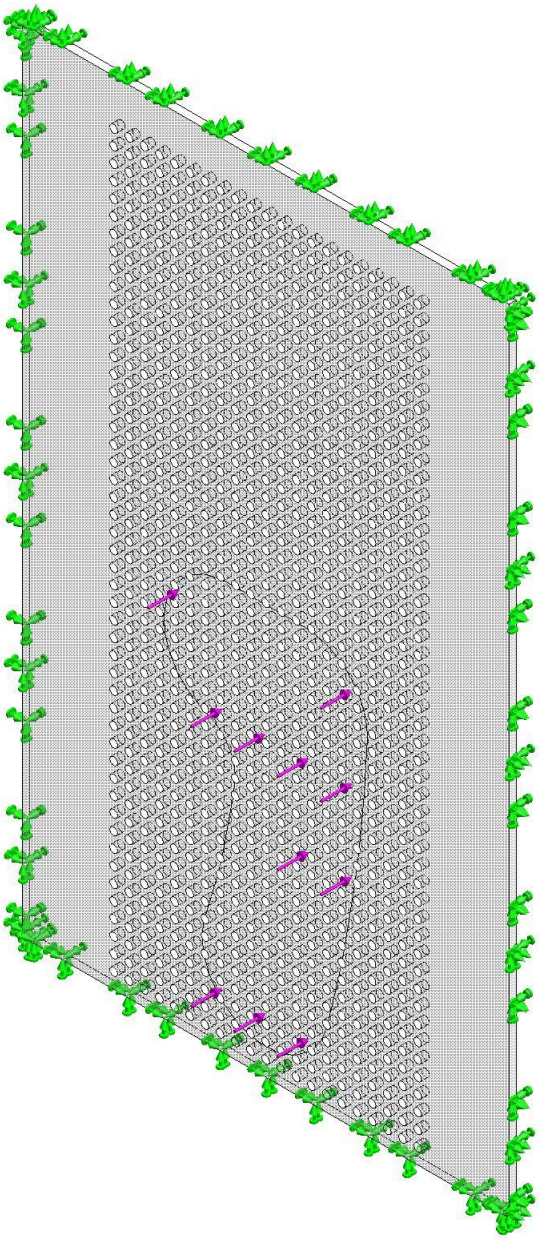

Figure 3-29: Foot Plate Boundary Conditions

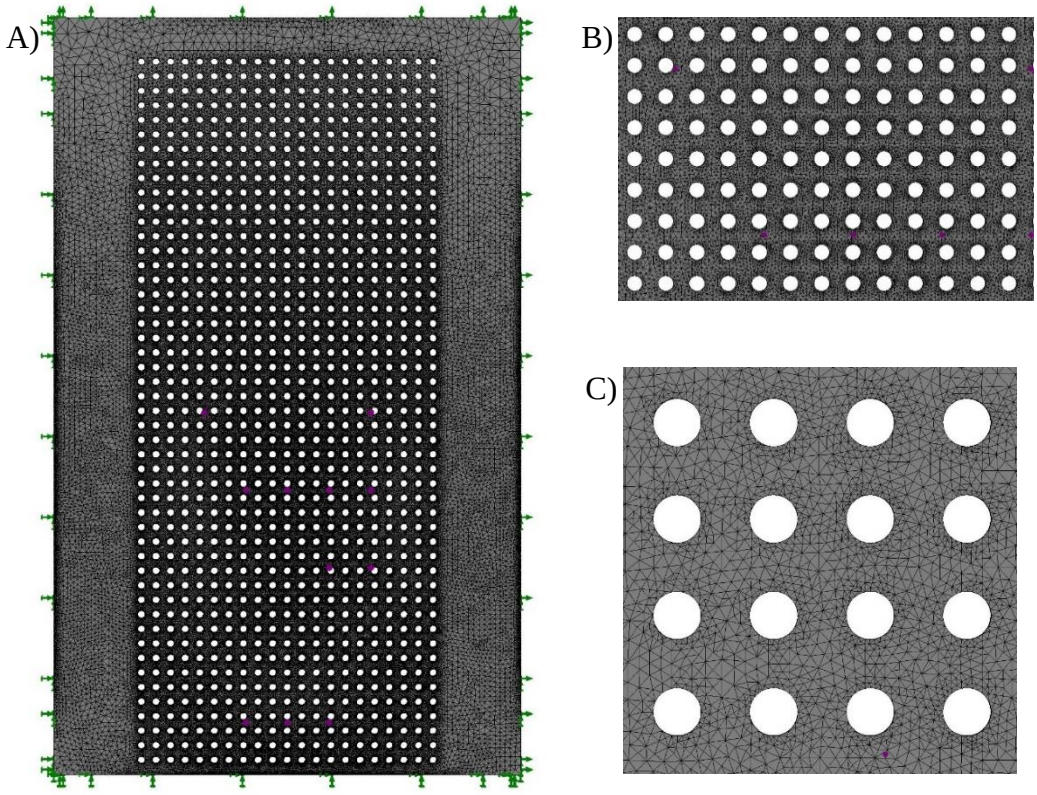

Figure 3-30: Foot Plate Final Mesh

A) Large Scale
B) Medium Scale
C) Small Scale

After running through all of the simulation studies for the various loading conditions the von Mises stress, normal stress, and resultant displacement were all examined. The results, presented in Table 3-3, show that greater amounts of force yielded higher amounts of stress and displacement in the foot plate. Consequently, this resulted in a factor of safety of 1.32 for the 50 lb. load when considering the von Mises criteria for failure. Figures 3-31 shows the von Mises stress plot on the foot plate, while Figures 3-32 and Figure 3-33, show the normal stress and resultant displacement plots, respectfully. Figure 3-31, Figure 3-32, and Figure 3-33 are all for the 50 lb. load and have a deformation scale of 5.9, which is why there is a lot of exaggeration with the visual plots. The plots showed that the foot plate deformed inward as a result of this load. In fact, the greatest amount of deflection was near the center of the foot plate and will deform by roughly 5.6 mm. The highest

states of stress are at the center of the foot plate and near the fixed edges. It should also be noted that all studies achieved a stress convergence after 5 iterations, Figure 3-34 shows the convergence plot for the foot plate loaded with 50 lbs. Ultimately these results show that the foot plate is safe to be used up to 50 lbs., which is unlikely to ever occur since the patient will be placing their foot against the plate and will never stand on it.

Table 3-9: Foot Plate FEA Results

Load (lbs)	Maximum von Mises Stress (MPa)	Maximum Normal Stress (MPa)	Maximum Resultant Displacement (mm)	Factor of Safety
10	6.814	1.976	1.116	6.60
20	13.64	3.937	2.233	3.30
30	20.46	5.755	3.349	2.20
40	27.28	7.873	4.466	1.65
50	34.10	9.865	5.582	1.32

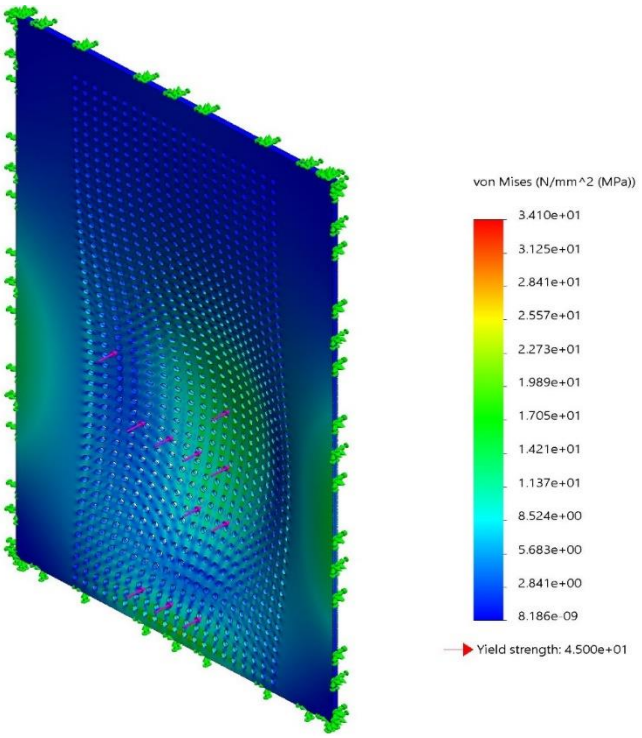

Figure 3-31: Foot Plate von Mises Stress Plot, 50 lbs.

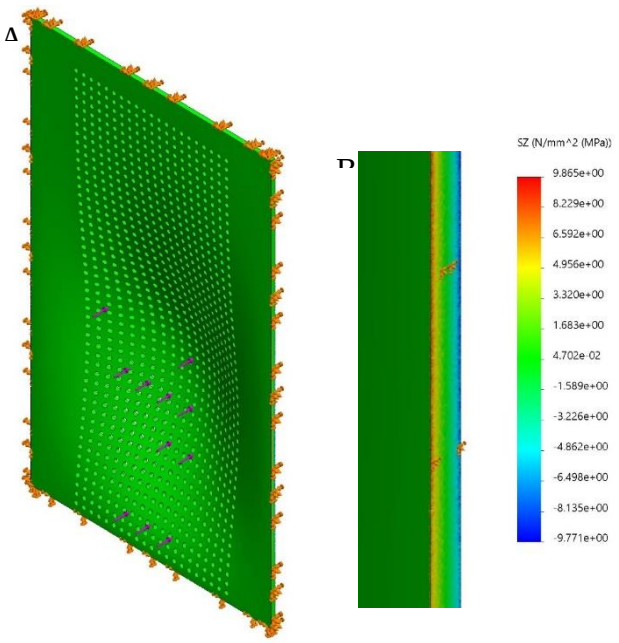

Figure 3-32: Foot Plate Normal Stress Plot, 50 lbs.

A) Pictorial View
B) Edge Closeup

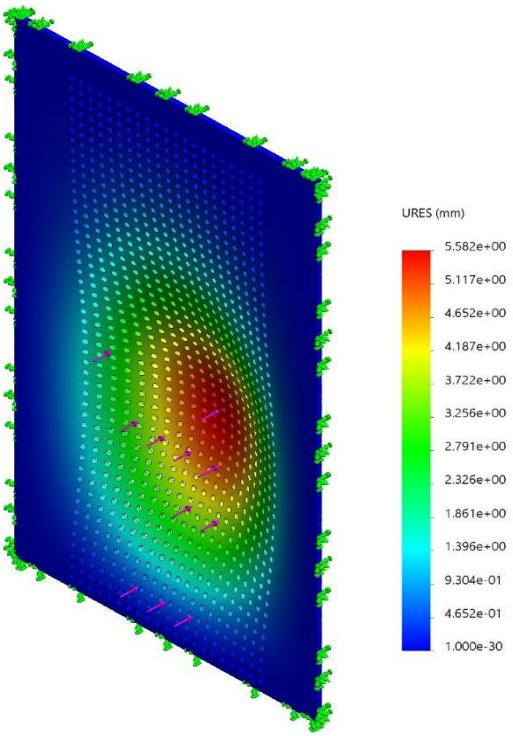

Figure 3-33: Foot Plate Resultant Displacement Plot, 50 lbs.

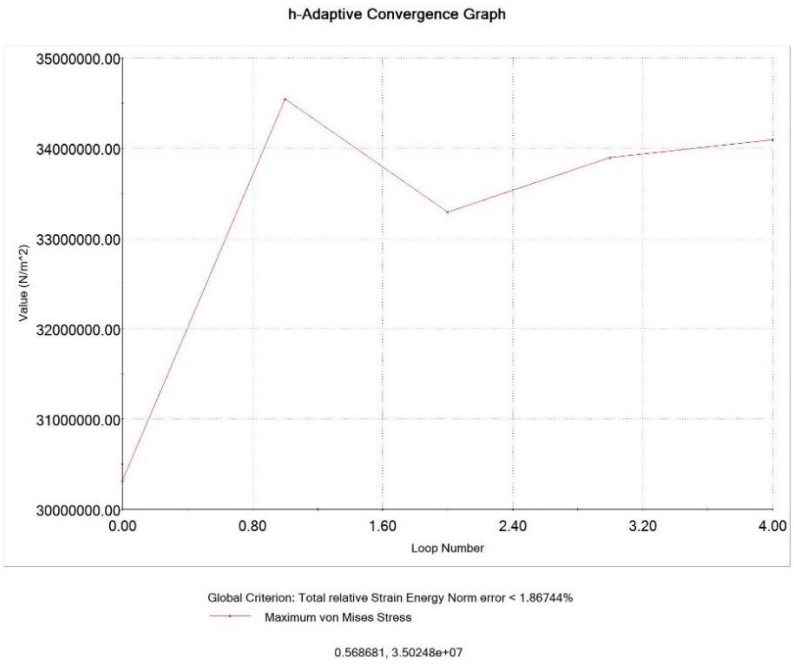

Figure 3-34: Foot Plate Convergence Plot, 50 lbs.

3.8 Design Validation

Mk1 and Mk2 both met the initial design objectives. The designs were modular and adaptable, Mk1 in particular was able to be upgraded over the course of a year until it was completed and was successfully built with only one individual. A large part of this was due to the use of extruded aluminum. It took roughly 12 hours to build the Mk1 prototype, but it is anticipated that the Mk2 prototype will be able to be assembled even faster. The Mk1 prototype was also assembled only using commonly found tools. The Mk1 prototype was roughly 45 pounds which was below the required minimum, however Mk2 will weigh closer to 60 pounds to account for the electronics cabinet. Although the weight of the device is no longer a significant objective since the device is attached to a cart with wheels. The machine remained noninvasive by using the standard nylon monofilament. The foot clamping mechanism is both comfortable, secures the foot, and is able to relocate the foot so that the same locations from a previous assessment can be reevaluated. All

surfaces of the foot clamping mechanism can be disinfected and are not sharp. The foot clamp was successfully designed to be used on 95% of the world's population. However the most important objective was that the device was able to produce multiple values of force stimuli, at minimum three. Not only was it able to produce a range of forces between 0.2 and 10.0 grams of force. In preliminary pilot testing the machine was able to achieve the ±0.5 grams of force accuracy, and when used on a microfiber towel it demonstrated a percent error of 14%. However data still needs to be collected on human subjects to further validate the accuracy of this device in an ideal setting. It was also able to achieve the 0.1 gram of force resolution, but future testing of the device will be used to analyze if it can actually achieve a greater resolution. The assessment time per foot was also optimized to only take between 7 and 12 minutes and will also be confirmed in human subject testing. Lastly the cost of the prototypes were $2,300.00 and $2,800.00 for the Mk1 and Mk2 prototypes, respectfully. Although this is a great amount of money it is still anticipated that at volume the cost can be improved closer to the $1,000.00 criteria.

Chapter 4: Semi-Automated Plantar Surface Sensation Detection Device-Provisional Patent Application

Provisional Application No.: 6/903,211

Auburn University Invention Disclosure #2019-032:
"A New Standardized Approach for Measuring Diabetic Neuropathy on the Plantar Surface of the Foot"

Inventors:
Jon Commander, MD
Thomas Burch, PhD, PE
Michael Zabala, PhD
Vitale Kyle Castellano, BS
Hayden Burch
Kenny Brock, PhD

4.1 Abstract

A device has been designed and developed that can be used to map the threshold sensitivity of the plantar surface of the foot in a semi-automatic fashion. The machine is based off of the monofilament pressure test, where a monofilament is applied to the surface of the foot until it buckles at a corresponding pressure. The patient indicates a positive or negative response, based on if they were able to feel the monofilament. After an initial setup by the operator, this device is able to automatically apply different amounts of pressures at different locations on the plantar surface, allowing for a patient's threshold sensitivity to be measured and mapped. Setup of the system utilizes a camera aimed at the plantar surface of the foot through a transparent plate to select locations for evaluation, which are then randomized for testing. The machine continues to reevaluate a location until a threshold sensitivity is determined. False positive checks may also be utilized whereby no pressure is applied but the patient is asked to determine if the stimulation was felt.

This machine may be used to systematically quantify the extent of an individual's neuropathy by generating a threshold sensitivity map of the plantar surfaces of the feet. This technology may also be used to validate potential treatments of neuropathy and serve as a means of detecting the disease earlier during initial stages of development.

4.2 Diagrams

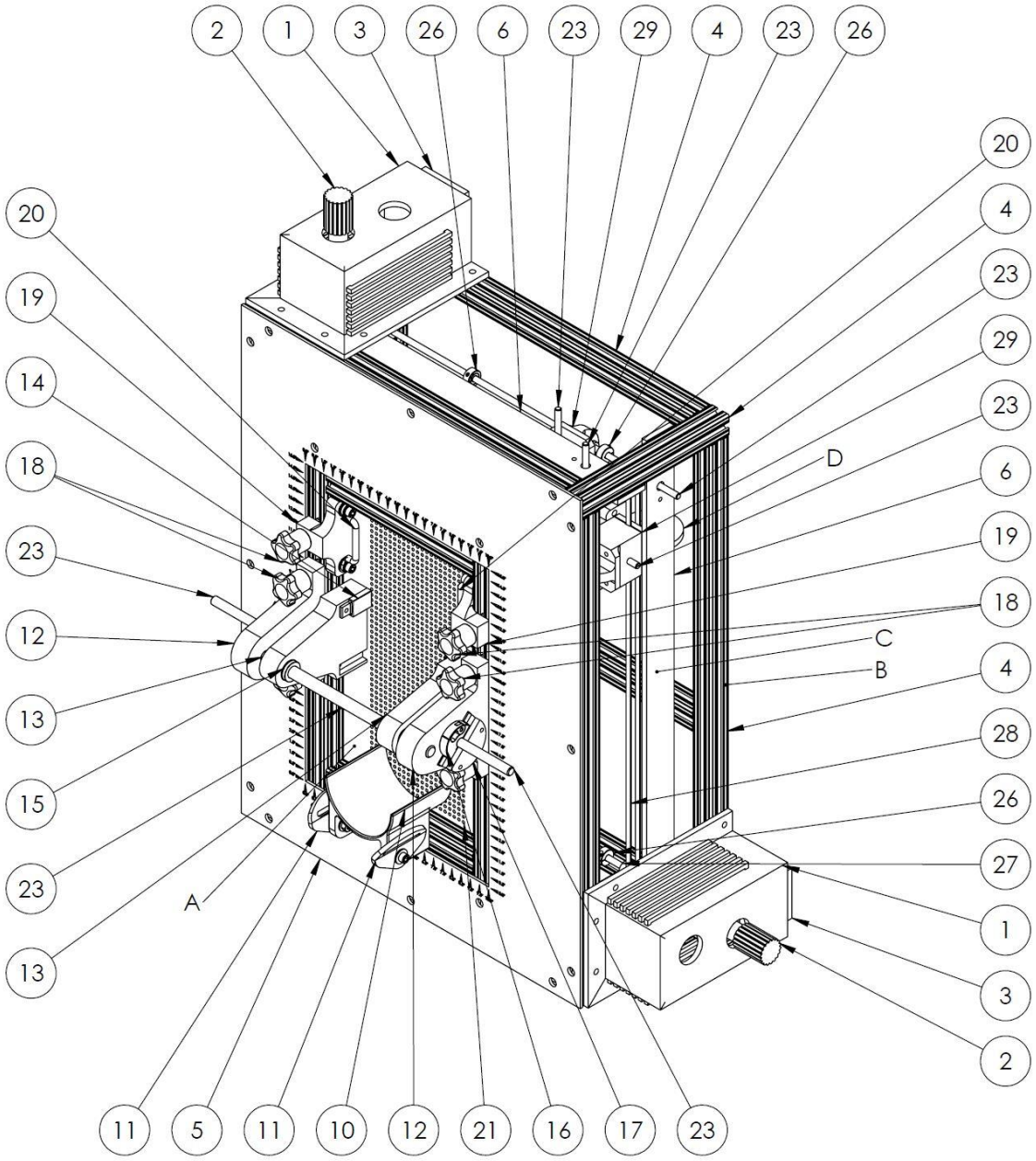

Figure 4-1: Neuropathy Diagnostic Tool

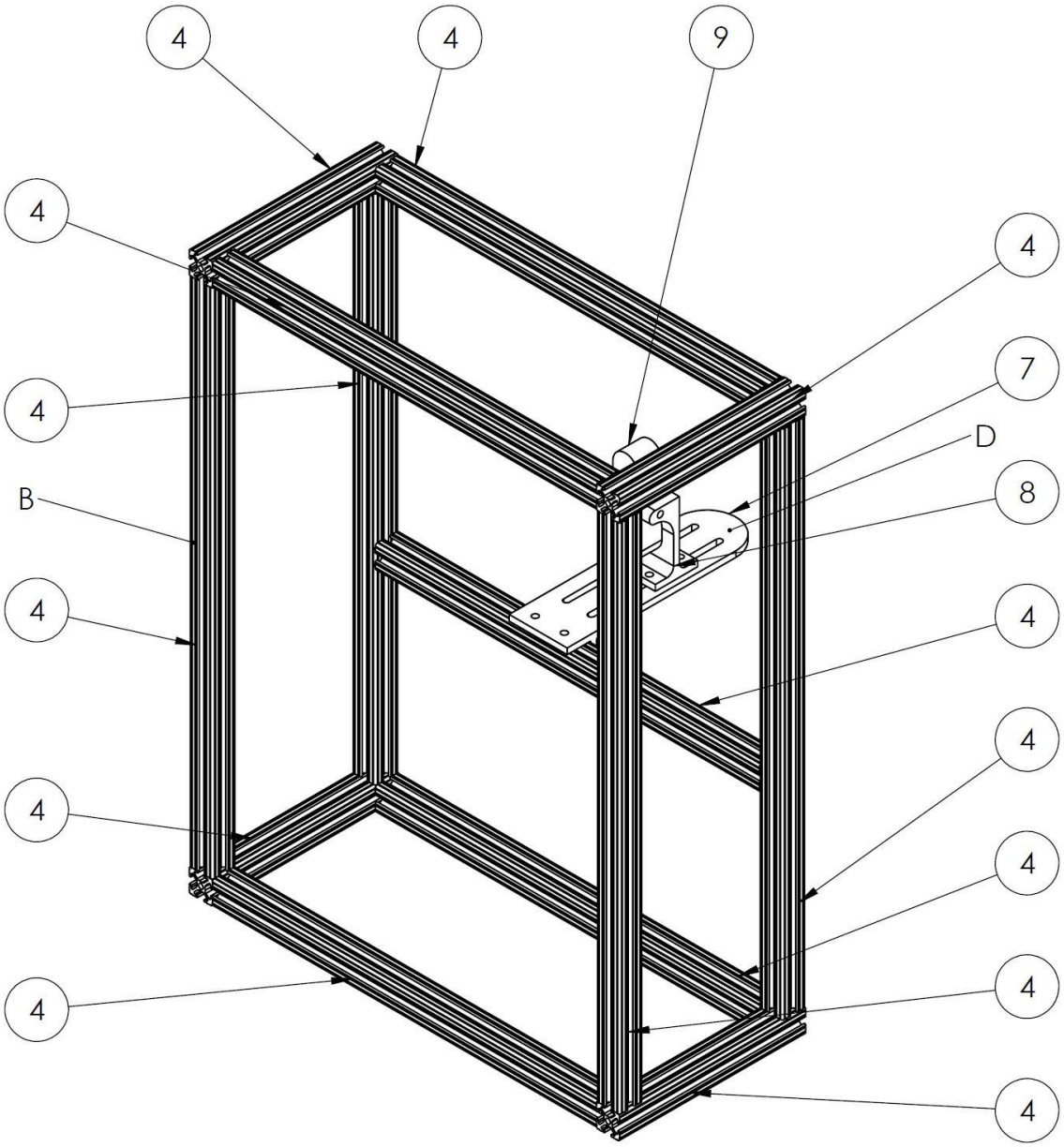

Figure 4-2: Chassis

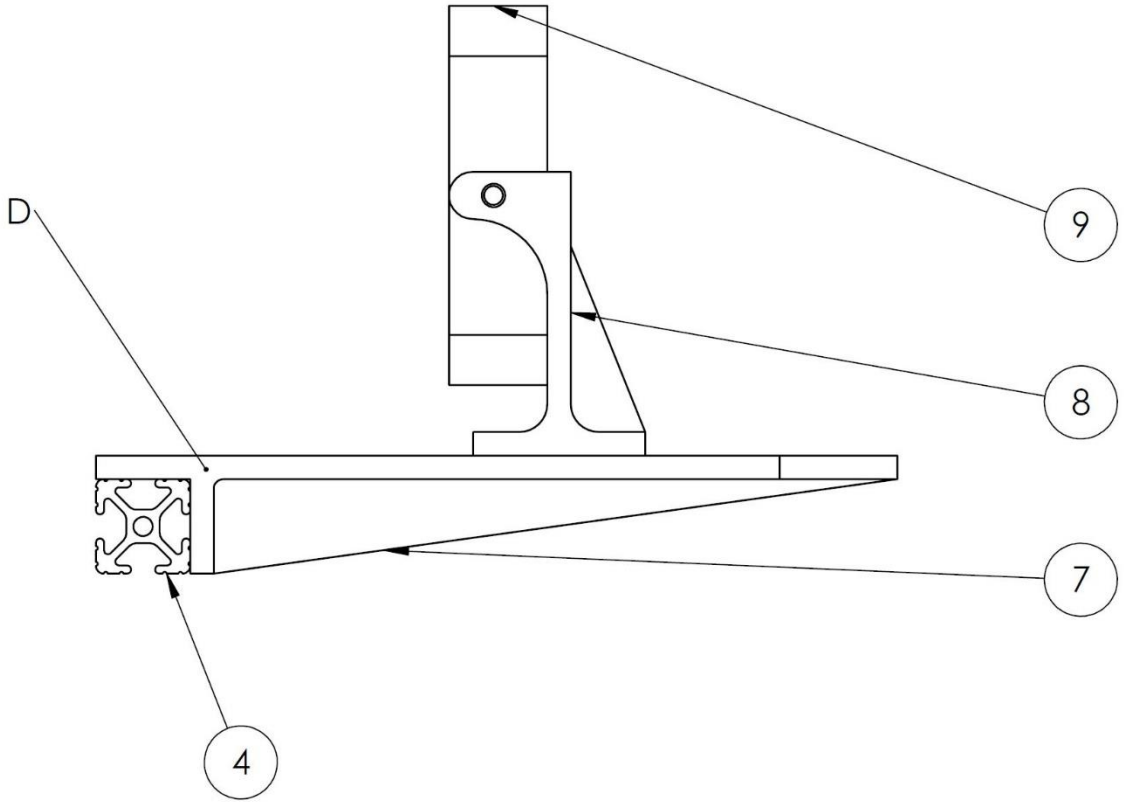

Figure 4-3: Camera Subassembly

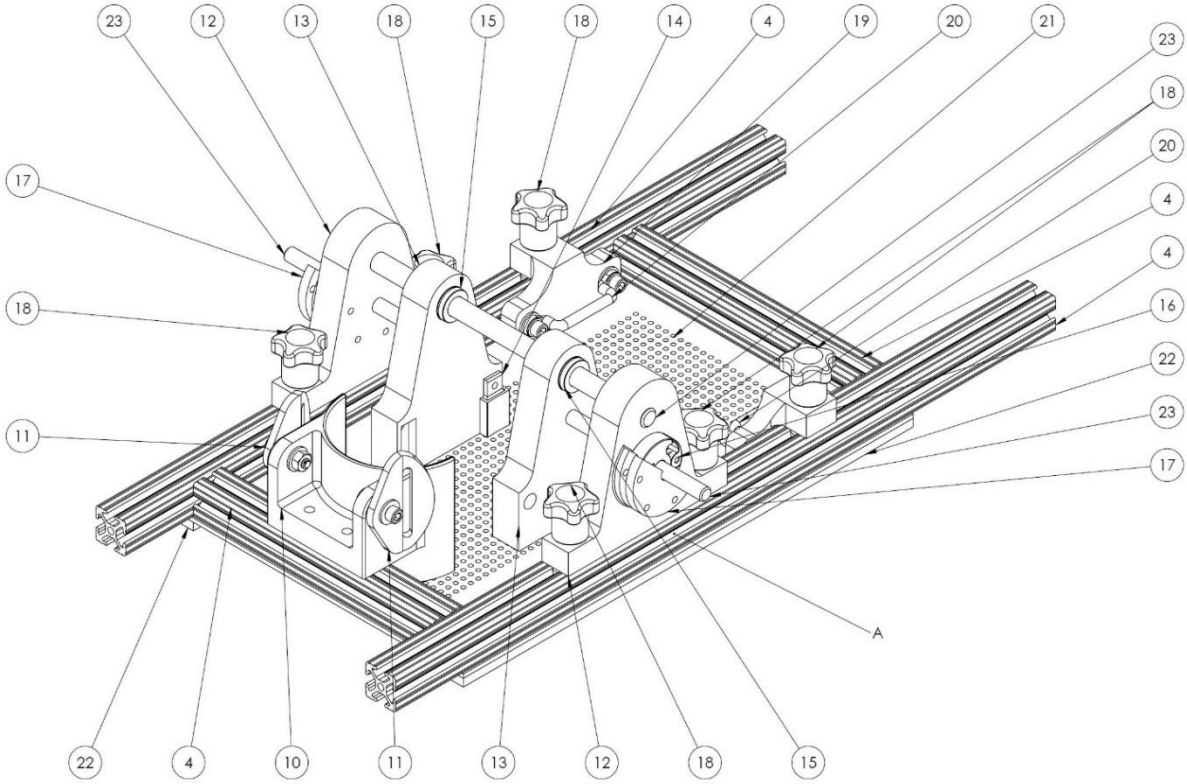

Figure 4-4: Foot Clamp Mechanism

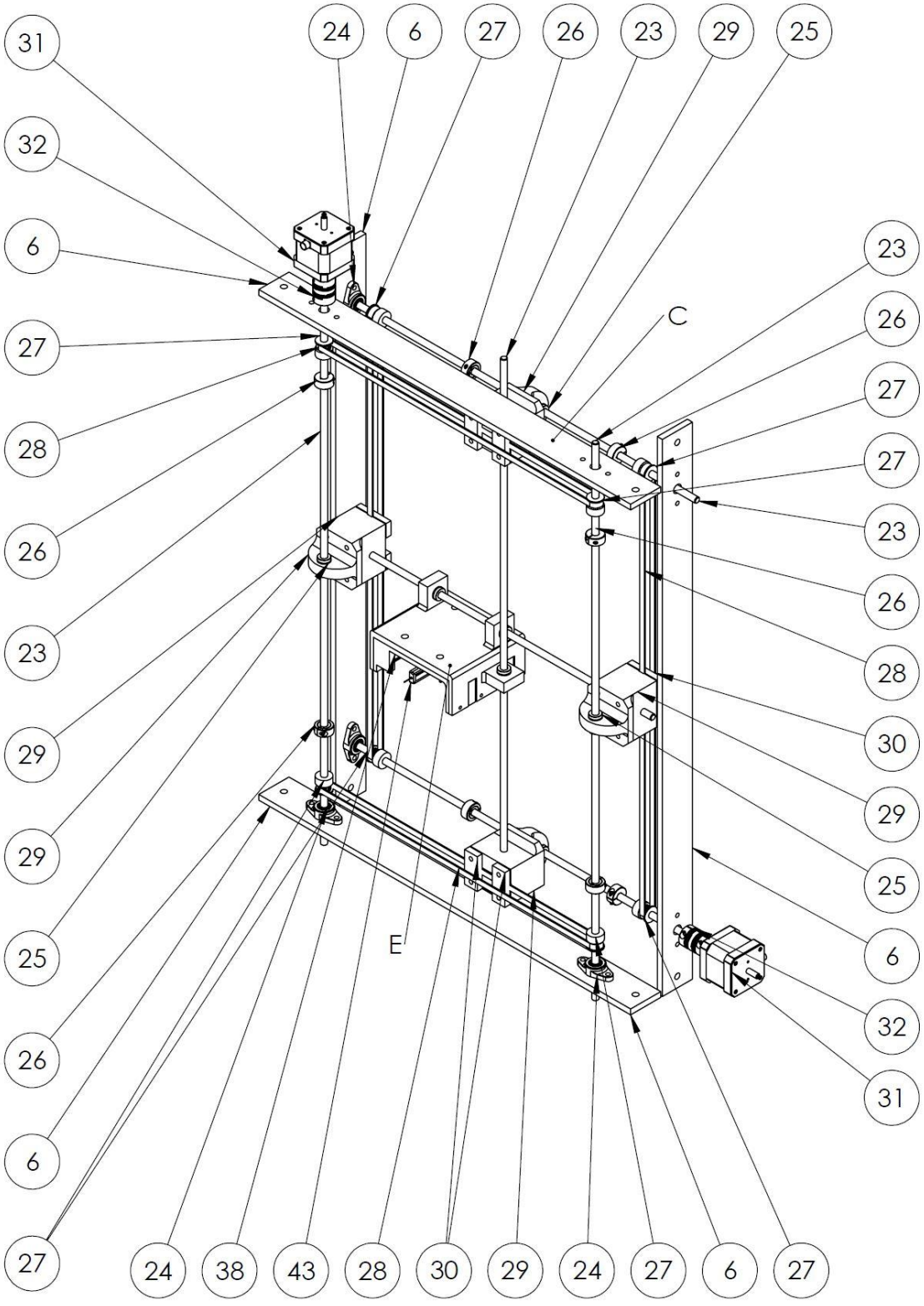

Figure 4-5: Gantry Pictorial A

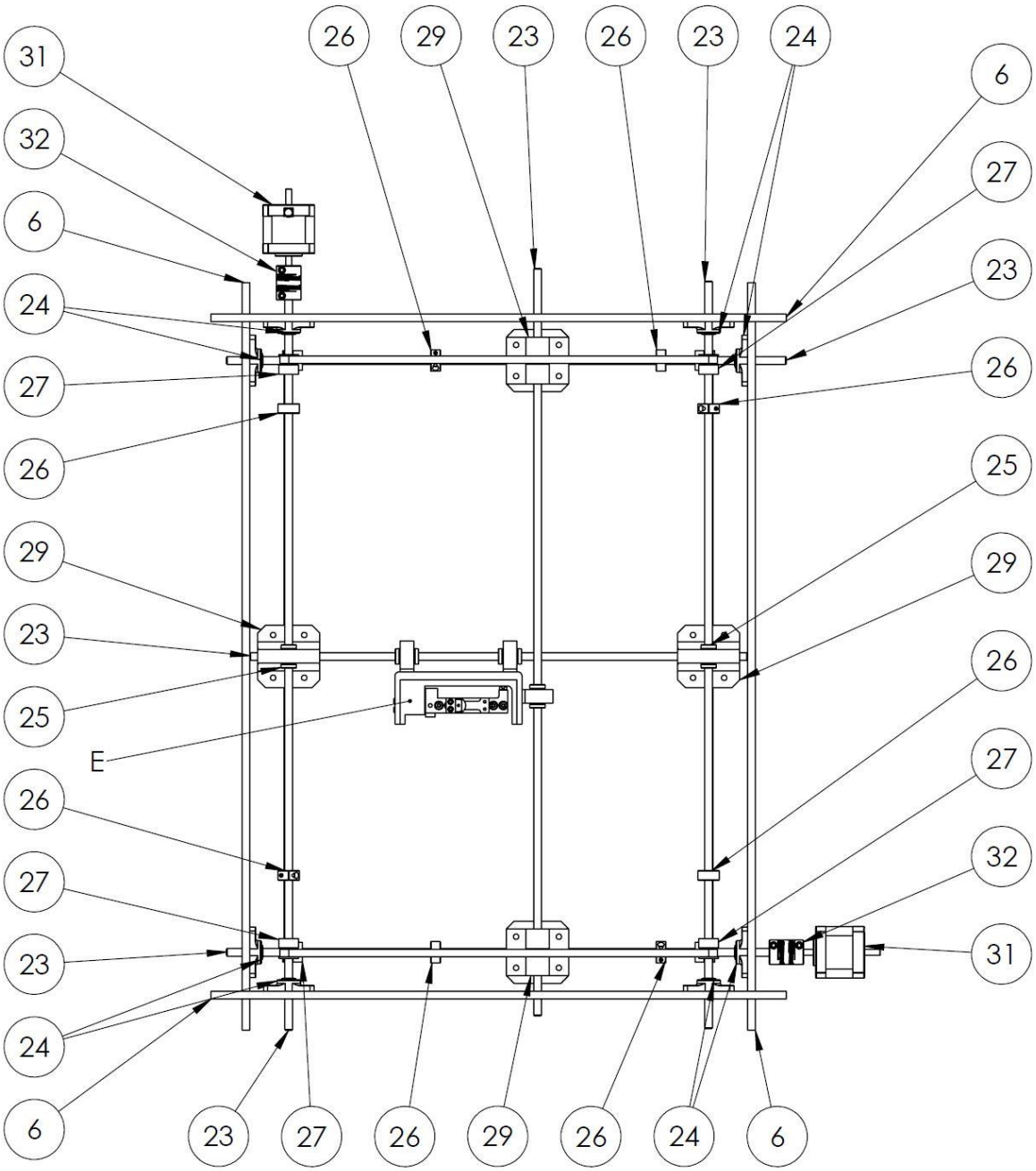

Figure 4-6: Gantry Pictorial B

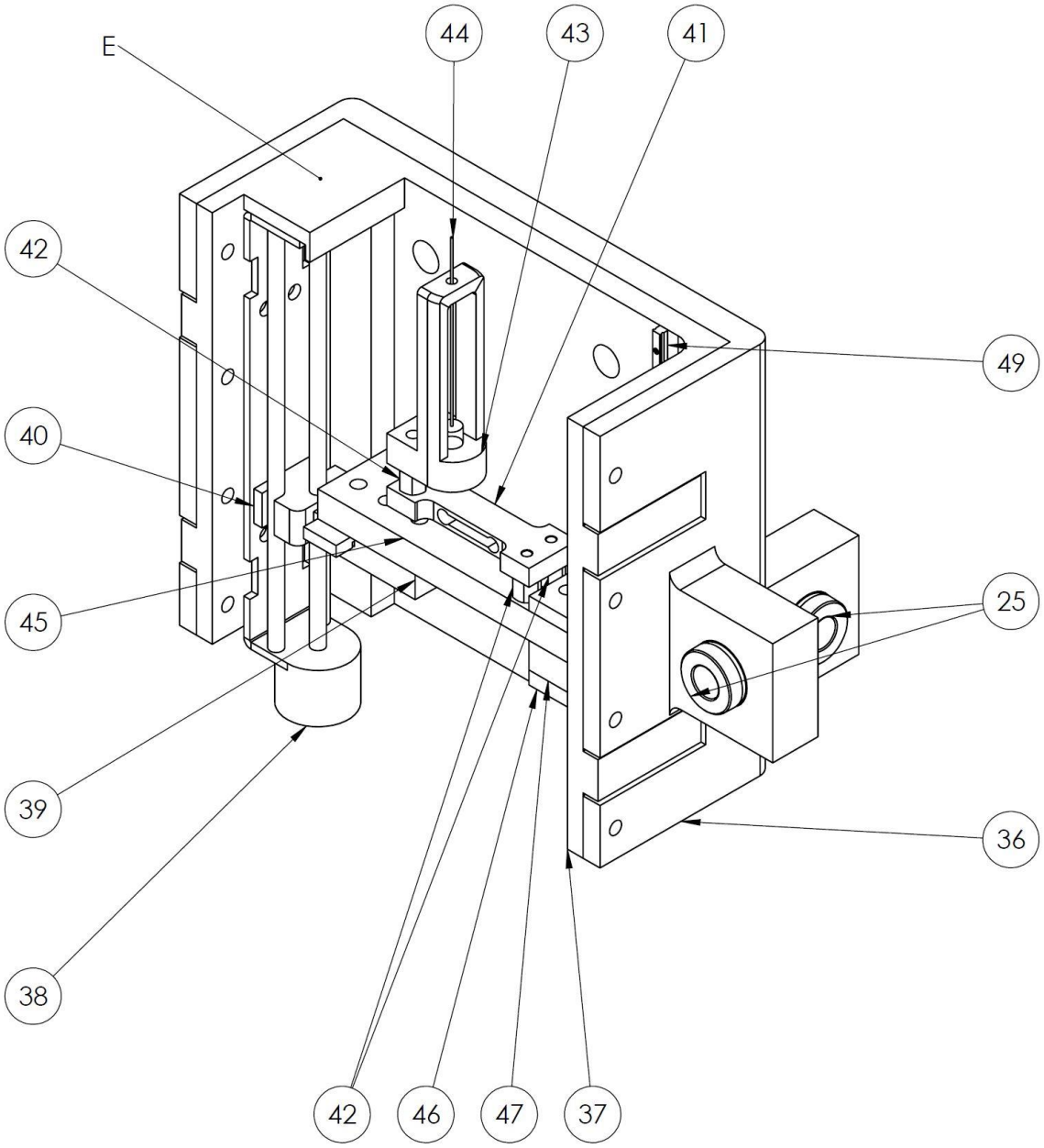

Figure 4-7: Monofilament Holder Pictorial A

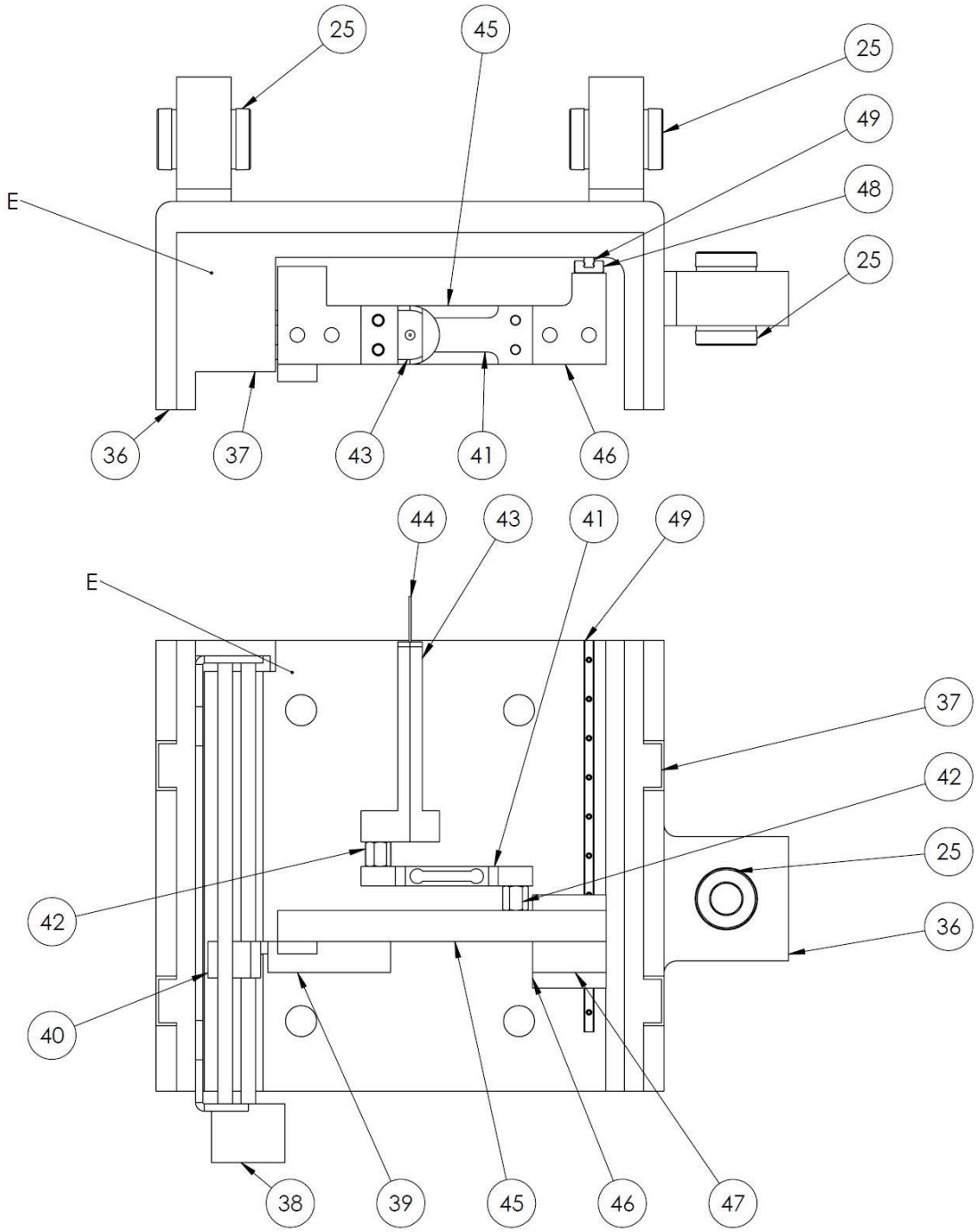

Figure 4-8: Monofilament Holder Pictorial B

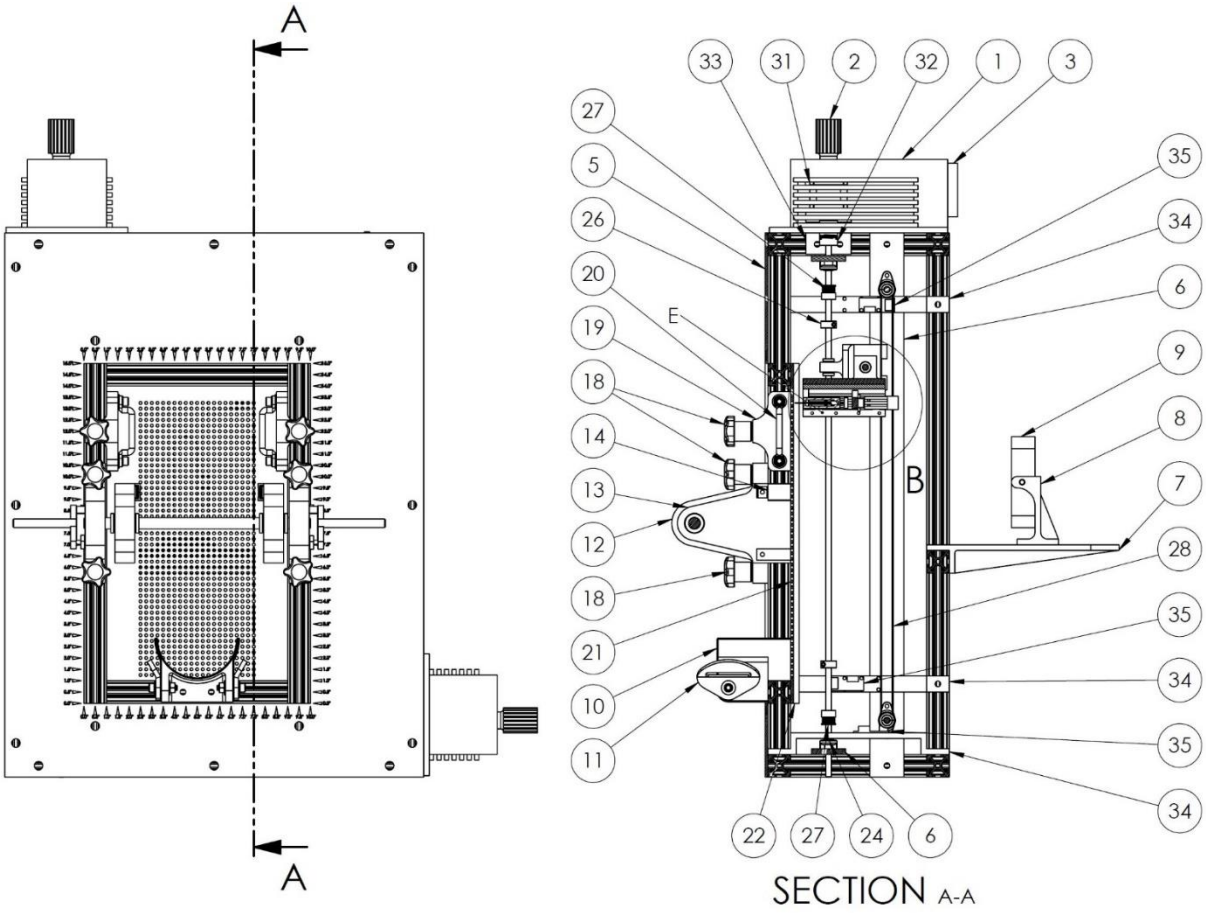

Figure 4-9: Neuropathy Diagnostic Tool Cross Section

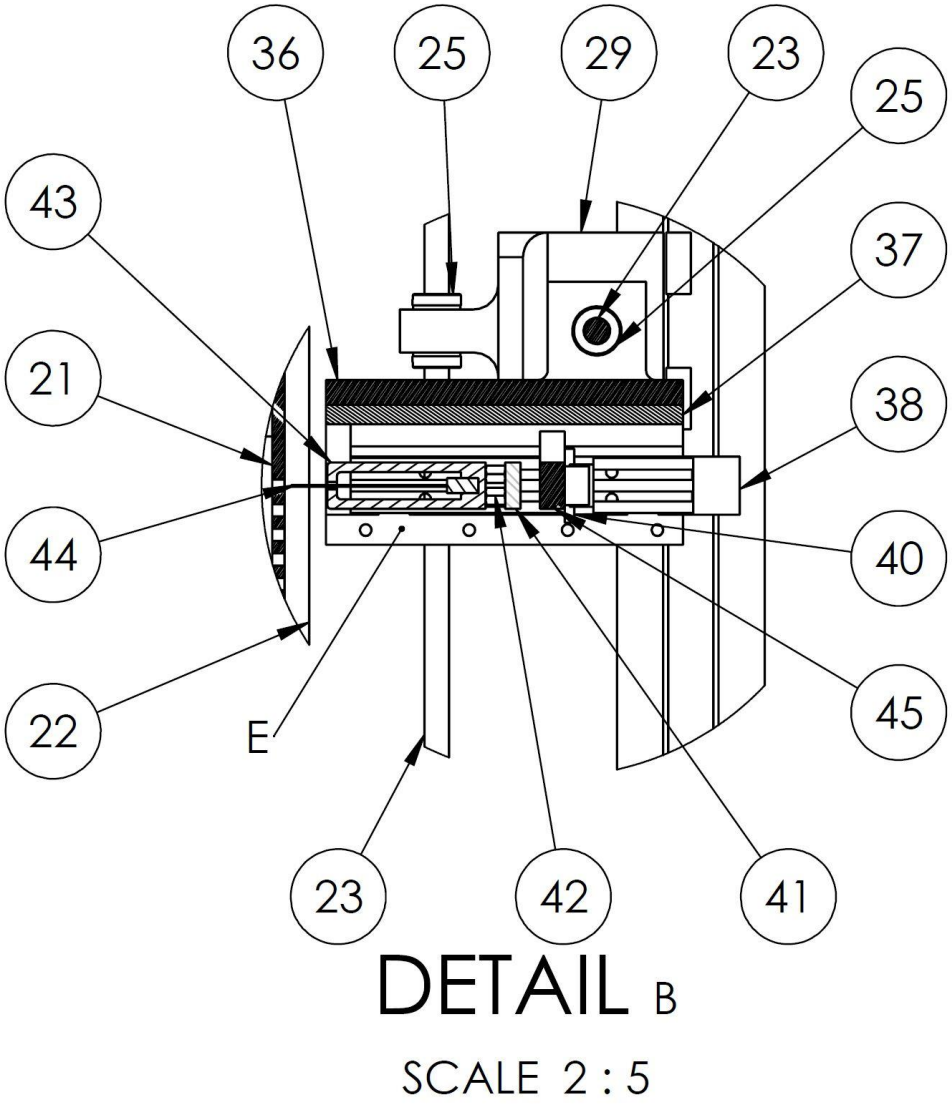

Figure 4-10: Monofilament Holder Close-Up

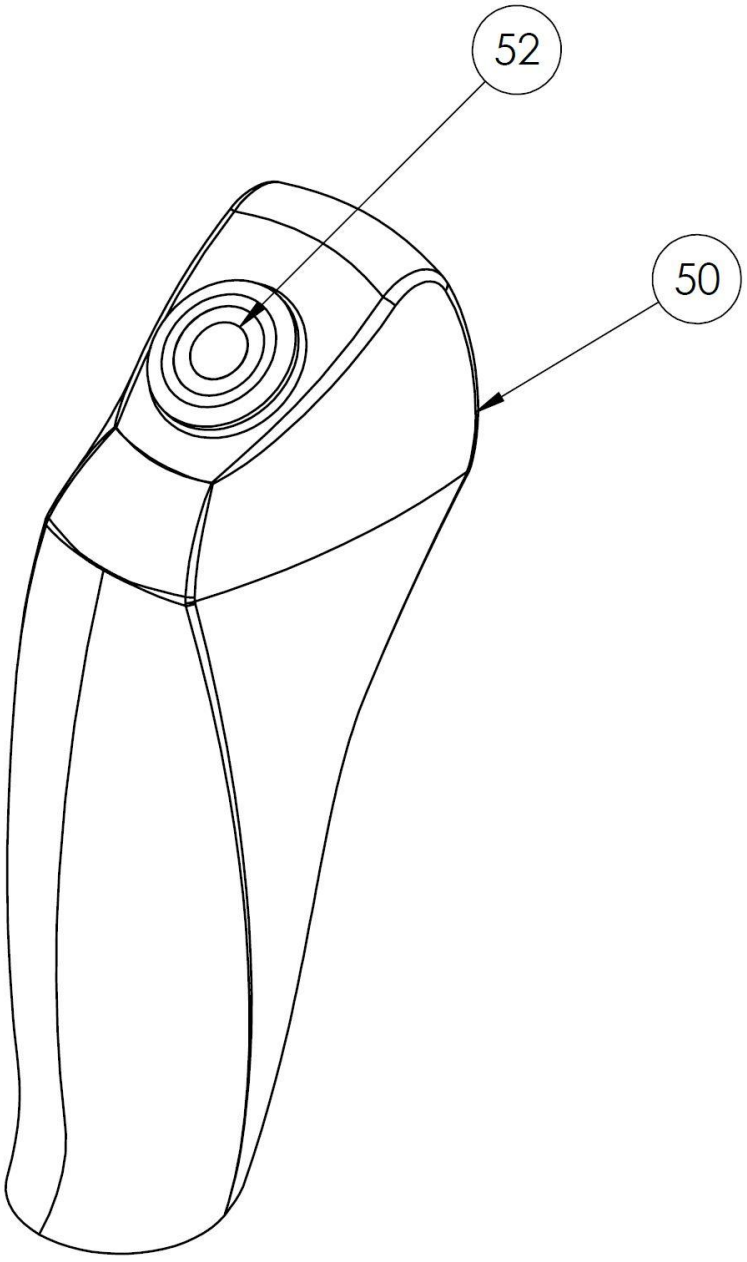

Figure 4-11: Response Handle Pictorial A

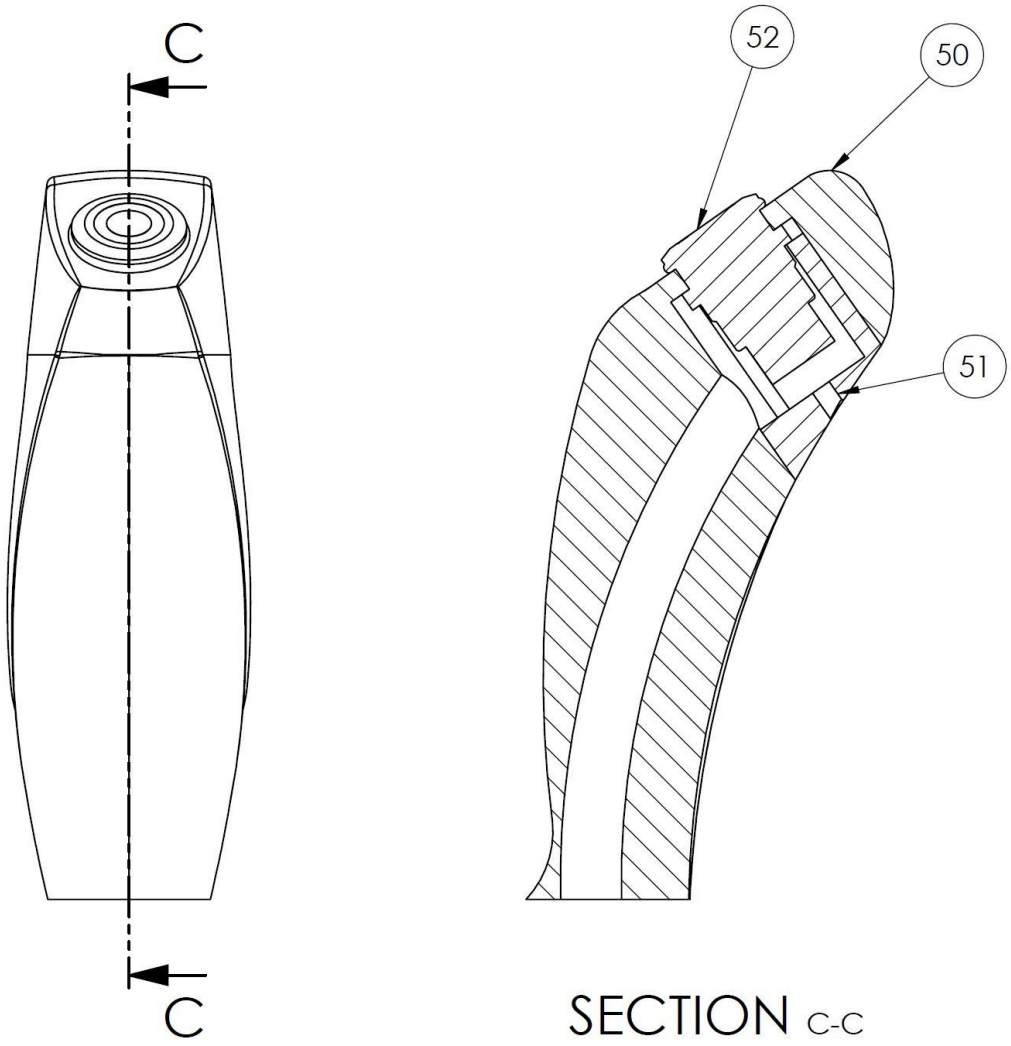

Figure 4-12: Response Handle Pictorial B

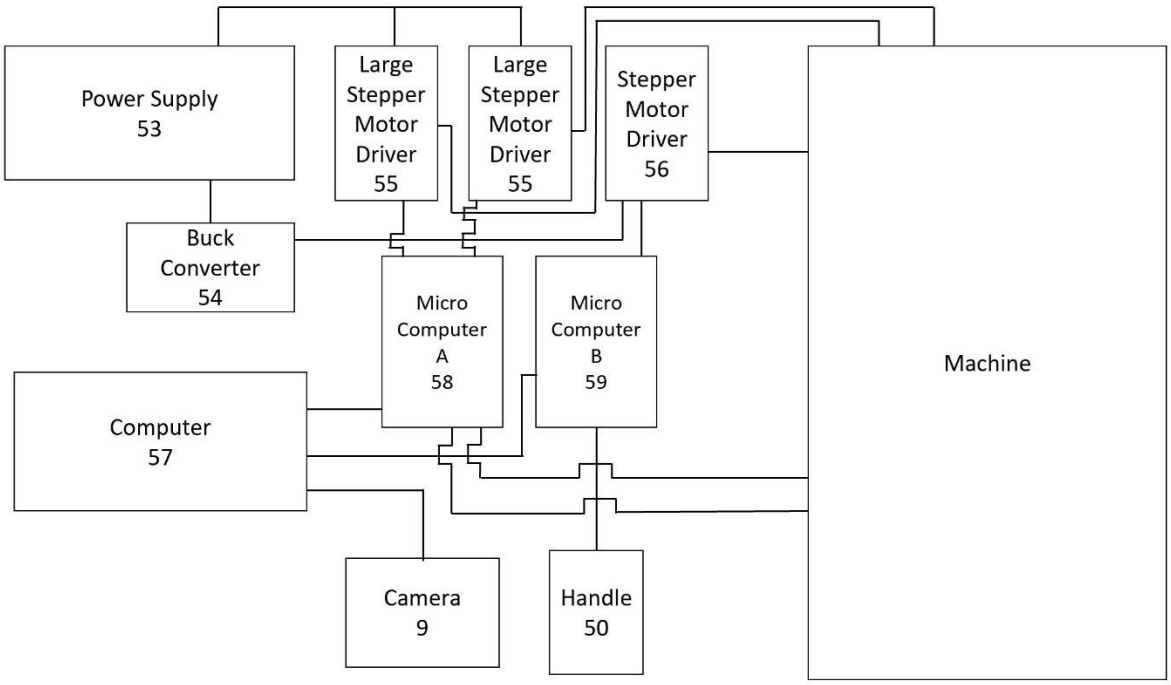

Figure 4-13: Machine Component Hookup Diagram

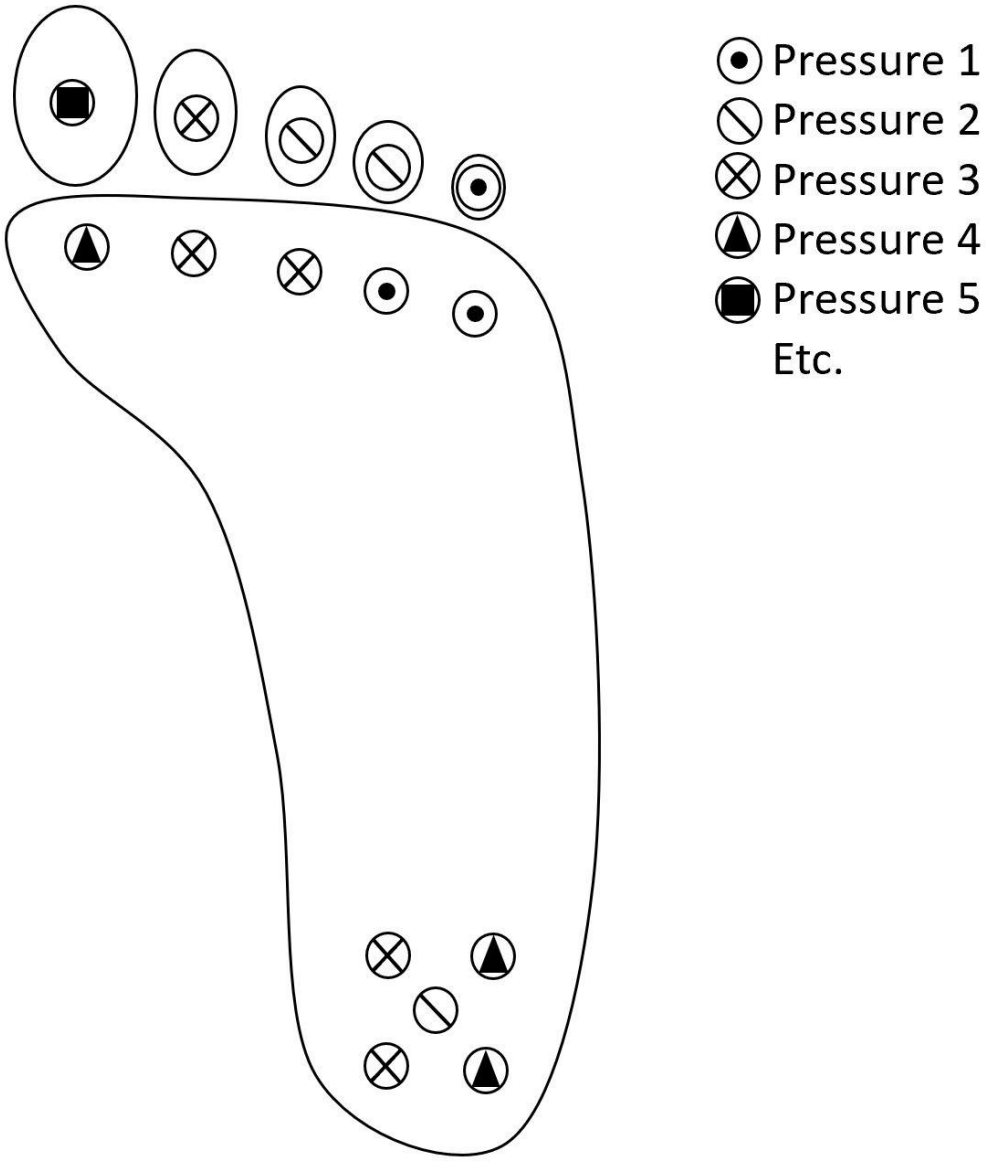

Figure 4-14: Threshold Sensitivity Map Example

4.3 Background Description

Diabetes is an ever-increasing diagnosis that carries with it numerous neuropathic complications. It is estimated that over 7.5% of adults in the United States have diabetes; this number reaches as high as 30 million Americans with the inclusion of children [51, 52].

The cost of care of diabetes is fast approaching $300 billion per year with at least 60% of this cost directed toward hospitalizations and treatment of complications. Diabetic foot complications are the most common and too often lead to ulcerations, and sadly, amputation. The cost of diabetic foot disease is estimated at over $10 billion per year, above the cost of routine diabetic care. Eighty-five percent of all amputations are attributed to preceding foot ulcerations [53]. The standard for evaluation of diabetic feet has traditionally included: foot inspection, checking for peripheral pulses, the ability to detect vibration and ankle reflex, the sensing of pinprick, the ability to distinguish between hot and cold, and the monofilament test. Different studies have evaluated various clinical tools for diabetic foot assessment such as MNSI (The Michigan Neuropathy Screening Instrument), and a United Kingdom screening test. Both of these tools use inspection, vibration sense of the great toe, and evaluation of the Achilles tendon reflex. A few instruments have been used to assess diabetic neuropathy such as the Vibratron II (Physitemp Instruments), NC-stat (Neurometrix) and Neutron RSCPT (Neutron Inc.). The conclusion of one study was that Vibratron II and MNSI showed the highest sensitivity (85%), while the monofilament test had the highest specificity (98%) [54]. One study out of Egypt looked at the biomechanics of the feet and was able to correlate pressure points with the likelihood of developing neuropathy [55].

The importance of understanding and diagnosing neuropathy has led to the design and development of a machine, which is able to apply a pressure stimulus at the plantar surface of the foot. It utilizes the current method of neuropathy assessment by applying a monofilament which

when applied produces a certain amount of pressure. These monofilaments are often a set length with varying cross sections to supply different pressures. The most common is a 10-gram rated monofilament, which is considered the threshold of developing severe neuropathy. They are commonly referred to as Semmes-Weinstein monofilaments. When the 10-gram monofilament buckles it produces a corresponding pressure at the testing site. For some individuals with severe neuropathy they may step on a nail and not even feel it. This can lead to infections, ulceration, and amputations. An amputation may start off with just one small part of the foot but can progress in the amputation of a limb. The monofilament testing method is often referred to as the gold standard of neuropathy assessment. However, it is subjected to inaccuracies. A physician may apply the monofilament at too high a speed, which results in the monofilament applying a greater pressure than it should have. Additionally, the monofilament may be inserted at an angle. Furthermore, this doesn't consider the topography of the skin, such as smoothness versus roughness and fatty versus boney surfaces. Quality control is another issue with using the current hand applied methods, where the monofilaments may differ in length and may not be perfectly uniform. These monofilaments may also be slightly bent out of the box. Achieving accurate repeatable measurements is paramount for neuropathy assessment and the current hand application method does not accomplish this. Hence a machine was developed that would standardize the testing process and would be able to improve upon the current monofilament test shortcomings.

This device can change the landscape of diabetic neuropathy assessment by making it affordable, portable, and able to provide reproducible results. The clinical significance of this instrument could identify neuropathy earlier and indicate which sites on an individual's foot are at greatest risk for ulceration and other complications. Also, it would be advantageous to detect neuropathy in patients before they develop symptoms. The machine collects data on the patient's foot in order to

determine if they are suffering from a loss of sensitivity at different amounts of pressure. A threshold sensitivity map is then generated from the data. This map more accurately and better quantifies the degree of neuropathy the patient is suffering. Such information would allow for individualization of foot health treatment and greatly assist in prevention of foot ulcerations and amputation.

4.4 Technical Description

A device that measures the threshold touch sensitivity of individuals by applying various noninvasive pressures at multiple locations upon the plantar surface of the foot. Locations are selected for pressure evaluation from an image of the plantar surface against the plate and then randomized to determine the sensation limit at that location. Patient responses are recorded, and the data generates a threshold sensation map visually showing the results of the assessment. The results can validate the effectiveness of potential treatments for diseases, such as peripheral neuropathy.

This machine works by moving a monofilament in 3D space in order to apply a pressure stimulus on the plantar surface of the foot. This translation is achieved with the use of stepper motors which when paired with belts and pulleys allow the monofilament to be positioned anywhere within the constraints of the machine. A stepper motor attached to a lead screw is used to insert the monofilament, noninvasively, until it makes contact with the patient's foot at a prescribed pressure. The monofilament is part of a complex assembly involving a load cell, which measures the pressure of the monofilament. However, it takes it a step further by analyzing the contact pressure until it reaches the prescribed value. This means that the machine can be set to apply an equivalent pressure of 1 gram and once it reaches this value on the plantar surface of the foot it will retract the monofilament. The monofilament is rated for 10 grams and the machine can comfortably be

used at any value between 0.2 and 10 grams; however, it has been able to produce values exceeding 10 grams and below 0.2 grams. Using different monofilaments, with different lengths, cross sectional areas, and materials can be used to alter this range. To ensure an accurate applied pressure a load cell reads at a fast rate and a system is set in place to slow the insertion of the monofilament until it reaches the desired value. The machine's ability to not only produce a pressure, but to measure and analyze the pressure during evaluation, allows the machine to map the threshold sensitivity of the patient's foot over many locations. All of the machine's components can be secured inside of a chassis made out of aluminum support materials, however other rigid materials can be substituted. This structure is lightweight and gives the machine its overall shape. The supports also allow for components to be moved and repositioned as needed. The implementation of a camera normal to the plantar surface allows for the selection of test locations. The overall results of the evaluation are plotted on an image taken from the camera in order to display an individual's threshold sensitivity.

During a plantar surface evaluation, the patient will put their foot on a perforated plate, containing numerous holes, through which the monofilament will be able to go. Each hole corresponds to a potential testing location and with the use of a camera, the operator can select points of interest. Additionally, a clamping structure may be used to keep the individual's foot in place during testing. The current design utilizes straps and an adjustable clamp to keep light contact between the patient's foot and the transparent plate.

A computer script was written to control all aspects of the machine. Specifically, this code sends instructions through USB ports on the computer to microcomputer A and microcomputer B. The microcomputers then interpret the instructions and with the use of the stepper motors, the load cell, the camera, and other electrical components, the machine is able to semi-automatically map the

threshold sensitivity of the foot. First a homing sequence is initiated to prepare the machine for the test. The patient's foot is then placed in the foot clamp apparatus and strapped in with light pressure. Next a picture is taken of the plantar surface of the foot using the camera mounted on the backside. This image is then used to select test locations. These locations are then randomized to avoid bias. False positives are also randomly assigned to the testing locations. At every location a prescribed pressure value, ranging from 0.2-10.0 grams of equivalent pressures, will be applied, whose range can be modified with different monofilaments and subtle changes to the device. The patient will then give a response using a tactile LED pushbutton, where a positive response means that they were able to feel the monofilament. Once the monofilament has been applied to the prescribed pressure and returned to its origin the LED will start to blink for five seconds. During these five seconds the patient will depress the button if they felt the monofilament. This feature can also work during a false positive check. If the patient did not feel the monofilament, this location will be retested at a new value until they are able to feel the monofilament or until they reach the 10-gram maximum pressure threshold. The data will be plotted on the image of the person's foot once all test locations have been assessed. A map will show the threshold sensitivity of the foot and will indicate which areas are healthy and which are demonstrating a loss of sensation or even neuropathy.

Completing the evaluation as quickly as possible (for example five to ten minutes), while also getting accurate measurements is paramount because desensitization could occur as a result of potentially repeating the pressure stimulus at different values. It is also important that the patient remain comfortable while being evaluated. As such, the patient can be laying on their back during the test. Furthermore, the foot clamp apparatus has foam padding placed in the ankle support and foot clamps to provide comfort.

4.5 Descriptions of Diagrams

Table 4-1: Diagnostic Tool Components

Table 1: Components	
ITEM NO.	PART NAME
1	Motor Cover
2	Motor Knob
3	Fan
4	Support
5	Cover Plate
6	Chassis Support Plate
7	Camera Mounting Plate
8	Camera Mount
9	Camera
10	Ankle Support
11	Ankle Strap Plate
12	Clamp Base
13	Foot Clamp
14	Locator
15	Large Sleeve Bearing
16	Clamp Lock
17	Lock Cover
18	Lock Handle
19	Toe Clamp
20	Foot Strap Plate
21	Foot Plate
22	Foot Plate Support Bracket
23	Shaft
24	Bearing
25	Sleeve Bearing
26	Hard Stops
27	Pulley
28	Belt
29	X/Y Axis Connector
30	Belt Tension Plate
31	Large Stepper Motor
32	Motor Coupling

33	Motor Mount
34	Limit Switch Mount
35	Limit Switch
36	Head Connector
37	Head Chassis
38	Small Stepper Motor
39	Monofilament Support Connector
40	Slider
41	Load Cell
42	Standoff
43	Monofilament Load Cell Adapter
44	Monofilament
45	Load Cell Connector Plate
46	Monofilament Support Holder
47	Monofilament Support Plate
48	Guide
49	Rail
50	Handle
51	Handle Cap
52	LED Button
53	Power Supply
54	Buck Converter
55	Large Stepper Motor Driver
56	Stepper Motor Driver
57	Computer
58	Microcomputer A
59	Microcomputer B

Figure 4-1 represents the machine in its entirety. It shows the machine it its upright position, making note of item **A**, **B**, **C**, and **D**. Item **A** is the foot clamp apparatus, item **B** is the chassis, item **C** is the linear motion translation assembly, and item **D** is the camera assembly. The motor cover **1** shields the large stepper motor **31** but allows ventilation for cooling via the fan **3**. The motor cover **1** also protects individuals from coming into contact with the large stepper motors **31**. Although the large stepper motors **3** are controlled via microcomputer A **58** they can be manually rotated by the motor knob **2** to facilitate linear motion. The motor cover **1** is connected to the

supports **4**. Affixed to the chassis is the cover plate **5**, which acts as the front face of the machine. In this iteration of the machine it is made from a transparent material, but can be made from a plethora of solid materials. The cover plate **5** also has position markers located on its face to aid in foot relocation and position applications. Item **A** is comprised of multiple components. The ankle support **10**, retains the ankle in a secure position during evaluation. Furthermore, with the use of both ankle strap plates **11**, the ankle can be strapped down to maintain a secure position by applying a minimal amount of compression on the ankle. In order to prevent the foot from rotating within the ankle support **10**, a clamp base **12** and a foot clamp **13** are joined together to create a clamping structure. There are two clamping structures. Both clamp bases **12** are connected to each other by a shaft **23**. The foot clamps **13** house a large sleeve bearing **15** which linearly translates on the shaft **23** that connects both clamp bases **12**. Each foot clamp **13** houses a shaft **23** which interconnects to the clamp base **12** and can be locked in place with clamp lock **16**. A lock cover **17** applies compression to the clamp lock **16** in order to hold in the clamp base **12**. The foot clamp **13** also uses a locator **14** which can be used to help position the foot in the clamping apparatus. Additionally, the toes are compressed with the use of two toe clamps **19**, each of which includes a foot strap plate **20**. A strap is inserted in the foot strap plate **20** resulting in compression on the toes. The clamp base **12** structures and the toe clamp **19** structures are secured to the support **4** with lock handles **18**. However, by loosening the lock handles **18** slightly the clamp base **12** and toe clamp **19** are able to translate linearly along the support **4** in order to accommodate varying foot sizes. One of the most important components of the device is the foot plate **21**, which is a manufactured from a transparent material. The foot plate **21** is comprised of numerous holes which accommodates for varying foot sizes in additional to other elements of item **A**. Moreover, item **B** and item **C** are connected together with chassis support plates **5**. This figure also shows that hard

stops **26**, pulleys **27**, belts **28**, and the X/Y axis connector **29** are all assembled in item **C**, which is ultimately what allows for linear translation of the monofilament **44**.

Figure 4-2 reveals the chassis, item **B**, of the device unobstructed by all other components. It is entirely made up of supports **4** which create a hollow rectangular shape. Furthermore, the camera mounting plate **7** connects to this chassis. The camera **9** connects to the camera mount **8** which is fixed onto the camera mounting plate **7**. These features are all part of item **D**.

Figure 4-3 shows an unobstructed view of item **D**, the camera assembly. Here it clearly shows how the camera mounting plate **7**, the camera mount **8**, and the camera **9** all connect to a support **4**. The camera mount **8** can be moved along the camera mounting plate **7** to accommodate for different types of cameras **9**. This allows for the optimal location for the camera **9** to be placed at. The camera **9** takes a photo of the patient's foot when placed in the device and this photo is then used to select testing locations. At the end of the evaluation the data is plotted on this image.

Figure 4-4 is a close up of item **A**, the foot clamp apparatus. Its overall shape is made up of four supports **4**. Connected to the supports **4** is the foot plate **21**, which houses an array of holes in order to accommodate for different foot sizes. The foot plate **21** is further reinforced by two foot plate support brackets **22**, which apply compression to this part and connect to the supports **4**. Likewise, this figure also highlights the clamping features of the machine. The ankle support **10** and the ankle strap plates **11** are used to fix the ankle in place during testing. The clamp bases **12**, foot clamps **13**, and locators **14** are assembled together with shafts **23** and large sleeve bearings **15**. When these parts are combined, they create a structure used to keep the foot from rotating by applying minimal compression. This is achieved by using the clamp locks **16** and the lock covers **17**. The toes are compressed by an assembly of toe clamps **19** and the foot plate straps **20**. The toe clamps **19** and the clamps bases **12** translate linearly along the support **4** and lock in place with the use of lock

handles **18**. All of these features allowing for varying foot sizes to be tested and also allow for the foot to be reasonable relocated to for future evaluations.

Figure 4-5 is the linear translation assembly, item **C**, and it highlights the major components of the system used to move the monofilament **44** to locations of interest. The chassis support plates **6** serve two purposes. One is to provide additional rigidity to the chassis, item **B**, while the second is to hold all of the linear translation components together. Bearings **24** are fastened to the chassis support plates **6**, in which shafts **23** are capable of rotation. Two large stepper motors **31** provide the means of rotary motion by the use of motor couplings **32** to the shafts **23**. In order to turn the rotary motion of the large stepper motors **31** into linear motion a shaft **23** is placed parallel to the shaft **23** directly connected to the large stepper motor **31**. These assemblies are then connected to each other by pulleys **27**, fixed on the shafts **23**, and belts **28**. Also attached to the shafts **23** are four X/Y axis connectors **29**. These connectors join the opposing shafts **23** together and when combined with the large stepper motors **31** move the head, item **E**, to a plethora of valid testing locations on the foot plate **21**. The head sleeve bearings **25** attached to the X/Y axis connectors **29** and glide over the shafts **23**. The belts **28** are secured to the X/Y axis connectors **29** via the belt tension plates **30**. This all creates a system to move the monofilament in 3D space and although the positioning is controlled with software, hard stops **26** are still employed for safety. The hard stops **26** act as a limit by defining the range of motion the monofilament can move in.

Figure 4-6 pictures the linear translation assembly in a normal orientation. Here it can easily be witnessed how the two large stepper motors **31** each drive a shaft **23** and transmit rotation movement to a parallel shaft **23** with the use of pulleys **27** and belts **28**. Interconnected to these shafts are X/Y axis connectors **29** which translates the head, item **E**. Bearings **24** and sleeve bearings **25** allow for smooth translation between surfaces and the hard stops **26** act as safety limits,

which constrains the range of motion of the machine. All of which is connected to the chassis support plates **6**.

Figure 4-7 depicts the head, item **E**, and is arguable the most important aspect of this machine. The head connector **36** houses all of the parts in this subassembly and is also what directly connects to the linear translation assembly, item **C**. Three sleeve bearings **25** are used to facilitate smooth linear travel of the head. A head chassis **37** fastens to the head connector **36** and it also houses the small stepper motor **38**. This motor is attached to a lead screw which converts rotation movement to linear movement. A slider **40** is driven by the small stepper motor **38** and is attached to the load cell connector **45**. A monofilament support connector **39**, a monofilament support holder **46** and monofilament support plate **47** are used to fasten the load cell connector plate **45** to the slider **40** and the rail **49**. This allows for smooth linear motion of the monofilament when it is being inserted into the patient's foot, noninvasively. This is paramount for accurate repeatable measurements from the load cell **41**. The load cell **41** is a device that uses a Wheatstone bridge to convert a change in electrical resistance to a change in mass. The load cell **41** is secured to the load cell connector plate **45** with standoffs **42**. The monofilament **44** is inserted into the monofilament load cell adapter **43**, which is also attached to the load cell **41** with additional standoffs **42**.

Figure 4-8 further highlights the components of the head, item **E**. Here is can be seen that the head connector **36** houses three sleeve bearings **25**, and also retains the head chassis **37**. The small steeper motor **38** and its slider **40** are also highlighted here. Moreover, the intricate assembly involving the monofilament support connector **39**, the load cell connector plate **45**, the monofilament support holder **46**, and the monofilament support plate **47** is present. This assembly when connected to the slider **40** and the rail **49**, with the use of guide **48**, creates a stable platform

for the load cell **41**. The load cell **41** fixes to this assembly with the use of standoffs **42** and connects to the monofilament **44** via the load cell adapter with additional standoffs **42**.

Figure 4-9 represents a section view of the machine, Section **A-A**. Here is can be observed how complex the machine is. The supports **4** are used to house everything together. The motor cover **1**, the motor knob **2**, and the fan **3** are positioned in proximity of the large stepper motor **31**. Additionally, the large stepper motor **31** is not only connected to the shaft **23** with the motor coupling **32** but is connected to support **4** with the motor mount **33**. Also present are pulleys **27**, belts **28**, bearings **24**, and hard stops **26**, all of which aid in the linear translation assembly. Moreover, this view also shows the limit switch mounts **34** and the limit switches **35**, which are used to run a homing sequence upon machine start up. This homing sequence is used to position the machine accurately upon every evaluation. Although the limit switches **35** are meant to define the range of motion in the software side of things, hard stops **26** are still installed for additional safety precautions. The chassis support plates **6** refines the overall structure providing rigidity and fastening points for the linear translation assembly. The camera mounting plate **7**, camera mount **8**, and the camera **9** are all present in this view and connect to a support **4**. The cover plate **5** attached to the support **4**, while the foot plate **21**, with the use of the foot plate support bracket **21**, also fastens down on supports **4**. Aspects of the foot clamp apparatus are also accounted for, including the ankle support **10** and the ankle strap plate **11**, which in tandem are used to fix the ankle in place. The clamp base **12**, foot clamp **13**, and the locator **14** prevent rotation during evaluation. The toe clamp **19** and the foot strap plate **20** also prevent motion during the test. These components are able to translate, can be adjusted for different foot sizes, and can lock in place with the use of lock handles **18**. All of these components help the head, item **E**, during the evaluation

process by moving it from location to location while the patient's foot is securely fixed to the machine.

Figure 4-10 showcases Detail **B** of the head, item **E**. This figure shows how the monofilament **44** goes through the holes of the foot plate **21**. The foot plate **21** is reinforced with the foot plate support bracket **22**. Furthermore, the head connector **36** houses the head chassis **37**, which retains the small stepper motor **38** used to drive the monofilament **44** through the holes of the foot plate **21**. The slider **40** converts the rotational movement of the small stepper motor **38** lead screw into linear translation. The slider **40** connects to the load cell connector plate **45** creating a stable platform. This platform is used to secure the load cell **41** with the use of standoffs **42**. The load cell **41** is then attached to the monofilament load cell adapter **43**, with standoffs **42**, which houses the monofilament **44**. Additionally, the head connector **36** utilizes sleeve bearings **25** which glide through shaft **23**. This shaft **23** is secured to the X/Y axis connector **29** which also has a sleeve bearing **25** guided through an additional shaft **23**.

Figure 4-11 represents a pictorial view of the handle **50**, which is used to collect the patient's response during evaluation. It houses a LED pushbutton **52** that will blink for five seconds indicating to the patient when they should depress the button if they felt the monofilament **44**. The handle **50** is designed to be ergonomic and is hand neutral. It can also be held in multiple ways to accommodate the patient's needs.

Figure 4-12 shows a section view, Section **C-C**, of the handle **50**. It details how the LED pushbutton **52** is connected to the handle **50**. A handle cap **51** is also used to hide all electrical connections coming from the LED pushbutton **52**. A hollow cavity inside the handle **50** is used to channel the wires.

Figure 4-13 details the wiring diagram for the machine. A power supply **53** supplies power for the large stepper motor drivers **55**. The power supply **53** is also connected directly to the buck converter **54** which is then used to power the stepper motor driver **56**. A computer **57**, which houses the script to run the machine, is connected to microcomputer A **58** and microcomputer B **59**. The computer **57** is also connected to camera **9**, which is also controlled by the script. Microcomputer A **58** is used to control the large stepper motor drivers **55**. These drivers hook up to the large stepper motors **31**, used for linear translation. Furthermore, the microcomputer A **58** hooks up to the limit switches **35**, which are used for the homing sequence and for additional safety features. Microcomputer B **59** directly connects to the stepper motor driver **56** which hooks up to the small stepper motor **38**. Small stepper motor **38** assists in inserting the monofilament **44** noninvasively into the foot. Lastly microcomputer B **59** is linked to the handle **50**, which houses the LED pushbutton **52**. This is used to gather the patient's response following administration of a pressure stimulus.

Figure 4-14 represents a threshold sensitivity map of the plantar surface of the foot. Once the machine has evaluated all locations the corresponding threshold sensitivity pressures are plotted per location. Various magnitudes of pressures can be used for evaluation, such as pressure 1, pressure 2, pressure 3, etc. Furthermore, the results are plotted on an image of the actual patient's foot and not an arbitrary pictorial. This readily allows for the person's threshold sensitivity to be examined and understood by both the patient and the physician. This image serves as a way to quantify the degree of neuropathy an individual is suffering from and can be used to monitor changes as part of potential treatments.

4.6 Capabilities of the Device

The device is capable of applying a pressure stimulus of various magnitudes with a monofilament to the plantar surface of the foot. The device can produce various pressures using the same monofilament, which can be altered with changes in the length and cross-sectional area. The monofilament is inserted slowly until it makes contact with the skin, after which its insertion speed is gradually reduced until it reaches the targeted pressure. This test is noninvasive and does not cause harm to the patient. The monofilament is moved in 3D space with translation elements, such as belts, pulleys, and lead screws. The machine also secures the foot with a clamping apparatus which applies minimal pressure and provides comfort during evaluation. The device has a built-in homing sequence which is mandatory for the machine to be calibrated within the overall system. A camera is used to take a photo of the patient's testing surface and with a computer script test locations are selected from this image. The device is also able to record the response data from the patient with a LED pushbutton, whereby a push of the button indicates that the patient felt the monofilament. A pressure stimulus is applied until the individual's threshold sensitivity has been determined. This data is then plotted on the image of the plantar surface of the patent's foot showing a threshold sensitivity map. Ultimately this device can be used to better quantify neuropathy, can validate potential treatments, and potentially detect diseases such as neuropathy earlier.

4.7 Future Improvements

Future improvements of the machine include the addition of a mobile cart which will serve as a self-contained unit for all components of the machine, both hardware and electronics. The cart will also have an adjustable height feature to allow the machine to be placed in an optimal ergonomic position during testing. Additionally, a computer will be added onto the cart system. Vibration

dampening features will also be considered in the future. Subtle changes to the foot clamp apparatus will be investigated in order to make sure that individuals can be securely strapped in place during testing and to allow for relocation for future evaluations. Other minor hardware changes will be different tension mechanisms for the belts and slight changes to the head, which houses the monofilament and load cell assembly. Materials may also be subjected to change and could include aluminum, steel, and plastics. Some components could be manufactured using injection modeling techniques.

Regarding electronics, an alternative microcomputer will be considered, which could potentially replace the need of a computer to interface with the machine and or the necessity of one or both current microcomputers. A tablet may also be incorporated into the device which would allow for patients to indicate a response and where they felt the monofilament on their foot. Wireless communication between different electronic components of the machine will also be considered in future revisions.

The machine can be reconfigured to evaluate diminished sensations of other body surfaces such as the face, palm, lower back, buttock, and thigh.

4.8 Claims

1. A device for mapping of threshold sensitivity on the plantar surface of the foot, said device comprising:

   a. A support frame;

   b. A monofilament;

   c. A foot plate;

   d. A motor;

   e. A power supply;

f. A series of belts and pulleys;

Wherein said device can be operated to apply pressure via the monofilament at different locations on the plantar surface of the foot.

2. The device of claim 1 wherein operation can be semi-automatic.

3. The device of claim 1 wherein the pressure applied ranges from about 0.2 to about 10 grams.

4. The device of claim 3 wherein the same monofilament can be used to apply different pressures.

5. The device of claim 4 wherein the pressures applied via the monofilament are applied noninvasively using variable speed control.

6. The device of claim 5 wherein the pressure applied noninvasively via the monofilament stops after reaching a prescribed value measured by a load cell.

7. The device of claim 1 wherein the motor and series of belts and pulleys can move the monofilament three dimensionally to any location within a grid array on the foot plate.

8. The device of claim 1 further comprising a camera.

9. The device of claim 8 further comprising a microcomputer that documents and displays the plantar surface sensitivity results by an operator selecting testing locations from a photograph taken by a camera mounted to the device.

10. The device of any one of claims 1 through 9 wherein the foot is secured during evaluation.

11. The device of claim 10 wherein the device can accommodate multiple foot sizes.

12. The device of claim 11 wherein during a separate examination, the previously examined foot of a patient can be relocated to the same position in the device using the microcomputer and built-in features of the clamping apparatus.

Chapter 5: Conclusion and Future Work

5.1 Conclusion

Neuropathy is a disease, often developed in older type-2 diabetics. There are many complications associated with neuropathy, but the loss of sensation in the extremities has been directly associated with infections, amputations, and even death. Although there are current screening tools that are effective in diagnosis and monitoring sensation lost due to neuropathic complications, these methods are subjective to both the clinician and the patient. Some of the current diagnostic tools can only be applied on specific locations on the foot and are incapable of mapping out a person's threshold sensitivity over an entire body part, i.e. the plantar surface of the foot. The Semmes-Weinstein monofilament is a very popular assessment tool used to apply a specific amount of force at a targeted location. However, these monofilaments have been shown to be very subjective to the amount of insertion depth and the diameter via theoretical contact mechanics and finite element analysis. The results of these equations were depicted as surface plots which showed that higher amounts of insertion depths yielded greater amounts of contact force and normal stress. However the reduction in the monofilament diameter created lower amounts of contact force and higher levels of stress. The finite element analysis for the 10 gram monofilament correlated closely to the theoretical contact mechanics considering linear elastic human skin mechanical properties. Moreover, these results showed that it is very challenging to apply a monofilament to produce its rated contact force. Some clinicians may be able to overcome these influences and can constantly apply the correct amount of applied force but others may not be able to. Caution is recommended with the use of hand applied monofilaments, but this makes it very challenging to monitor disease progression and to validate potential treatments for neuropathy. A new automated testing methodology was developed, which has taken the current hand applied monofilament assessment

and standardized it. Using a force-based control method with a load cell and stepper motor in a feedback loop proved to be very effective in pilot testing. This allowed the machine to not only apply an accurate amount of force but was capable of applying a range of forces. This new methodology is independent of the length, diameter, and the quality of the monofilament and is more dependent on the skin properties. This device can be used on 95% of the world's population because of the large testing area and the adjustable foot clamp. This diagnostic tool also removed both clinician and patient bias by incorporating randomization during the assessment. False positive checks were also placed into the testing protocol to ensure that patients would respond truthfully. The use of randomization and false positives during the evaluation are currently absent from the manual monofilament test and when combined with the threshold sensitivity homing sequence created a potentially new standardized approach for neuropathy assessment. With this automated method a person's threshold sensitivity can be mapped out and documented. This visual can be used to monitor a person's neuropathy over time and to validate treatments. This diagnostic tool has the potential to not only being a better device used to diagnosis neuropathy but can also become a better documenting tool used to monitor disease progression and the efficacy of treatments.

5.2 Future Work

Building the Mk2 prototype is one of the biggest tasks to complete in the future. This will require components to be ordered and parts to be manufactured. Assembling the Mk2 prototype will only take two weeks once all components have been made and delivered, as a result of the improvements made in this design. Although Mk2 is considered the final iteration of the diagnostic tool there are still some improvements that can be implemented. One of the most important

improvements is an update to the code used to control the machine. In the current code the machine moves from one location to another based on the default GRBL feed rate. It would be advantageous to implement a variable feed rate control function in the code so that it can move faster. This can be accomplished by calculating the relative distance between two locations and then defining a range of feed rates. If the distance is relatively large a faster feed rate should be used, whereas a smaller distance would require a smaller feed rate. This variable feed rate parameter can be added onto the G-code generated in the MATLAB function. Determining the variable feed rate parameter goes hand in hand with measuring the positional accuracy of the device for multiple distance (0.25, 0.50, 1.00, 2.00, 3.00 inches, etc.). Similarly the accuracy of actual force applied to the surface of the skin needs to be analyzed and verified that it is within the ±0.5 gram force tolerance. Ideally this will be accomplished over multiple applications of a monofilament. Also studying force-time plots (impulse) as it relates to the accuracy of the stepper motor feedback loop system would be very insightful in validating this automated assessment method. Furthermore, a new function in the MATLAB script needs to be incorporated, which allows testing locations from a previous assessment to be loaded back into the program for reassessment. This would allow the machine to be used for treatment validation by testing the same locations over a period of time. A graphical user interface (GUI) is also recommended, especially for a commercial version of the diagnostic tool. The code could also be modified to reflect the predicted health of the patient. In essence this would mean that if the clinician believed that the patient had a minor sensation loss the machine could execute a bottom up approach, where it increases the magnitude of the force until their threshold is reached. Likewise, if the patient is believed to suffer from a high degree of sensation loss than a top down approach would be recommended. The methodology proposed in this thesis is best for those individuals in the middle but is also sufficient for conducting clinical trials needed

to validate the device. Having the ability to select which of the three testing protocols would be a beneficial feature in a commercial variant of the diagnostic tool. Another improvement is to find a way to reduce from two Arduinos down to one. This would require finding a way to combine GRBL with the custom Arduino function developed to apply the monofilament. A custom microcontroller could also be considered, or even a Raspberry Pi controller. Another future improvement is to convert the MATLAB scripts and functions into a different computing language (C+ or ROS). Although MATLAB has been very effective and is fully capable of controlling the machine, a commercial version of the machine will need to be controlled with a more robust code. In the current iteration of the machine the picture taken by the webcam suffers from some lens distortion, as such a better camera should be sourced to correct this.

Nonetheless, the most important work that remains with the diagnostic tool is to collect data in a clinical setting, in order to determine this device's feasibility to detect and monitor neuropathy. A future study will include 200 individuals, all 40 years of age or greater. These individuals will be divided into four cohorts: control, type 2 diabetes without neuropathy symptoms, type 2 diabetes with neuropathy symptoms, and type 2 diabetes with a history of ulcers and amputations as a result of neuropathy. All diabetic patients must have had their diabetes diagnosis for over five years and have to have an ankle-brachial index of greater than 1.0 to be included in the study. The subjects will be evaluated using a manually applied 10 gram monofilament and a 128 Hz tuning fork, in addition to being assed using the diagnostic tool. The neuropathy device will be used to apply forces ranging from 0.2 to 10.0 grams of force. Each foot will be tested at 13 locations and the results will be used to map out the individual's threshold sensitivity. Demonstrating that the machine is safe, reliable, and accurate is the first step towards obtaining FDA certification. Finally, the results obtained using the machine and the hand applied methods will be compared to one

another to ultimately determine if an automated process for neuropathy assessment is a more effective method to quantify an individual's loss of sensation and if this method can detect the presence of neuropathy earlier than conventional tests.

References

[1] American Diabetes Assoication, "Peripheral Neuropathy," [Online]. Available: https://www.diabetes.org/diabetes/complications/neuropathy/peripheral-neuropathy.

[2] American Diabetes Association, "Neuropathy," [Online]. Available: https://www.diabetes.org/diabetes/complications/neuropathy.

[3] J. J. Brown, S. L. Pribesh, K. G. Baskette, A. I. Vinik and S. R. Colberg, "A Comparison of Screening Tools for the Early Detection of Peripheral Neuropathy in Adults with and without Type 2 Diabetes," *Journal of Diabetes Research,* vol. 2017, pp. 1-11, 2017.

[4] International Diabetes Federation, "IDF Diabetes Atlas, 9th edn.," 2019. [Online]. Available: https://www.diabetesatlas.org.

[5] WebMD, "Understanding Peripheral Neuropathy -- the Basics," [Online]. Available: https://www.webmd.com/brain/understanding-peripheral-neuropathy-basics#1.

[6] B. A. Brouwer, M. Bakkers, J. G. J. Hoeijmakers, C. G. Faber and I. S. J. Merkies, "Improving assessment in small fiber neuropathy," *Journal of the Peripheral Nervous System,* vol. 20, no. 3, pp. 333-340, 2015.

[7] A. J. M. Boulton, D. G. Armstrong, S. F. Albert, R. G. Frykberg, R. Hellman, M. S. Kirkman, L. A. Lavery, J. W. LeMaster, J. L. Mills, M. J. Mueller, P. Sheehan and D. K. Wukich, "Comprehensive Foot Examination and Risk Assessment," *Diabetes Care,* vol. 31, no. 8, pp. 1679-1685, 2008.

[8] A. M. Aring, D. E. Jones and J. M. Falko, "Evaluation and Prevention of Diabetic Neuroapthy," *American Family Physician,* vol. 71, no. 11, pp. 2123-2128, 2005.

[9] R. J. Tanenberg and P. D. Donofrio, "Chapter 3-Neuropathic Problems of the Lower Limbs in Diabetic Patients," in *Levin and O'Neal's: The Diabetic Foot,* 2008, pp. 33-74.

[10] K. G. Prabhu, D. Agrawal, K. M. Patil and S. Srinivasan, "Parameters for analysis of walking foot pressures at different levels of diabetic neuropathy and detection of plantar ulcers at early stages," *IRBM,* vol. 22, no. 3, pp. 159-169, 2001.

[11] J. Dros, A. Wewerinke, P. J. Bindels and H. C. V. Weert, "Accuracy of Monofilament Testing to Diagnose Peripheral Neuropathy: A Systematic Review," *Annals of Family Medicine,* vol. 7, no. 6, pp. 555-558, 2009.

[12] A. Nather, W. K. Lin, Z. Aziz, C. H. J. Ong, B. M. C. Feng and C. B. Lin, "Assessment of sensory neuropathy in patients with diabetic foot problems," *Diabetic Foot & Ankle,* vol. 2, no. 1, pp. 1-5, 2011.

[13] A. P. Popov, A. V. Bykov and I. V. Meglinski, "Influence of probe pressure on diffuse reflectance spectra of human skin measured in vivo," *Journal of Biomedical Optics,* vol. 22, no. 11, pp. 1-4, 2017.

[14] M. H. Haloua, I. Sierevelt and W. J. Theuvenet, "Semmes-Weinstein Monofilaments: Influence of Temperature, Humidity, and Age," *The Journal of Hand Surgery,* vol. 36, no. 7, pp. 1191-1196, 2011.

[15] M. J. G. Bradman, F. Ferrini, C. Salio and A. Merighi, "Practical mechanical threshold estimation in rodents using von Frey hairs/Semmes–Weinstein monofilaments: Towards a rational method," *Journal of Neuroscience Methods,* vol. 255, pp. 92-103, 2015.

[16] Y. Feng, F. J. Schlösser and B. E. Sumpio, "The Semmes Weinstein monofilament examination as a screening tool for diabetic peripheral neuropathy," *Journal of Vascular Surgery,* vol. 50, no. 3, pp. 675-682, 2009.

[17] J. A. Bell-Krotoski, E. E. Fess, J. H. Figarola and D. Hiltz, "Threshold Detection and Semmes-Weinstein Monofilaments," *Journal of Hand Therapy,* vol. 8, no. 2, pp. 155-162, 1995.

[18] M. Chikai and S. Ino, "Buckling Force Variability of Semmes–Weinstein Monofilaments in Successive Use Determined by Manual and Automated Operation," *SENSORS,* vol. 19, no. 4, pp. 1-9, 2019.

[19] F. Wang, J. Zhang, J. Yu, S. Liu, R. Zhang, X. Ma, Y. Yang and P. Wang, "Diagnostic Accuracy of Monofilament Tests for Detecting Diabetic Peripheral Neuropathy: A Systematic Review and Meta-Analysis," *Journal of Diabetes Research,* vol. 2017, pp. 1-12, 2017.

[20] M. McGill, L. Molyneaux and D. K. Yue, "Use of the Semmes–Weinstein 5.07/10 Gram Monofilament: the Long and the Short of it," *Diabetic Medicine,* vol. 15, pp. 615-617, 1998.

[21] M. Viceconti, S. Olsen, L. P. Nolte and K. Burton, "Extracting clinically relevant data from finite element simulations," *Clinical Biomechanics,* vol. 20, no. 5, pp. 451-454, 2005.

[22] I. N. Sneddon, "The Relation Between Load and Penetration in the Axisymmetric Boussinesq Problem for a Punch Arbitrary Profile," *International Journal of Engineering Science,* vol. 3, no. 1, pp. 47-57, 1965.

[23] K. I. Johnson, "Indention by a rigid flat punch," in *Contact Mechanics 1st ed.*, Cambridge University Press, 1985, pp. 35-42.

[24] C. Li, G. Guan, R. Reif, Z. Huang and R. K. Wang, "Determining elastic properties of skin by measuring surface waves from an impulse mechanical stimulus using phase-sensitive optical coherence tomography," *Journal of the Royal Society Interface,* vol. 9, no. 70, pp. 831-841, 2012.

[25] M. Zhang and A. F. T. Mak, "In vivo friction properties of human skin," *Prosthetics and Orthotics International,* vol. 23, no. 2, pp. 135-141, 1999.

[26] X. Dong, X. Yin, Q. Deng, B. Yu, H. Wang, P. Weng, C. Chen and H. Yuan, "Local contact behavior between elastic and elastic–plastic bodies," *International Journal of Solids and Structures,* vol. 150, no. 1, pp. 22-39, 2018.

[27] P. M. Kurowski, "12: Static analysis of a bracket using adaptive solution methods," in *Engineering Analysis with SolidWorks Simulation 2016*, Mission: SDC Publications, 2016, pp. 211-227.

[28] D. L. Russell and L. W. White, "An Elementary Nonlinear Beam Theory with Finite Buckling Deformation Properties," *SIAM Journal on Applied Mathematics,* vol. 62, no. 4, pp. 1394-1413, 2002.

[29] R. Szalai, "Impact Mechanics of Elastic Structures with Point Contact," *Journal of Vibration and Acoustics,* vol. 136, no. 4, pp. 1-16, 2014.

[30] H. Joodaki and M. B. Panzer, "Skin Mechanical Properties and Modeling: A Review," *Proceedings of the Institution of Mechanical Engineers Part H-Journal of Engineering in Medicine,* vol. 232, no. 4, pp. 323-343, 2018.

[31] T. R. Kuphaldt, "13.5 Stepper Motors," in *Lessons In Electric Circuits, Volume II – AC*, All About Circuits, 2007, pp. 426-437.

[32] B. Porter, "One Step at a Time- What's a Stepper Motor Driver & Why Do I Need It?," All3DP, 6 April 2019. [Online]. Available: https://all3dp.com/2/what-s-a-stepper-motor-driver-why-do-i-need-it/. [Accessed 5 June 2020].

[33] B. Earl, "All About Stepper Motors," 17 Feburary 2020. [Online]. Available: https://cdn-learn.adafruit.com/downloads/pdf/all-about-stepper-motors.pdf. [Accessed June 2020].

[34] Dejan, "How a Stepper Motor Works," HowToMechatronics, [Online]. Available: https://howtomechatronics.com/how-it-works/electrical-engineering/stepper-motor/. [Accessed 5 June 2020].

[35] M. Budimir, "Microstepping Myths," Machine Design, 09 October 2003. [Online]. Available: https://www.machinedesign.com/archive/article/21812154/microstepping-myths. [Accessed 16 June 2020].

[36] Faulhaber, "Stepper Motor Technical Note: Microstepping Myths and Realities," Faulhaber Group, [Online]. Available: https://www.faulhaber.com/en/support/technical-support/motors/tutorials/stepper-motor-tutorial-microstepping/. [Accessed 16 June 2020].

[37] Bantam Tools, "Histroy of CNC Machining, Part 1: The People, Stories, and Inventions That Made Today's Tech Possible," Medium, 12 April 2019. [Online]. Available: https://medium.com/cnc-life/history-of-cnc-machining-part-1-2a4b290d994d. [Accessed 7 June 2020].

[38] Bantam Tools, "History of CN Machining, Part 2: The Evolution from NC to CNC," Medium, 12 April 2019. [Online]. Available: https://medium.com/cnc-life/history-of-cnc-machining-part-2-the-evolution-from-nc-to-cnc-4b9fe1653536. [Accessed 7 June 2020].

[39] Autodesk, "Getting Started with G-Code," Autodesk Inc, [Online]. Available: https://www.autodesk.com/industry/manufacturing/resources/manufacturing-engineer/g-code. [Accessed 7 June 2020].

[40] Bantam Tools, "History of CNC Machining, Part 3: From the Factory Floor to the Desktop," Medium, 12 April 2019. [Online]. Available: https://medium.com/cnc-life/history-of-cnc-machining-part-3-from-the-factory-floor-to-the-desktop-b16cc35ef7be. [Accessed 7 June 2020].

[41] S. Al-Mutlaq, "Getting Started with Load Cells," SparkFun, [Online]. Available: https://learn.sparkfun.com/tutorials/getting-started-with-load-cells/all. [Accessed 6 June 2020].

[42] Omega, "Load Cells & Force Sensors," Omega Engineering, March 12 2020. [Online]. Available: https://www.omega.com/en-us/resources/load-cells. [Accessed 6 June 2020].

[43] "Wheatstone Bridge Circuit Equations and Derivation," Engineers Edge, [Online]. Available: https://www.engineersedge.com/instrumentation/wheat_stone_bridge.htm. [Accessed 6 June 2020].

[44] Electronics Tutorials, "Wheatstone Bridge," AspenCore, Inc, [Online]. Available: https://www.electronics-tutorials.ws/blog/wheatstone-bridge.html. [Accessed 6 June 2020].

[45] L. Peebles and B. Norris, ADULTDATA-The Handbook of Adult Anthropometric and Strength Measurement-Data for Design Safety, 1998.

[46] F. P. Beer, E. R. Johnston, J. T. DeWolf and D. F. Mazurek, "Chapter 16-Columns," in *Statics and Mechanics of Materials*, New York, McGraw-Hill, 2011, pp. 641-674.

[47] B. Wang, Y. Si, C. Chadha, J. T. Allison and A. E. Patterson, "Nominal Stiffness of GT-2 Rubber-Fiberglass Timing Belts for Dynamic System Modeling and Design," *Robotics*, vol. 7, no. 4, pp. 1-8, 2018.

[48] Automation Direct, "Sure Step™ Stepping Systems User Manual," 29 April 2020. [Online]. Available: https://cdn.automationdirect.com/static/manuals/surestepmanual/surestepmanual.html. [Accessed 16 June 2020].

[49] Amazon, "DC 12V Drive Stepper Motor Screw with Linear Nut Slider for DIY Laser Engraving Machine," [Online]. Available: https://www.amazon.com/Stepper-Linear-Slider-Engraving-Machine/dp/B07H3XC3DD. [Accessed 16 June 2020].

[50] Robot Shop, "100g Micro Load Cell," [Online]. Available: https://www.robotshop.com/en/100g-micro-load-cell.html?gclid=Cj0KCQjwn8_mBRCLARIsAKxi0GJvlujAosrZC1mOoxS4J9px6CIAvgIlaJeF93v-4eNAoPBR2ozeNDwaAly7EALw_wcB. [Accessed 16 June 2020].

[51] Centers for Diesease Control and Prevention, "2011 National Diabetes Fact Sheet," 2011. [Online]. Available: http://www.cdc.gov/diabetes/pubs/pdf/ndfs_2011.pdf. [Accessed 20 June 2013].

[52] American Diabetes Association, "The Cost of Diabetes," 06 March 2013. [Online]. Available: http://www.diabetes.org/advocacy/news-events/cost-of-diabetes.html .

[53] M. LepCantalo, J. Apelqvist and C. Setacci, "Diabetic Foot," *Chapter V*, pp. S60-S74, Dec. 2011.

[54] G. Pambianco, T. Costacou, E. Strotmeyer and T. Orchard, "The assessment of clinical distal symmetric polyneuropathy in type 1 diabetes: A comparison of methodologies from the Pittsburgh Epidemiology of Diabetes Complications Cohort.," *Diabetes Research and Clinical Practice*, vol. 92, no. 2, pp. 280-287, 2011.

[55] O. A. Fawzy, A. I. Arafa, M. A. El Wakeel and S. H. Abdul Kareem, "Plantar Pressure as a Risk Assessment Tool for Diabetic Foot Ulceration in Egyptian Patients with Diabetes," 02 Dec. 2014. [Online]. Available: https://www.ncbi.nlm.nih.gov/pmc/articles/PMC4257475.

Appendix A (Provisional Patent Application Submission)

AUBURN UNIVERSITY | Office of Innovation Advancement and Commercialization

DATE: September 20, 2019

RE: Newly filed Provisional Application No.: 62/903,211

Title: "Semi-automated Plantar Surface Sensation Detection Device"

Innovator(s): Michael Edgar Zabala; Vitale K. Castellano; Kenny V. Brock; Thomas Burch; Hayden G. Burch; Jonathan Commander

File Date: September 20, 2019

Expiration Date:

September 20,

2020 AU IP No.:

2019-032-01

The above-referenced provisional application was filed electronically with the United States Patent and Trademark Office on **September 20, 2019,** and a copy of the Electronic Acknowledgement Receipt has been attached for your records. Copies of the provisional application, as filed, are available to all listed innovators upon request.

Provisional applications provide the means to establish an early effective filing date in any future non-Provisional patent application filings; additionally, the term "patent pending" may be applied in connection with the description of the intellectual property (IP). Provisional applications have a pendency of 12 months from the date of filing and cannot be extended. Within this one-year period, the provisional application will be evaluated to determine whether further evaluation and or development and/or what, if any, patent, copyright, trademark and/or plant variety protection is needed.

Best Regards & War Eagle!

Misty W. Schwieker

As required by the Bayh-Dole Act (1980), Auburn University (AU) requires all AU innovators to execute the Patent and Copyright Agreement for Auburn University Personnel. Signed copies may be returned via email to iac_innovations@auburn.edu with originals to follow by campus mail. Please note that only one fully-executed agreement per innovator is required. Additional agreements will not be required on future intellectual property disclosure submissions, trademark, copyright, and/or provisional or patent application filings.

Track the status and progress of this and all your Intellectual Property (IP), Agreement(s) and MTA request(s) by logging into the AU Innovator Portal. IAC Innovator Portal ID login requests may be made via e-mail to iac@auburn.edu or by telephone to (334) 844-4977.

570 Devall Drive ▪ Suite 102 ▪ Auburn, AL 36832 ▪ P: (334) 844-4977 ▪ iac_innovations@auburn.edu

Appendix B (IRB Consent Document)

EDWARD VIA COLLEGE OF OSTEOPATHIC MEDICINE (VCOM)

CONSENT TO TAKE PART IN A BIOMEDICAL RESEARCH STUDY

Title: A Novel Clinical Tool for Neuropathic Grade Assessment

Investigator(s):

Dr. Jon Commander, MD, MS (Principle Investigator)
Dr. Michael Zabala, Auburn University
Dr. Kenny Brock, VCOM
Dr. Thomas Burch, Auburn University
Vitale Kyle Castellano, Auburn University
Hayden Burch, Auburn University
Jessica Remy, VCOM
Madison Blackwell, VCOM
David McGregor, VCOM
Joshua Maher, VCOM
Kayla Garner, VCOM
David Levin, VCOM
Rachel Dykes, VCOM
Ryan Pollard, VCOM
Jonothon Segars, VCOM
Elizabeth Sullivan, VCOM

I. SUMMARY

Neuropathy is defined as a sensation in the body such as burning, tingling, numbness, warm or cool patches, a sensation of a sock on the foot, or a sponge under the foot.

The most common cause of neuropathy is type 2 diabetes mellitus. Neuropathic symptoms are most common in the foot but can occur in the hand, the trunk of the body or the lower back into the legs. The cause of neuropathy is not well understood. Some of the causes include an inherited trait, poor blood sugar control, and poor circulation to the feet.

The purpose of the study is to compare the standard foot exam to an examination done with a newly invented device. A standard foot exam includes hand applied monofilaments and vibratory analysis using a tuning fork. Your participation in this study is voluntary; it is your choice. You have the right to withdraw from the study at any point. The information from this research study will be confidential, kept anonymous, and maintained in a secure computer system under a coded protocol.

Our hope is that the data will give you new information about the health of your feet. The collected information will lead to better foot care for you and for all other diabetics in the future.

The study staff will explain this study in detail to you. Ask questions about anything that is not clear at any time. You may take home an unsigned copy of this consent form to think about and discuss with family or friends.

Please read this consent form carefully.

II. WHAT IS INFORMED CONSENT?

You are being asked to take part in a research study that will study that may benefit individuals who have diabetic foot neuropathy, a condition causing pain in various places on the foot. Before you decide whether to take part in the research, you should be told about the risks and benefits with this study. This process is known as informed consent. This consent form will give you information about this study and your rights as a research subject. Your decision to (or not to) participate in the voluntary study will in no way influence or affect your medical care and treatment at Internal Medicine Associates.

III. WHY IS THIS RESEARCH BEING DONE?

The purpose of this research it to develop a method of examining the sensitivity of the foot using a device using a monofilament. The research involves an office visit to examine your feet using the device.

IV. WHAT WILL HAPPEN IN THIS RESEARCH STUDY?

After you have given consent you the VCOM student will generate a study code unique to you. All of your data and results will be deidentified using this code as to remove your identity from the results. During the exam you will be asked to remove shoes, socks, stockings, and or knee highs to expose the foot and ankle. If you have a long sleeve shirt, a gown will be provided to check your blood pressure. Your blood pressure, BMI, and ABI will be evaluated and recorded on a data sheet. Your age, gender, and any symptoms related to neuropathy will also be recorded on the datasheet. During the exam a pressure will be checked at your ankle and top of your foot. Your medical record at IMA will be accessed for your last three fasting blood sugars and last three HgbA1c readings and will be written down on the datasheet. Furthermore, you will be subjective to a standard exam using hand applied monofilaments and vibratory analysis using a tuning fork on both of your feet. After this you will be tested with the new device by either a VCOM student or an Auburn University student. While you are lying on the exam table the neuropathic device will be placed up against the sole of your foot. Care will be taken to assume proper placement. Comfort is important so no part of your foot will feel excess pressure. The device will then measure 13 points from the toes down to your heel. Different pressures will be used at random locations, until your minimum threshold sensitivity is

determined. You will be given a handheld pushbutton, which blinks to request a response from you. If you feel the applied pressure, please press the button during the blinking cycle. If you are not sure if you can feel the pressure, do not hit the button. False positives are thrown into the assessment to make sure you are being honest with your responses. Both of your feet will be assed using the new device A photograph will be taken of each foot for use with the device and for future analysis. You will consent to have your medical record assessed by Dr. Commander and the VCOM students and for the photographs taken.

V. WHAT ARE THE RISKS OF BEING IN THIS RESEARCH STUDY?

The examination of the foot using the monofilament should present minimal risk to you. In taking part in this research may harm you in unknown ways. As this study involves the use of your identifiable, personal information, there is a chance that a loss of confidentiality will occur. The researchers have procedures in place to lessen the possibility of this happening (see "What about confidentiality?" section below).

VI. WHAT ARE THE BENEFITS OF BEING IN THIS REASEARCH STUDY?

We cannot promise any benefits to your from taking part in the study. At the completion of the examination you will be given a copy of the datasheet with all of your results, including your threshold sensitivity of your feet using hand applied methods and the new device. However, the results using the new device cannot be used for the diagnosis of diseases, since it is not an FDA regulated device. Although you may not personally benefit from taking part in this study, the knowledge gained may benefit others.

VII. ARE THERE ANY OPTIONS TO BEING IN THIS REASEARCH STUDY?

The only alternative to participation is to choose not to participate.

VIII. WILL I RECEIVE NEW INFORMATION ABOUT THIS RESEARCH STUDY?

You will not receive any new information about this research study beyond the results of the examination.

IX. WHAT ABOUT CONFIDENTIALITY?

After you sign this consent form, the VCOM student will make a study code unique to you. This code will be used throughout this examination. This code will deidentify your data and your results collected through this study, in addition to the photographs of your feet. There will be no record that connects your name with your study code, you will be the only person who knows your own study code. At the end of the evaluation you will get a copy of this consent document and a copy of your datasheet. The

investigators' copy of your signed consent form and datasheet will be keep in a locked filing cabinet and will be separated into different folders. The new machine will use your study code to save your deidentified results and data on password protected computers owned by the investigators of this study. Your datasheet will also include a summary of this results. Your identity will not be used in any sort of published report without your written permission.
Your identity in this study will be treated as confidential. The results of the study, including laboratory or any other data, may be published but will not give your name or include any identifiable references to you. This includes your blood pressure, BMI, ABI, last three fasting blood sugars, last three HgbA1c levels, age, gender, symptoms related to neuropathy, and data results from the standard foot exam and from the new device, and the photographs of your feet. However, any records or data obtained as a result of your participation in this study may be inspected by the persons conducting this study and/or The Edward Via College of Osteopathic Medicine's Institutional Review Board, provided that such inspectors are legally obligated to protect any identifiable information from public disclosure, except where disclosure is otherwise required by law or a court of competent jurisdiction. These records will be kept private in so far as permitted by law.

X. AUTHORIZATION TO USE YOUR HEALTH INFORMATION?

There is a federal law that protects the privacy of health information. This law is known as HIPAA. HIPAA stands for the "Health Insurance Portability and Accountability Act." Because of this law, your health information cannot be looked at, collected or shared with others without your permission.

Signing this consent and authorization form means you allow the Principal Investigator for this study and members of the investigator's research team to create, get, use, store and share information that identifies you for the purposes of this research.

After the VCOM student goes through this document with you and you sign it, they will go through your medical record and document the last three fasting blood sugars, and the last three HgbA1c readings on your datasheet. The datasheet will be noted with your unique study code, used to deidentify you from your data. Your blood pressure, BMI, ABI, age, gender, and any symptoms related to neuropathy will all be evaluated and documented on your datasheet. The datasheet will also document the results of your standard foot exam and your examination using the new device.

XI. WILL IT COST ME MONEY TO TAKE PART IN THE RESEARCH?

There is no cost to you to take part in the research study. If while participating, you think you have an injury or illness related to this study, contact the study staff right away. The study staff will treat you or refer you for treatment. If referred, you will be responsible for the cost of such treatment.

XII. WILL I BE PAID FOR TAKING PART IN THIS RESEARCH?

There will be no compensation for taking part in this research study.

XIII. WHAT IF I WANT TO STOP BEING IN THE STUDY BEFORE IT IS FINISHED?

At any time during the examination, you can choose to not participate and end the examination. You can also request to be removed from this study at any time, in which case your results will be removed.

XIV. CAN I BE REMOVED FROM THIS RESARCH WITHOUT MY APPROVAL?

The person in charge of this research can remove you from this research without your approval. There are three cases where this might occur, the first is if your ABI is less than one. The second is if you hit to many false positive checks while being evaluated with the new device. The third is if you have any open wounds on your feet.

XV. ARE RESEARCHERS BEING PAID TO DO THIS STUDY?

This research study is funded by VCOM, which has paid for the development of the device, raw materials, the Auburn University graduate research assistant's salary and Auburn University undergraduate research assistant salary. Other than the Auburn University graduate and undergraduate students, none of the investigators or research staff will receive money or other types of payment from this study.

XVI. WHAT ARE MY RESPONSIBILITES IF I CHOOSE TO PARTICIPATE IN THIS RESEARCH STUDY?

If you choose to participate, an appointment will be scheduled for your examination. The examination will require that you lay still and place your foot in a device. Furthermore, you will be tested with hand applied monofilaments and a tuning fork. The examination should not take longer than 60 minutes to complete.

XVII. WHO ARE THE CONTACT PERSONS FOR THIS STUDY?

If you encounter complications or have any questions about the study you may call:

Investigator Name: Dr. Jon Commander, MD

Address: Internal Medicine Associates, 121 North 20th St. #6, Opelika, AL 36801

Phone #: (334) 749-3385

Email Address: jcommander@imaopelika.com

This research is being overseen by the Edward Via College of Osteopathic Medicine Institutional Review Board (IRB). An IRB is a group of people who perform independent review of research studies. You may talk with the Chairman of the IRB by calling (540) 231-4981 if:

- You have questions, concerns, or complaints that are not being answered by the research team.
- If you have questions about your rights as a research subject.
- If you need to report a research-related injury.

XVIII. CONSENT SIGNATURES

PARTICIPANT: The research study described in this consent form, including the risks and benefits, has been explained to me and all my questions have been answered. I consent to take part in this research study. My consent is given willingly and voluntarily. I understand that I am free to withdraw my consent at any time. I will receive a signed copy of this consent form.

I give my permission to the researchers to use my medical records as described in this consent form.

_____ _____

Printed Name of Participant Signature of participant Date

PERSON OBTAINING CONSENT: I certify I was present for the informed consent discussion. The subject or legally authorized representative had an opportunity to ask questions about the study and appeared to understand the information presented. The subject or legally authorized representative agreed to take part voluntarily in the research and I obtained his/her signature.

_____ _____

Printed Name of Person Obtaining Consent Signature of Person Obtaining Consent Date

Appendix C (Patient Datasheet)

Patient Code: _____

Gender: _____
Age: _____
(if older than 89 indicate 90+)

Cohort

- ☐ Control
- ☐ DM2, no symptoms
- ☐ DM2, with symptoms
- ☐ DM2, history of ulcers, amputation

Vital Signs

BP: _____
BMI: _____
ABI Screen: _____
Last 3 Fasting Blood Sugars
_____,_____,_____
Last 3 HgbA1c
_____,_____,_____

Sig PMH

- ☐ CKDz, Proteinuria
- ☐ Neuropathy
- ☐ Vascular Disease
- ☐ Peripheral Vascular Disease
- ☐ None

Symptoms

- ☐ Burning
- ☐ Tingling
- ☐ Numbness
- ☐ Warm Patches
- ☐ Cold Patches
- ☐ False Sensation
- ☐ Other: _____
  _____
  _____
- ☐ None

Patient Code: _____

Standard Foot Exam

	Right		Left	
	M	V	M	V
Toe 1				
2				
3				
4				
5				
MT 1				
2				
3				
4				
5				
H 1				
2				
3				

New Device Foot Exam*

	Right	Left
Toe 1		
2		
3		
4		
5		
MT 1		
2		
3		
4		
5		
H 1		
2		
3		

*Note: Results obtained using the new device cannot be used for the diagnosis of diseases, since this is not an FDA regulated device

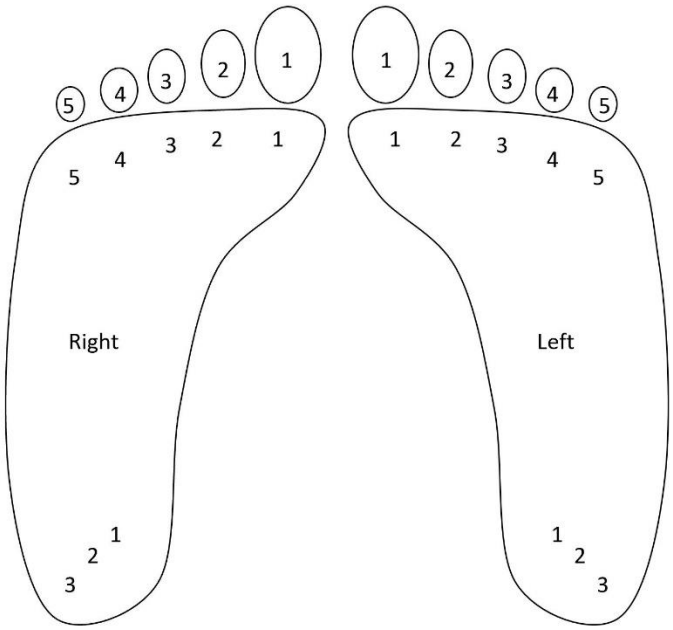

**Note: Pictorial shows the plantar surface of the foot, locations and size are not exact or to scale

Appendix D (Research Volunteer Flyer for IMA Lobby)

Attachment for Questionnaire for enrollment, Consent for Collaborative Clinical Research and Poster for IMA Lobby

Poster for IMA Lobby

Dr. Jon Commander of Internal Medicine Associates

Auburn University Samuel Ginn College of Engineering's Mechanical Engineering Department

Edward Via College of Osteopathic Medicine (VCOM)

Request your participation!

A research study on diabetic neuropathy of the feet using a newly invented tool for analyzing neuropathy.

Seeking:

- 50 patients, at least 40 years-old, no health risks for diabetes/neuropathy
- 50 patients, at least 40 years-old, with type II diabetes for at least 5 years, no symptoms of neuropathy
- 50 patients, at least 40 years-old, with type II diabetes for at least 5 years, with symptoms of neuropathy
- 50 patients, at least 40 years-old, with type II diabetes and history of foot ulcers and/or partial amputation

If you meet the requirements of one of these groups, please take a flyer/request information during vital signs, and you may participate in this FREE test. Results will be provided to you. There is no compensation for this free examination. This study is not open to type I diabetics or anyone less than 40 years of age. Also if you have an Ankle-Brachial Index less than 1.0 you will be excluded from this study. Patient's with unhealed ulcers or unhealed amputations will be excluded. The entire evaluation will take no more than 60 minutes.

Recruitment Script

Thank you for your interest in being included in this research on neuropathy. As a control patient you must be at least 40 years of age with no know history of peripheral vascular disease nor symptoms of neuropathy. All Type 2 DM volunteers must be at least age 40 and have had DM 2 for at least 5 years. Also if you have an Ankle-Brachial Index less than 1.0 you will be excluded from this study. Patient's with unhealed ulcers or unhealed amputations will be excluded. During the evaluation you will have a standard foot exam on each foot, which includes hand applied monofilaments and vibratory analysis using a tuning fork. You will also be evaluated using the new tool. You will also receive an ABI exam to document your blood flow to your feet. You will be given a copy of your results which you can share with your primary care physician, however since this is not an FDA approved device the results cannot be used to diagnosis a disease. There will be no compensation provided for participation. The entire evaluation will take no more than 60 minutes. An appointment time will be scheduled for the free exam.

Appendix E (Neuropathy Device Code)

This code was written by Vitale Kyle Castellano

```
clc
clear all
close all

Mega=serial('COM3', 'BaudRate', 115200);
fopen(Mega);
pause(3)
Uno=serial('COM6', 'BaudRate', 9600);
Uno.Terminator= 'LF';
Uno.timeout=30;
fopen(Uno);
pause(3)
fprintf(Mega, '$X \n');
pause(3)
fprintf(Mega, '$H \n');
pause(3)
fprintf(Mega, 'G20 \n');
pause(3)
fprintf(Mega, 'G28.1 \n');
pause(3)
fprintf(Mega, 'G10 L20 P1 X0 Y0 Z0 \n');
pause(3)
mycam=webcam('Logitech');
mycam.Resolution = '1920x1080';
pause(10)


PatientData=inputdlg({'Patient Identifier:', 'Gender:', 'Age:',
'Time:', 'Date:', 'Operator Initials:'}, 'Documentation', [1
50]);
PatientIdentifierChar=char(PatientData(1));

answer=questdlg('Left Foot or Right Foot?', 'Foot Type', 'Left',
'Right', 'Left');

switch answer
    case 'Left'
        Type1st='LeftFoot';
        Type2nd='RightFoot';
    case 'Right'
        Type1st='RightFoot';
        Type2nd='LeftFoot';
end
```

```
Directory='D:\Documents\Graduate Research Neuropathy
Project\Matlab Research Files';
NewDirectory=sprintf('%s\\%s',Directory, PatientIdentifierChar);

if ~exist(NewDirectory, 'dir')
    mkdir(fullfile(Directory,PatientIdentifierChar))
end

PatientIdentifierCharType1st=sprintf('%s%s',PatientIdentifierCha
r, Type1st);
PatientIdentifierCharType2nd=sprintf('%s%s',PatientIdentifierCha
r, Type2nd);
SubDirectory1st=sprintf('%s\\%s', NewDirectory,
PatientIdentifierCharType1st);
SubDirectory2nd=sprintf('%s\\%s', NewDirectory,
PatientIdentifierCharType2nd);

if ~exist(SubDirectory1st, 'dir')
    mkdir(fullfile(NewDirectory, PatientIdentifierCharType1st))
end

if ~exist(SubDirectory2nd, 'dir')
    mkdir(fullfile(NewDirectory, PatientIdentifierCharType2nd))
end

filenamex1st=sprintf('%s.xlsx', PatientIdentifierCharType1st);
filenamex2nd=sprintf('%s.xlsx', PatientIdentifierCharType2nd);
filenamew=sprintf('%s.mat', PatientIdentifierChar);
filenamef1st=sprintf('%s.fig', PatientIdentifierCharType1st);
filenamef2nd=sprintf('%s.fig', PatientIdentifierCharType2nd);
tic

for H=1:2

    if H==1

        [T1, T2, T3, RS1]=NeuropathyScriptFunction1(Uno, Mega,
mycam, 1);
        answer5=questdlg('Offer the Patient a break', 'Break',
'Okay', 'Okay');
        fprintf(Mega, '$X \n');
        pause(3)
        fprintf(Mega, '$H \n');
        pause(3)
        fprintf(Mega, 'G20 \n');
        pause(3)
```

```
        fprintf(Mega, 'G28.1 \n');
        pause(3)
        fprintf(Mega, 'G10 L20 P1 X0 Y0 Z0 \n');
        pause(3)
        answer6=questdlg('Place the Patient''s other foot in the
machine', 'Insert Foot', 'Okay', 'Okay');
        answer7=questdlg('Click Okay to resume the test once the
Patient''s other foot has been placed in the machine', 'Resume
Test', 'Okay', 'Okay');
    end

    if H==2

        [T4, T5, T6, RS2]=NeuropathyScriptFunction1(Uno, Mega,
mycam, 2);

    end

end

endTime=toc;

fclose(Mega);
pause(3)
fclose(Uno);

writetable(T1, filenamex1st, 'sheet', 'sheet1')
writetable(T2, filenamex1st, 'sheet', 'sheet2')
writetable(T3, filenamex1st, 'sheet', 'sheet3')
writetable(T4, filenamex2nd, 'sheet', 'sheet1')
writetable(T5, filenamex2nd, 'sheet', 'sheet2')
writetable(T6, filenamex2nd, 'sheet', 'sheet3')

savefig(1, PatientIdentifierCharType1st)
savefig(2, PatientIdentifierCharType2nd)
save(PatientIdentifierChar)

movefile(filenamex1st, SubDirectory1st)
movefile(filenamex2nd, SubDirectory2nd)
movefile(filenamew, NewDirectory)
movefile(filenamef1st, SubDirectory1st)
movefile(filenamef2nd, SubDirectory2nd)
```

Appendix F (Neuropathy Script Function)

This code was written by Vitale Kyle Castellano

```
function [T1, T2, T3, rs]=NeuropathyScriptFunction1(Uno, Mega,
mycam, N)

figure(N)
img=snapshot(mycam);
imwrite(img, 'PatientNew.tiff');
I=imread('PatientNew.tiff');
imshow(I);
axis on

[c,r]=getpts(figure(N));

c1=c(1);
c2=c(2);
CLength=c2-c1;
xratio=12/CLength;
cd=CLength/48;

r1=r(1);
r2=r(2);
RLength=r2-r1;
yratio=5/RLength;
rd=RLength/20;

hold on;

for col=c1:cd:c2
    line([col, col], [r2, r1], 'Color', 'w');
end

for row=r1:rd:r2
    line([c2, c1], [row, row], 'Color', 'w');
end

R=r1:rd:r2;
C=c1:cd:c2;

fprintf(Mega, 'G54 X0.225 Y1.265 \n');
pause(3)
fprintf(Mega, 'G30.1 \n');
pause(3)
fprintf(Mega, 'G10 L20 P2 X0 Y0 Z0 \n');
pause(0.1)
```

```
[~, ~, ~] = NeuropathyUnoFunction2("0", Uno);
pause(0.1)


for L=1:3
    if L==1
        fprintf("Region 1-Toes \n")
        answer1=questdlg('Please select locations on the
metatarsal heads', 'Region 1', 'Okay', 'Okay');
    end

    if L==2
        fprintf("Region 2-Ball of the Foot \n")
        answer2=questdlg('Please select locations on the ball of
the foot', 'Region 2', 'Okay', 'Okay');
    end

    if L==3
        fprintf("Region 3-Heel \n")
        answer3=questdlg('Please select locations on the heel',
'Region 3', 'Okay', 'Okay');
    end

[x,y]=getpts(figure(N)); %Collects data on figure
hold on

Data=[x y]; %Mouse click Data stored
DataConversion=Data-[c1 r1];
DataInch=DataConversion.*[xratio yratio];

[rowInch, ~]=size(DataInch); %Determines how many points there
are
NumberRows=rowInch; %Counts rows

accuracy=0.25; %rounded to nearest 0.25 inch
DataRounded=round(DataInch/accuracy)*accuracy;
DataRoundedLimit=max(DataRounded, 0); %Converts negative numbers
to zero

XData=DataRoundedLimit(: ,1); %X axis data to less than or equal
to 12
XData(XData>12)=12;

YData=DataRoundedLimit(: ,2); %Y axis data to less than or equal
to 5
YData(YData>5)=5;
```

```
DataFinal=[XData YData];
DataFinalPixels=DataFinal./[xratio yratio];

DataPixels=DataFinalPixels+[c1 r1];
DataPixelsX=DataPixels(: ,1);
DataPixelsY=DataPixels(: ,2);
plot(DataPixelsX,DataPixelsY, 'c*');
hold on

GcodeCell=cell(1, NumberRows);
for i=1:NumberRows
    DataPoint=DataFinal(i, :); %Selects a row of data for
indexed value or rounded set
    DataPointX=DataPoint(2); %X coordinate for indexed value
    DataPointY=DataPoint(1); %Y coordinate for indexed value
    Gcode=sprintf('G55 X%0.2f Y%0.2f', DataPointX, DataPointY);
%String printf of Gcode
    GcodeCell{i}=Gcode;  %Stores all indexed Gcode in a Cell
end

    if L==1
        R1Gcode=GcodeCell;
        R1DataPixels=DataPixels;
        R1DataPixelsX=DataPixelsX;
        R1DataPixelsY=DataPixelsY;
        Length1=NumberRows;
    end

    if L==2
        R2Gcode=GcodeCell;
        R2DataPixels=DataPixels;
        R2DataPixelsX=DataPixelsX;
        R2DataPixelsY=DataPixelsY;
        Length2=NumberRows;
    end

    if L==3
        R3Gcode=GcodeCell;
        R3DataPixels=DataPixels;
        R3DataPixelsX=DataPixelsX;
        R3DataPixelsY=DataPixelsY;
        Length3=NumberRows;
    end
end
```

```
M1=plot(-1,-1, 'o', 'LineWidth',2, 'MarkerEdgeColor','k',
'MarkerFaceColor','g', 'MarkerSize',10, 'DisplayName', '0.200
grams');
M2=plot(-1,-1, 'o', 'LineWidth',2, 'MarkerEdgeColor','k',
'MarkerFaceColor','b', 'MarkerSize',10, 'DisplayName', '0.700
grams');
M3=plot(-1,-1, 'o', 'LineWidth',2, 'MarkerEdgeColor','k',
'MarkerFaceColor','y', 'MarkerSize',10, 'DisplayName', '2.00
grams');
M4=plot(-1,-1, 'o', 'LineWidth',2, 'MarkerEdgeColor','k',
'MarkerFaceColor','m', 'MarkerSize',10, 'DisplayName', '4.00
grams');
M5=plot(-1,-1, 'o', 'LineWidth',2, 'MarkerEdgeColor','g',
'MarkerFaceColor','r', 'MarkerSize',10, 'DisplayName', '6.00
grams');
M6=plot(-1,-1, 'o', 'LineWidth',2, 'MarkerEdgeColor','c',
'MarkerFaceColor','r', 'MarkerSize',10, 'DisplayName', '8.00
grams');
M7=plot(-1,-1, 'o', 'LineWidth',2, 'MarkerEdgeColor','r',
'MarkerFaceColor','k', 'MarkerSize',10, 'DisplayName', '10.00
grams');
M8=plot(-1,-1, 'o', 'LineWidth',2, 'MarkerEdgeColor','k',
'MarkerFaceColor','k', 'MarkerSize',10, 'DisplayName', 'Greater
than 10.00 grams');

legend([M1, M2, M3, M4, M5, M6, M7, M8],'AutoUpdate','off');


rng shuffle
rs=rng;

TestingOrder=randi(4);
if TestingOrder==1
    %1-2-3

    T1Gcode=R1Gcode;
    T1DataPixels=R1DataPixels;
    T1DataPixelsX=R1DataPixelsX;
    T1DataPixelsY=R1DataPixelsY;
    T1Length=Length1;

    T2Gcode=R2Gcode;
    T2DataPixels=R2DataPixels;
    T2DataPixelsX=R2DataPixelsX;
    T2DataPixelsY=R2DataPixelsY;
    T2Length=Length2;
```

```
    T3Gcode=R3Gcode;
    T3DataPixels=R3DataPixels;
    T3DataPixelsX=R3DataPixelsX;
    T3DataPixelsY=R3DataPixelsY;
    T3Length=Length3;

elseif TestingOrder==2
    %2-1-3

    T1Gcode=R2Gcode;
    T1DataPixels=R2DataPixels;
    T1DataPixelsX=R2DataPixelsX;
    T1DataPixelsY=R2DataPixelsY;
    T1Length=Length2;

    T2Gcode=R1Gcode;
    T2DataPixels=R1DataPixels;
    T2DataPixelsX=R1DataPixelsX;
    T2DataPixelsY=R1DataPixelsY;
    T2Length=Length1;

    T3Gcode=R3Gcode;
    T3DataPixels=R3DataPixels;
    T3DataPixelsX=R3DataPixelsX;
    T3DataPixelsY=R3DataPixelsY;
    T3Length=Length3;

elseif TestingOrder==3
    %3-1-2

    T1Gcode=R3Gcode;
    T1DataPixels=R3DataPixels;
    T1DataPixelsX=R3DataPixelsX;
    T1DataPixelsY=R3DataPixelsY;
    T1Length=Length3;

    T2Gcode=R1Gcode;
    T2DataPixels=R1DataPixels;
    T2DataPixelsX=R1DataPixelsX;
    T2DataPixelsY=R1DataPixelsY;
    T2Length=Length1;

    T3Gcode=R2Gcode;
    T3DataPixels=R2DataPixels;
    T3DataPixelsX=R2DataPixelsX;
    T3DataPixelsY=R2DataPixelsY;
    T3Length=Length2;
```

```
else
    %3-2-1

    T1Gcode=R3Gcode;
    T1DataPixels=R3DataPixels;
    T1DataPixelsX=R3DataPixelsX;
    T1DataPixelsY=R3DataPixelsY;
    T1Length=Length3;

    T2Gcode=R2Gcode;
    T2DataPixels=R2DataPixels;
    T2DataPixelsX=R2DataPixelsX;
    T2DataPixelsY=R2DataPixelsY;
    T2Length=Length2;

    T3Gcode=R1Gcode;
    T3DataPixels=R1DataPixels;
    T3DataPixelsX=R1DataPixelsX;
    T3DataPixelsY=R1DataPixelsY;
    T3Length=Length1;
end

for K=1:3

    if K==1
        [T1] = NeuropathyFunction3(T1Length, T1Gcode,
T1DataPixelsX, T1DataPixelsY, Mega, Uno);
    end

    if K==2
        [T2] = NeuropathyFunction3(T2Length, T2Gcode,
T2DataPixelsX, T2DataPixelsY, Mega, Uno);
    end

    if K==3
        [T3] = NeuropathyFunction3(T3Length, T3Gcode,
T3DataPixelsX, T3DataPixelsY, Mega, Uno);
    end

end

fprintf(Mega, 'G30 \n');
pause(3)
answer4=questdlg('Please remove the Patient''s foot Inserand
click okay when done', 'Remove Foot', 'Okay', 'Okay');
```

Appendix G (Neuropathy Function)

This code was written by Vitale Kyle Castellano

```
function [T] = NeuropathyFunction3(TLength, TGcode,
TDataPixelsX, TDataPixelsY, Mega, Uno)

TotalNumberofTrialVector=1:TLength; %Creates row vector of total
number of points selected
VectorTranspose=TotalNumberofTrialVector'; %Creates cloumn
vector of total number of points selected
RandomizedVector=TotalNumberofTrialVector(randperm(length(TotalN
umberofTrialVector))); %Randomizes the vector, used to randomize
the test locations
RandomizedVectorTranspose=RandomizedVector'; %Takes random
vector and transposes it
Y=RandomizedVector;

GcodeCelltoString=string(TGcode); %Converts cell array Gcode to
strings
GcodeCelltoStringTranspose=GcodeCelltoString'; %Transposes a
Gcode string array
Z=GcodeCelltoString;

FalsePositiveRandomizationVector=randi([1 10],1,TLength); %Flase
Positive Randmization
FalsePositiveRandomizationVectorTranspose=FalsePositiveRandomiza
tionVector';  %Flase Positive Randomization Transpose
W=FalsePositiveRandomizationVector;
X=TLength;

TestLocationCellArray=cell(1, X);
dataout0=zeros(1, X);
dataout1=zeros(1, X);
dataout2=zeros(1, X);
dataout3=zeros(1, X);
dataout4=zeros(1, X);
dataout5=zeros(1, X);
dataout6=zeros(1, X);
dataout7=zeros(1, X);
ResponseIndex0=zeros(1,X);
ResponseIndex1=zeros(1,X);
ResponseIndex2=zeros(1,X);
ResponseIndex3=zeros(1,X);
ResponseIndex4=zeros(1,X);
ResponseIndex5=zeros(1,X);
ResponseIndex6=zeros(1,X);
```

```
ResponseIndex7=zeros(1,X);
PercentError0=zeros(1,X);
PercentError1=zeros(1,X);
PercentError2=zeros(1,X);
PercentError3=zeros(1,X);
PercentError4=zeros(1,X);
PercentError5=zeros(1,X);
PercentError6=zeros(1,X);
PercentError7=zeros(1,X);
FalsePositiveCheckIndex=zeros(1,X);

for i=1:X
    TestLocation=Z(Y(i)); %Selects a random point to test at
    fprintf(Mega, '%s  \n',TestLocation); %Sends Gcode (X and Y)
to the arduino over serial usb connection
    TestLocationCellArray{i}=TestLocation; %Stores location data
    fo=0;

        while fo==0 %feedback loop
            flushinput(Mega);
            pause(1)
            fprintf(Mega, '? \n');
            C=fscanf(Mega);
            CC=strtok(C, '|');
            CCC=convertCharsToStrings(CC);

                if CCC=="<Idle"
                    fo=1;
                end
        end

    for j=1

        if W(i)==10
            %false positive code
            FalsePositiveCheckRandomizationVector=randi(2);

FalsePositiveCheckIndex(i)=FalsePositiveCheckRandomizationVector
;

            if FalsePositiveCheckRandomizationVector==2
                fprintf('False Positive Test at End \n');
                fprintf('Z axis move \n');
                pause(0.1);
                F="0.2";
                [ResponseIndex1(i), dataout1(i),
PercentError1(i)] = NeuropathyUnoFunction2(F, Uno);
```

```
                if ResponseIndex1(i)==1
                    ResponseIndex2(i)=101;
                    ResponseIndex3(i)=101;
                    ResponseIndex4(i)=101;
                    ResponseIndex5(i)=101;
                    ResponseIndex6(i)=101;
                    ResponseIndex7(i)=101;
                    dataout2(i)=0;
                    dataout3(i)=0;
                    dataout4(i)=0;
                    dataout5(i)=0;
                    dataout6(i)=0;
                    dataout7(i)=0;
                    PercentError2(i)=0;
                    PercentError3(i)=0;
                    PercentError4(i)=0;
                    PercentError5(i)=0;
                    PercentError6(i)=0;
                    PercentError7(i)=0;
                end

                if ResponseIndex1(i)==0
                    fprintf('Z axis move \n'); %Z axis moves
                    pause(0.1);
                    F="10";
                    [ResponseIndex2(i), dataout2(i),
PercentError2(i)] = NeuropathyUnoFunction2(F, Uno);
                end

                if ResponseIndex2(i)==1
                    fprintf('Z axis move \n'); %Z axis moves
                    pause(0.1);
                    F="4";
                    [ResponseIndex3(i), dataout3(i),
PercentError3(i)] = NeuropathyUnoFunction2(F, Uno);
                end

                if ResponseIndex2(i)==0
                    ResponseIndex3(i)=101;
                    ResponseIndex4(i)=101;
                    ResponseIndex5(i)=101;
                    ResponseIndex6(i)=101;
                    ResponseIndex7(i)=101;
                    dataout3(i)=0;
                    dataout4(i)=0;
                    dataout5(i)=0;
```

```
                    dataout6(i)=0;
                    dataout7(i)=0;
                    PercentError3(i)=0;
                    PercentError4(i)=0;
                    PercentError5(i)=0;
                    PercentError6(i)=0;
                    PercentError7(i)=0;
                end

                if ResponseIndex3(i)==1
                    fprintf('Z axis move \n'); %Z axis moves
                    pause(0.1);
                    F="0.7";
                    [ResponseIndex4(i), dataout4(i),
PercentError4(i)] = NeuropathyUnoFunction2(F, Uno);

                    if ResponseIndex4(i)==1
                        ResponseIndex5(i)=101;
                        ResponseIndex6(i)=101;
                        ResponseIndex7(i)=101;
                        dataout5(i)=0;
                        dataout6(i)=0;
                        dataout7(i)=0;
                        PercentError5(i)=0;
                        PercentError6(i)=0;
                        PercentError7(i)=0;
                    end

                    if ResponseIndex4(i)==0
                        fprintf('Z axis move \n'); %Z axis moves
                        pause(0.1);
                        F="2";
                        [ResponseIndex6(i), dataout6(i),
PercentError6(i)] = NeuropathyUnoFunction2(F, Uno);

                        ResponseIndex5(i)=101;
                        ResponseIndex7(i)=101;
                        dataout5(i)=0;
                        dataout7(i)=0;
                        PercentError5(i)=0;
                        PercentError7(i)=0;
                    end

                end

                if ResponseIndex3(i)==0
                    fprintf('Z axis move \n'); %Z axis moves
```

```
                    pause(0.1);
                    F="8";
                    [ResponseIndex5(i), dataout5(i),
PercentError5(i)] = NeuropathyUnoFunction2(F, Uno);

                    if ResponseIndex5(i)==1
                        fprintf('Z axis move \n'); %Z axis moves
                        pause(0.1);
                        F="6";
                        [ResponseIndex7(i), dataout7(i),
PercentError7(i)] = NeuropathyUnoFunction2(F, Uno);

                        ResponseIndex4(i)=101;
                        ResponseIndex6(i)=101;
                        dataout4(i)=0;
                        dataout6(i)=0;
                        PercentError4(i)=0;
                        PercentError6(i)=0;
                    end

                    if ResponseIndex5(i)==0
                        ResponseIndex4(i)=101;
                        ResponseIndex6(i)=101;
                        ResponseIndex7(i)=101;
                        dataout4(i)=0;
                        dataout6(i)=0;
                        dataout7(i)=0;
                        PercentError4(i)=0;
                        PercentError6(i)=0;
                        PercentError7(i)=0;
                    end

                end

                fprintf('False Positive Z \n');
                pause(0.1);
                F="0";
                [ResponseIndex0(i), dataout0(i),
PercentError0(i)] = NeuropathyUnoFunction2(F, Uno);

            else
                fprintf('False Positive at Beginning \n');
                fprintf('False Positive Z \n');
                pause(0.1);
                F="0";
                [ResponseIndex0(i), dataout0(i),
PercentError0(i)] = NeuropathyUnoFunction2(F, Uno);
```

```
                fprintf('Z axis move \n');
                pause(0.1);
                F="0.2";
                [ResponseIndex1(i), dataout1(i),
PercentError1(i)] = NeuropathyUnoFunction2(F, Uno);

                if ResponseIndex1(i)==1
                    ResponseIndex2(i)=101;
                    ResponseIndex3(i)=101;
                    ResponseIndex4(i)=101;
                    ResponseIndex5(i)=101;
                    ResponseIndex6(i)=101;
                    ResponseIndex7(i)=101;
                    dataout2(i)=0;
                    dataout3(i)=0;
                    dataout4(i)=0;
                    dataout5(i)=0;
                    dataout6(i)=0;
                    dataout7(i)=0;
                    PercentError2(i)=0;
                    PercentError3(i)=0;
                    PercentError4(i)=0;
                    PercentError5(i)=0;
                    PercentError6(i)=0;
                    PercentError7(i)=0;
                end

                if ResponseIndex1(i)==0
                    fprintf('Z axis move \n'); %Z axis moves
                    pause(0.1);
                    F="10";
                    [ResponseIndex2(i), dataout2(i),
PercentError2(i)] = NeuropathyUnoFunction2(F, Uno);
                end

                if ResponseIndex2(i)==1
                    fprintf('Z axis move \n'); %Z axis moves
                    pause(0.1);
                    F="4";
                    [ResponseIndex3(i), dataout3(i),
PercentError3(i)] = NeuropathyUnoFunction2(F, Uno);
                end

                if ResponseIndex2(i)==0
                    ResponseIndex3(i)=101;
                    ResponseIndex4(i)=101;
```

```
                    ResponseIndex5(i)=101;
                    ResponseIndex6(i)=101;
                    ResponseIndex7(i)=101;
                    dataout3(i)=0;
                    dataout4(i)=0;
                    dataout5(i)=0;
                    dataout6(i)=0;
                    dataout7(i)=0;
                    PercentError3(i)=0;
                    PercentError4(i)=0;
                    PercentError5(i)=0;
                    PercentError6(i)=0;
                    PercentError7(i)=0;
                end

                if ResponseIndex3(i)==1
                    fprintf('Z axis move \n'); %Z axis moves
                    pause(0.1);
                    F="0.7";
                    [ResponseIndex4(i), dataout4(i),
PercentError4(i)] = NeuropathyUnoFunction2(F, Uno);

                    if ResponseIndex4(i)==1
                        ResponseIndex5(i)=101;
                        ResponseIndex6(i)=101;
                        ResponseIndex7(i)=101;
                        dataout5(i)=0;
                        dataout6(i)=0;
                        dataout7(i)=0;
                        PercentError5(i)=0;
                        PercentError6(i)=0;
                        PercentError7(i)=0;
                    end

                    if ResponseIndex4(i)==0
                        fprintf('Z axis move \n'); %Z axis moves
                        pause(0.1);
                        F="2";
                        [ResponseIndex6(i), dataout6(i),
PercentError6(i)] = NeuropathyUnoFunction2(F, Uno);

                        ResponseIndex5(i)=101;
                        ResponseIndex7(i)=101;
                        dataout5(i)=0;
                        dataout7(i)=0;
                        PercentError5(i)=0;
                        PercentError7(i)=0;
```

```
                    end

                end

                if ResponseIndex3(i)==0
                    fprintf('Z axis move \n'); %Z axis moves
                    pause(0.1);
                    F="8";
                    [ResponseIndex5(i), dataout5(i),
PercentError5(i)] = NeuropathyUnoFunction2(F, Uno);

                    if ResponseIndex5(i)==1
                        fprintf('Z axis move \n'); %Z axis moves
                        pause(0.1);
                        F="6";
                        [ResponseIndex7(i), dataout7(i),
PercentError7(i)] = NeuropathyUnoFunction2(F, Uno);

                        ResponseIndex4(i)=101;
                        ResponseIndex6(i)=101;
                        dataout4(i)=0;
                        dataout6(i)=0;
                        PercentError4(i)=0;
                        PercentError6(i)=0;
                    end

                    if ResponseIndex5(i)==0
                        ResponseIndex4(i)=101;
                        ResponseIndex6(i)=101;
                        ResponseIndex7(i)=101;
                        dataout4(i)=0;
                        dataout6(i)=0;
                        dataout7(i)=0;
                        PercentError4(i)=0;
                        PercentError6(i)=0;
                        PercentError7(i)=0;
                    end

                end

            end

        else
            fprintf('No False Positive \n');
            fprintf('Z axis move \n'); %Z axis moves
            pause(0.1);
            F="0.2";
```

```
            [ResponseIndex1(i), dataout1(i), PercentError1(i)] =
NeuropathyUnoFunction2(F, Uno);
            FalsePositiveCheckIndex(i)=0;

            if ResponseIndex1(i)==1
                    ResponseIndex0(i)=101;
                    ResponseIndex2(i)=101;
                    ResponseIndex3(i)=101;
                    ResponseIndex4(i)=101;
                    ResponseIndex5(i)=101;
                    ResponseIndex6(i)=101;
                    ResponseIndex7(i)=101;
                    dataout0(i)=0;
                    dataout2(i)=0;
                    dataout3(i)=0;
                    dataout4(i)=0;
                    dataout5(i)=0;
                    dataout6(i)=0;
                    dataout7(i)=0;
                    PercentError0(i)=0;
                    PercentError2(i)=0;
                    PercentError3(i)=0;
                    PercentError4(i)=0;
                    PercentError5(i)=0;
                    PercentError6(i)=0;
                    PercentError7(i)=0;
            end

            if ResponseIndex1(i)==0
                fprintf('Z axis move \n'); %Z axis moves
                pause(0.1);
                F="10";
                [ResponseIndex2(i), dataout2(i),
PercentError2(i)] = NeuropathyUnoFunction2(F, Uno);
            end

            if ResponseIndex2(i)==1
                fprintf('Z axis move \n'); %Z axis moves
                pause(0.1);
                F="4";
                [ResponseIndex3(i), dataout3(i),
PercentError3(i)] = NeuropathyUnoFunction2(F, Uno);
            end

            if ResponseIndex2(i)==0
                    ResponseIndex0(i)=101;
                    ResponseIndex3(i)=101;
```

```
                    ResponseIndex4(i)=101;
                    ResponseIndex5(i)=101;
                    ResponseIndex6(i)=101;
                    ResponseIndex7(i)=101;
                    dataout0(i)=0;
                    dataout3(i)=0;
                    dataout4(i)=0;
                    dataout5(i)=0;
                    dataout6(i)=0;
                    dataout7(i)=0;
                    PercentError0(i)=0;
                    PercentError3(i)=0;
                    PercentError4(i)=0;
                    PercentError5(i)=0;
                    PercentError6(i)=0;
                    PercentError7(i)=0;
            end

            if ResponseIndex3(i)==1
                fprintf('Z axis move \n'); %Z axis moves
                pause(0.1);
                F="0.7";
                [ResponseIndex4(i), dataout4(i),
PercentError4(i)] = NeuropathyUnoFunction2(F, Uno);

                if ResponseIndex4(i)==1
                        ResponseIndex0(i)=101;
                        ResponseIndex5(i)=101;
                        ResponseIndex6(i)=101;
                        ResponseIndex7(i)=101;
                        dataout0(i)=0;
                        dataout5(i)=0;
                        dataout6(i)=0;
                        dataout7(i)=0;
                        PercentError0(i)=0;
                        PercentError5(i)=0;
                        PercentError6(i)=0;
                        PercentError7(i)=0;
                end

                if ResponseIndex4(i)==0
                    fprintf('Z axis move \n'); %Z axis moves
                    pause(0.1);
                    F="2";
                    [ResponseIndex6(i), dataout6(i),
PercentError6(i)] = NeuropathyUnoFunction2(F, Uno);
```

```
                    ResponseIndex0(i)=101;
                    ResponseIndex5(i)=101;
                    ResponseIndex7(i)=101;
                    dataout0(i)=0;
                    dataout5(i)=0;
                    dataout7(i)=0;
                    PercentError0(i)=0;
                    PercentError5(i)=0;
                    PercentError7(i)=0;
                end

            end

            if ResponseIndex3(i)==0
                fprintf('Z axis move \n'); %Z axis moves
                pause(0.1);
                F="8";
                [ResponseIndex5(i), dataout5(i),
PercentError5(i)] = NeuropathyUnoFunction2(F, Uno);

                if ResponseIndex5(i)==1
                    fprintf('Z axis move \n'); %Z axis moves
                    pause(0.1);
                    F="6";
                    [ResponseIndex7(i), dataout7(i),
PercentError7(i)] = NeuropathyUnoFunction2(F, Uno);

                    ResponseIndex0(i)=101;
                    ResponseIndex4(i)=101;
                    ResponseIndex6(i)=101;
                    dataout0(i)=0;
                    dataout4(i)=0;
                    dataout6(i)=0;
                    PercentError0(i)=0;
                    PercentError4(i)=0;
                    PercentError6(i)=0;
                end

                if ResponseIndex5(i)==0
                        ResponseIndex0(i)=101;
                        ResponseIndex4(i)=101;
                        ResponseIndex6(i)=101;
                        ResponseIndex7(i)=101;
                        dataout0(i)=0;
                        dataout4(i)=0;
                        dataout6(i)=0;
                        dataout7(i)=0;
```

```
                        PercentError0(i)=0;
                        PercentError4(i)=0;
                        PercentError6(i)=0;
                        PercentError7(i)=0;
                    end

                end

            end
        end
end

TestLocationCelltoString=string(TestLocationCellArray);
TestLocationCelltoStringTranspose=TestLocationCelltoString';
ResponseIndexRecordI0=ResponseIndex0';
ResponseIndexRecordI1=ResponseIndex1';
ResponseIndexRecordI2=ResponseIndex2';
ResponseIndexRecordI3=ResponseIndex3';
ResponseIndexRecordI4=ResponseIndex4';
ResponseIndexRecordI5=ResponseIndex5';
ResponseIndexRecordI6=ResponseIndex6';
ResponseIndexRecordI7=ResponseIndex7';

FalsePositiveCheckIndexTranspose=FalsePositiveCheckIndex';

ForceIndexRecordD0=dataout0';
ForceIndexRecordD1=dataout1';
ForceIndexRecordD2=dataout2';
ForceIndexRecordD3=dataout3';
ForceIndexRecordD4=dataout4';
ForceIndexRecordD5=dataout5';
ForceIndexRecordD6=dataout6';
ForceIndexRecordD7=dataout7';

PercentErrorC0=PercentError0';
PercentErrorC1=PercentError1';
PercentErrorC2=PercentError2';
PercentErrorC3=PercentError3';
PercentErrorC4=PercentError4';
PercentErrorC5=PercentError5';
PercentErrorC6=PercentError6';
PercentErrorC7=PercentError7';

NumberofTrials=VectorTranspose;
LocationSelected=GcodeCelltoStringTranspose;
RandomizedOrder=RandomizedVectorTranspose;
RandomizedLocations=TestLocationCelltoStringTranspose;
```

```
FalsePositiveCheck=FalsePositiveRandomizationVectorTranspose;
FalsePositiveOrderofOccurance=FalsePositiveCheckIndexTranspose;
RandomizedPixelsX=TDataPixelsX(RandomizedVector);
RandomizedPixelsY=TDataPixelsY(RandomizedVector);

for i=1:X
    if ResponseIndex1(i)==1
        PositiveResponse1=find(ResponseIndex1==1);
        PositiveReponseX1=RandomizedPixelsX(PositiveResponse1);
        PositiveReponseY1=RandomizedPixelsY(PositiveResponse1);
        P1=plot(PositiveReponseX1,PositiveReponseY1, 'o',
'LineWidth',2, 'MarkerEdgeColor','k', 'MarkerFaceColor','g',
'MarkerSize',10, 'DisplayName', '0.200 grams');
    end

    if ResponseIndex1(i)==0 && ResponseIndex2(i)==0
        PositiveResponse8=find(ResponseIndex2==0);
        PositiveReponseX8=RandomizedPixelsX(PositiveResponse8);
        PositiveReponseY8=RandomizedPixelsY(PositiveResponse8);
        P8=plot(PositiveReponseX8,PositiveReponseY8, 'o',
'LineWidth',2, 'MarkerEdgeColor','k', 'MarkerFaceColor','k',
'MarkerSize',10, 'DisplayName', 'Greater than 10.00 grams');
    end

    if ResponseIndex1(i)==0 && ResponseIndex2(i)==1 &&
ResponseIndex3(i)==0 && ResponseIndex5(i)==0
        PositiveResponse2=find(ResponseIndex2==1);
        PositiveReponseX2=RandomizedPixelsX(PositiveResponse2);
        PositiveReponseY2=RandomizedPixelsY(PositiveResponse2);
        P2=plot(PositiveReponseX2,PositiveReponseY2, 'o',
'LineWidth',2, 'MarkerEdgeColor','r', 'MarkerFaceColor','k',
'MarkerSize',10, 'DisplayName', '10.00 grams');
    end

    if ResponseIndex3(i)==1 && (ResponseIndex7(i)==1 ||
ResponseIndex6(i)==0)
        PositiveResponse3=find(ResponseIndex3==1);
        PositiveReponseX3=RandomizedPixelsX(PositiveResponse3);
        PositiveReponseY3=RandomizedPixelsY(PositiveResponse3);
        P3=plot(PositiveReponseX3,PositiveReponseY3, 'o',
'LineWidth',2, 'MarkerEdgeColor','k', 'MarkerFaceColor','m',
'MarkerSize',10, 'DisplayName', '4.00 grams');
    end

    if ResponseIndex4(i)==1
        PositiveResponse4=find(ResponseIndex4==1);
        PositiveReponseX4=RandomizedPixelsX(PositiveResponse4);
```

```
        PositiveReponseY4=RandomizedPixelsY(PositiveResponse4);
        P4=plot(PositiveReponseX4,PositiveReponseY4, 'o',
'LineWidth',2, 'MarkerEdgeColor','k', 'MarkerFaceColor','b',
'MarkerSize',10, 'DisplayName', '0.700 grams');
    end

    if ResponseIndex5(i)==1 && ResponseIndex7(i)==0
        PositiveResponse5=find(ResponseIndex5==1);
        PositiveReponseX5=RandomizedPixelsX(PositiveResponse5);
        PositiveReponseY5=RandomizedPixelsY(PositiveResponse5);
        P5=plot(PositiveReponseX5,PositiveReponseY5, 'o',
'LineWidth',2, 'MarkerEdgeColor','c', 'MarkerFaceColor','r',
'MarkerSize',10, 'DisplayName', '8.00 grams');
    end

    if ResponseIndex6(i)==1
        PositiveResponse6=find(ResponseIndex6==1);
        PositiveReponseX6=RandomizedPixelsX(PositiveResponse6);
        PositiveReponseY6=RandomizedPixelsY(PositiveResponse6);
        P6=plot(PositiveReponseX6,PositiveReponseY6, 'o',
'LineWidth',2, 'MarkerEdgeColor','k', 'MarkerFaceColor','y',
'MarkerSize',10, 'DisplayName', '2.00 grams');
    end

    if ResponseIndex7(i)==1
        PositiveResponse7=find(ResponseIndex7==1);
        PositiveReponseX7=RandomizedPixelsX(PositiveResponse7);
        PositiveReponseY7=RandomizedPixelsY(PositiveResponse7);
        P7=plot(PositiveReponseX7,PositiveReponseY7, 'o',
'LineWidth',2, 'MarkerEdgeColor','g', 'MarkerFaceColor','r',
'MarkerSize',10, 'DisplayName', '6.00 grams');
    end

end

T=table(NumberofTrials, LocationSelected, RandomizedOrder,
RandomizedLocations, FalsePositiveCheck, ForceIndexRecordD0,
PercentErrorC0, ResponseIndexRecordI0,
FalsePositiveOrderofOccurance, ForceIndexRecordD1,
PercentErrorC1, ResponseIndexRecordI1, ForceIndexRecordD2,
PercentErrorC2, ResponseIndexRecordI2, ForceIndexRecordD3,
PercentErrorC3, ResponseIndexRecordI3, ForceIndexRecordD4,
PercentErrorC4, ResponseIndexRecordI4, ForceIndexRecordD5,
PercentErrorC5, ResponseIndexRecordI5, ForceIndexRecordD6,
PercentErrorC6, ResponseIndexRecordI6, ForceIndexRecordD7,
PercentErrorC7, ResponseIndexRecordI7);
end
```

Appendix H (Neuropathy Uno Function)

This code was written by Vitale Kyle Castellano

```
function [ResponseIndex, dataoutnum, PercentError] =
NeuropathyUnoFunction2(F, Uno)

flushinput(Uno);

%Uno=serial('COM6', 'BaudRate', 9600);
%fopen(Uno);
%pause(3)

fprintf(Uno,'%s\n', F);
foo=0;

while foo==0

    if Uno.BytesAvailable>=0
        dataoutLC=fscanf(Uno,'%s\n');
        dataoutH=fscanf(Uno,'%s\n');
        foo=1;
    end
end

if dataoutH=="y"
    ResponseIndex=1;
else
    ResponseIndex=0;
end

dataoutstr=convertCharsToStrings(dataoutLC);
dataoutnum=str2double(dataoutstr);
Fnum=str2double(F);

if Fnum==0
    PercentError=0;
else
PercentError=abs((Fnum-dataoutnum)/Fnum)*100;
end

%pause(0.25)
%fclose(Uno);
%pause(0.25)
%flushoutput(Uno);

end
```

Appendix I (Arduino Uno Function)

The code was written by Hayden Burch and Vitale Kyle Castellano

```
#include "Arduino.h"
#include "HX711N.h"
#include "AccelStepper.h"
#include <avr/wdt.h>

HX711N scale(3, 2);  // (DOUT, CLK)

double measuredload;
char response;
bool stop_motor = false;
int calibration_factor = 13280;
int trim_in_pin = A0;
int trim_value = 0;

// Motor steps per revolution. Most steppers are 200 steps or 1.8 degrees/step
#define MOTOR_STEPS 200

// Microstepping mode. If you hardwired it to save pins, set to the same value here.
#define MICROSTEPS 1

#define DIR 6
#define STEP 7

bool foo = 1;
bool foot = 0;
int foob = 1;
bool fee=0;
int fum=0;

AccelStepper stepper(AccelStepper::DRIVER, STEP, DIR); // Defaults to
AccelStepper::FULL4WIRE (4 pins) on 2, 3, 4, 5

float inputload;
int startt;
int endt;
int n;

void setup() {
  pinMode(8, INPUT_PULLUP);
  pinMode(9, OUTPUT);
  stepper.setMaxSpeed(1000);
  stepper.setSpeed(-100);
```

```
  Serial.begin(9600);
  //  Serial.println("HX711 calibration sketch");
  //  Serial.println("Remove all weight from scale");
  //  Serial.println("After readings begin, place known weight on scale");

  //  scale.set_scale();
  scale.tare(10); // Reset the scale to 0; Reads value 10 times, calculates average and uses it as
offset.

  //  long zero_factor = scale.read_average(); //Get a baseline reading
  //  Serial.print("Zero factor: "); //This can be used to remove the need to tare the scale. Useful in
permanent scale projects.
  //  Serial.println(zero_factor);
  //
  scale.set_scale(calibration_factor); //Adjust to this calibration factor
  stepper.setCurrentPosition(0);
}

void loop() {

  if(Serial.available()>0 && foot == 0 && foo == 1)
  {
    inputload = Serial.parseFloat();
    foot = 1;
    foo = 0;
  }
  // NOTE: LOOP HAS TO RUN QUICKLY FOR STEPPER TO MOVE SMOOTHLY. DO
NOT ADD DELAYS
  while (foot == 1){
    stepper.setSpeed(-100);
    stepper.setAcceleration(250);
    stepper.move(-300);
    stepper.runToPosition();
    foot = 0;
    delay(250);
    }

  if (scale.is_ready() && foo == 0){
    measuredload = scale.get_units_direct();

    if (measuredload < .25*inputload) {
      stop_motor = false;
      stepper.setSpeed(-20);
    }
    else if (measuredload < .5*inputload) {
```

```
    stop_motor = false;
    stepper.setSpeed(-15);
   }
   else if (measuredload < .75*inputload) {
    stop_motor = false;
    stepper.setSpeed(-10);
   }
   else if (measuredload < .9*inputload) {
    stop_motor = false;
    stepper.setSpeed(-7);
   }
   else if (measuredload < 1*inputload) {
    stop_motor = false;
    stepper.setSpeed(-5);
   }
   else {
    stop_motor = true;
    foo=1;
   }

 }

 if (stop_motor) {
   Serial.println(measuredload);
   stepper.moveTo(0);
   stepper.setSpeed(200);
   fee=0;
   while (fee==0){
    stepper.runToPosition();

    fee=1;

   }

   foo=1;
   foob = 1;
   fum=0;
      startt = millis();
      endt = startt;
         while ((endt - startt) <=5000 && fum==0){
            if (foob==1){

            if (n%2==0){
            digitalWrite(9, HIGH);
            delay(250);
            }
```

```
            if (n%2!=0){
            digitalWrite(9, LOW);
            delay(250);
            }

                if (digitalRead(8) == LOW){
                  response = 'y';
                  Serial.println(response);
                  //Serial.println("felt");
                  digitalWrite(9, HIGH);
                  foob = 2;
                  fum=1;
                }
            endt = millis();
            n=n+1;
          }
          }
           if (digitalRead(8) == HIGH && foo == 1){
           response = 'n';
           Serial.println(response);
           foob = 0;
           digitalWrite(9, LOW);
           }

           while (foob==0 || foob==2){
           //Serial.end();
           foo=0;
           reboot();

           }

           //Serial.end();
  }

  else{
    stepper.runSpeed();
  }

}

void reboot(){
  wdt_disable();
  wdt_enable(WDTO_15MS);
  while (1) {}
}
```